Optimization of Microarray Technology-Based Expression Profiling for Investigation of Different Animal Models of Pulmonary Hypertension

Inauguraldissertation

zur Erlangung des Grades eines Doktors der Humanbiologie

des Fachbereichs Medizin

der Justus-Liebig-Universität Giessen

vorgelegt von Jai Prakash

aus Neu Dehli, Indien

Giessen 2005

Aus dem Institut für Pathologie

des Fachbereichs Medizin der Justus-Liebig-Universität Giessen

Direktor: Prof. Dr. med. Andreas Schulz

Gutachter: PD Dr. L. Fink

Gutachter: Prof. Dr. J. Lohmeyer

Tag der Disputation: 17.05.2006

TABLE OF CONTENTS

ABBREVIATIONS

aRNA	Antisense or Amplified RNA
β-ME	Beta-mercaptoethanol
bp	Base pair(s)
cAMP	Cyclic adenosine monophosphate
CBTs	Cholesterol-binding toxins
cDNA	Complementary DNA
cGMP	Cyclic guanosine monophosphate
Cy3- dCTP	Cyanine 3- 2´-Deoxycytidine 5´-Triphosphate
Cy5- dCTP	Cyanine 5- 2´-Deoxycytidine 5´-Triphosphate
Cy3-UTP	Cyanine 3- Uridine-5'-Triphosphate
Cy5-UTP	Cyanine 5- Uridine-5'-Triphosphate
Cyclic AMP	Adenosine 3' 5'-cyclic monophosphate
DNA	Deoxyribonucleic acid
dNTP	Deoxynucleotide Triphosphates mix
dATP	2´-Deoxyadenosine 5´-Triphosphate
dCTP	2´-Deoxycytidine 5´-Triphosphate
dGTP	2´-Deoxyguanosine 5´-Triphosphate
dTTP	2´-Deoxythymidine 5´-Triphosphate
DKFZ	Deutsches Krebsforschungszentrum
DMSO	Dimethylsulfoxide
ds cDNA	Double stranded complementary DNA
DTT	Dithiothreitol
EDTA	Ethylendinitrilo-N,N,N',N',-tetra-acetate
EB	Elution buffer
FOI	Frequency of incorporation
IT	Intratracheal
IV	Intravenous
g	Gram, unit of weight
GAPDH	Glyceraldehyde-3-phosphate dehydrogenase
GTC	Guanidine isothiocyanate

HBSS	Hank's balanced salt medium
HEPES	4-(2-hydroxyethyl)-1-piperazineethanesulfonic acid
IL-8	Interleukine-8
IVT	*In-vitro* transcription
Kb	Kilobase(s)
MCT	Monocrotaline
MT	Monocrotaline+ Tolafentine
M	Molar
mM	Millimolar
mg	Milligram
ml	Millilitre
mRNA	Messenger RNA
nm	Nanometer
OD	Optical density
Oligos	Oligodeoxynucleotides
PA	Pyrrolizidine alkaloid
PAH	Pulmonary artery hypertension
PAP	Pulmonary artery pessure
PBGD	Porphobilinogen deaminase
PCR	Polymerase chain reaction
PH	Pulmonary hypertension
PDE	Phosphodiesterases
pH	Potential of hydrogen
PLY	Pneumolysin
PMT	Photo multiplier tube
pmol	Picomol
PPH	Primary pulmonary pypertension
RNA	Ribonucleic acid
rRNA	Ribosomal RNA
rpm	Revolutions per minute
RT	Reverse transcription
RTase	Reverse transcriptase

SDS	Sodium dodecylsulfate
SSC	Sodium chloride sodium citrate
TBE	Tris borate EDTA buffer
TE	Tris EDTA
TIFF	Tagged image file format
Tola	Tolafentrine
Tris	Tris-(hydroxymethyl)-aminomethane
T7-IVT	T7- *In-vitro* transcription
μ	Micro (10^{-6})
μl	Microlitre
μm	Micrometer
μg	Microgram
U	Enzyme unit
UV	Ultaviolet
ΔCt	Delta threshold cycle

LIST OF PUBLICATIONS

Journal Articles

1. Fink, L., Hölschermann, H., Kwapiszewaska, G., **Prakash Muyal, J**., Lengemann, B., Bohle, RM., Santoso, S. Characterization of platelet-specific mRNA by real-time PCR after laser-assisted microdissection. Thromb *Haemost 2003*, **90**:749-756

2. Pullamsetti, S., Kiss, L., Ghofrani, HA., Voswinckel, R., Haredza, P., Walter, K., Aigner, C., Fink, L., **Prakash Muyal, J**., Weissmann, N., Grimminger, F., Seeger, W., Schermuly RT. Increased levels and reduced catabolism of asymmetric and symmetric dimethylarginices in pulmonary hypertension. *FASEB J 2005*, **19**:1175-79

3. Wilhelm, J., **Prakash Muyal, J**., Best, J., Kwapiszewska, G., Stein, MM., Bohle, RM., Fink, L. Systemic comparison of RNA preamplification techniques in genome wide expression profiling. Submitted

Poster Presentations

1. **Prakash Muyal, J**., Wilhelm, J., Stein, MM., Seeger, W., Bohle, RM., Fink, L. Comparison of pre-amplification techniques for expression profiling using DNA-microarrays. American Thoracic Society 2005 San Diego 101th International Conference, U.S.A.

2. Grimminger, F., Fink, L., **Prakash Muyal, J**., Repsilber, D., Wilhelm, J., Weissmann, N., Srivasatva, M., Maus, U., Schermuly, RT., Darji, A., Rose, F., Hossain, H., Tchatalbachev, S., Walid, W., Domann, E., Lüttmann, S., Hoffmann, R., Bohle, RM., Lohmeyer, J., Ziegler, A., Seeger, W., Chakraborty, T. Transcriptional response of the mouse lung to pneumolysin challenge. American Thoracic Society 2004 Orlando 100th International Conference, U.S.A.

3. Fink, L., Izraeli, Z., **Prakash Muyal, J**., Kwapiszewska, G., Maus, U., Hanze, J., Rose, F., Grimminger, F., Seeger, W., Weissmann, N., Bohle, RM. Hypoxia induced gene regulation in alveolar macrophages. American Thoracic Society 2003 Seattle 99th Internationale Conference, U.S.A.

4. Kohlhoff, S., **Prakash Muyal, J**., Kwapiszewska, G., Stein, MM., Hanze, J., Weissmann, N., Rose, F., Seeger, W., Bohle, RM., Fink, L. Hypoxia induced expression profile differences from laser microdissected lung vessels and alveolar septum cells. Array User Conference (RZPD), DKFZ-Heidelberg, 14-16.05.2003, Germany.

5. Hölschermann, H., Fink, L., Kwapiszewska, G., **Prakash Muyal, J**., Lengemann, B., Bohle, RM., Tillmanns, H., Santoso, S. An improved method for characterization of platelet-specific mRNA by real-time PCR after laser assisted microdissection. Gesellschaft für Thrombose und Hämostaseforschung, 15-18.02.03, Innsbruck, Germany.

ACKNOWLEDGEMENTS

1   Introduction

The application of microarrays for expression profiling was first published in 1995.[1] Since this time, the number of publications related to microarrays increased exponentially (figure 1). This demonstrates the rapidly increasing impact of this technology on toxicological research[2], genetic diagnostics[3], drug discovery[4] and basic research applications.[5-8] DNA-microarrays are a large-scale and high-throughput technology to obtain information on relative abundances of up to many thousands of transcripts from a single biological sample simultaneously. This allows studying the complex interplay of all the genes in a cell. The global patterns of gene activities become observable with few microarray experiments. These expression patterns may provide clues to regulation and possible functions of previously uncharacterized genes or genes known in a different context. The combination with metabolic schematics can help to understand how pathways interact and change under varying conditions.
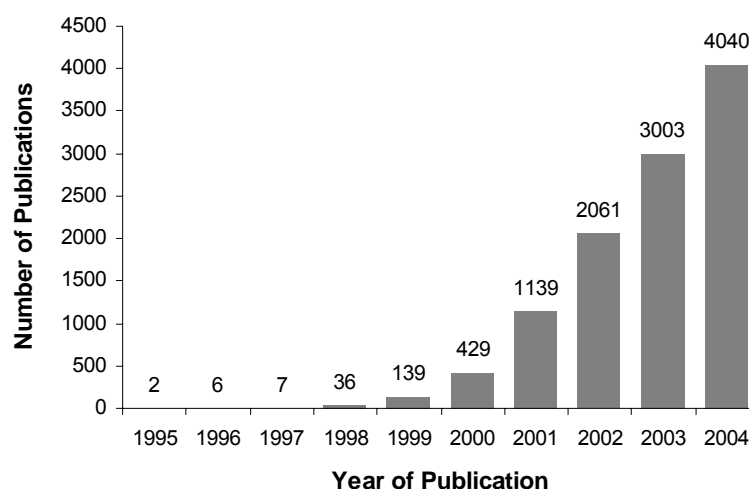
Figure 1. Number of publications about DNA-microarrays from 1995-2004. The given numbers are the amount of references found in PubMed [9] searching for publications related to microarrays.

1.1   DNA-Microarray Technology

Although there are many different kinds of DNA-microarrays available, the basic technology is for all types the same. DNA fragments with sequences unique for the genes or transcripts of interest are generated and immobilized at defined positions (spots or features) on a solid surface (matrix). Labelled nucleic acids from the samples are prepared and allowed to hybridize to the complementary probes spotted on the matrix. The amounts of hybridized samples are read out for each spot by appropriate imaging techniques, depending on the kind of label used. Changes in gene expression between two samples are determined by the difference in the intensities of the corresponding spots. When fluorescent labels are used, the two samples to be compared can be labelled with different colors (fluorophores) and hybridized to the same microarray. In this case, each spot contains the information of the abundance of one particular gene or transcript in both of the samples. Figure 2 shows the schematic of the whole process for the example of a competitive hybridization of two fluorescently labelled samples.

For the matrix, materials like nylon membrane, plastic or modified glass surfaces can be applied. The original membrane used for nucleic acid immobilization was nitrocellulose, selected by E. M. Southern for his Southern blotting method.[10] Recently, nylon has been promoted as a substrate for nucleic acid binding owing to its greater physical strength and binding capacity, and a wider range of available surface chemistries was offered for optimizing nucleic acid attachment. Immobilization on nylon membranes can be performed via physical adsorption, UV cross-linking, or chemical activation. Immobilization on nylon has been demonstrated to be more durable during repeated probe stripping than immobilization on nitrocellulose.[11] Nylon membranes have also been used in methods to detect DNA by colorimetry, fluorometry, and chemiluminescence.[12] The high background typically observed with nylon membranes is their principal disadvantage. This may be due to a nonspecific binding of the sample or detection system, or to some natural property of the membrane. Nitrocellulose has a lower binding capacity and is weaker than nylon, but it has far lower background for most detection systems. Traditional membranes such as nylon and nitrocellulose have been used in the production of macroarrays, but their use in microarrays is limited

because of the low spot resolution. Because these membranes exhibit lateral wicking characteristics, the label tends to spread from the point of application. This has been a limitation in the production of high-density arrays.
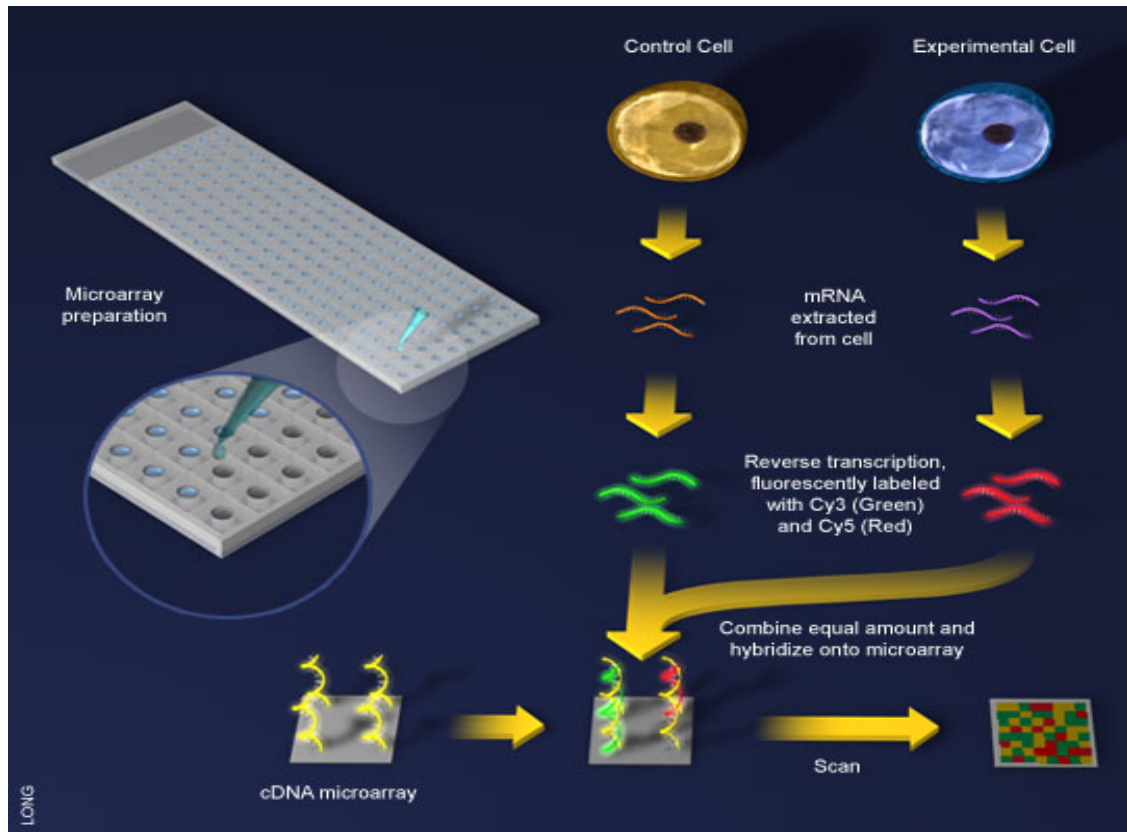
Figure 2. Schematic of microarray technology. A PCR product from a DNA clone is purified and spotted on a glass surface with the help of robotic printing. RNA is extracted from two different samples and converted into fluorescently labelled cDNA. The labelled cDNAs of the two samples are then mixed and hybridized to the array. The array is finally scanned to get the relative fluorescence intensities for each spot. Picture taken from http://www.bioteach.ubc.ca/ MolecularBiology/microarray.

Modified glass surfaces (epoxy-, aminosilan, or poly-L-lysine coated) are the most commonly used matrices for high-density microarrays. Similar to the application on membranes, the probes can be mechanically spotted on the surface and subsequently be immobilized by UV-crosslinking or baking. Figure 3 show a spotting robot for glass arrays and a print-tip head in action.
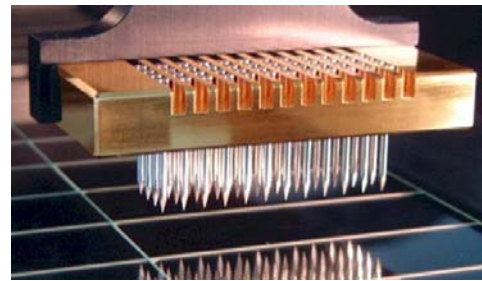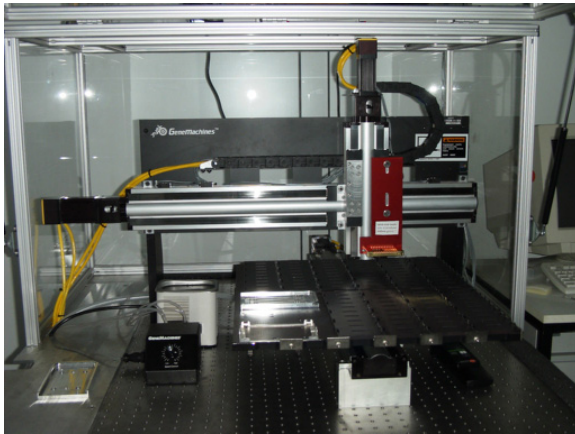
Figure 3. Microarray spotting robot *(left)* and detail View of a Print-Tip Head *(right)*. The *left* pictures was taken from http://www.dkfz-heidelberg.de/kompl_genome/, the *right* picture was taken from http://arrayit.com/Products/ Printing/Stealth/stealth.html.

The Affymetrix Company holds the patent on a robust method to synthesize short oligonucleotides (25mers) directly on the glass surface with a combination of photolithography and combinatorial chemistry.[13-14] This system is named GeneChip™ technology. Another unique feature of Affymetrix GeneChip™ arrays is the probe design: the sequences of the transcripts of interest are addressed by a set (5-20) of different 25mer oligonucleotides. To be able to correct for cross-hybridization of the samples with the relatively short probes, each probe set is complemented by a set of similar probes containing a base substitution in the middle of the probe sequence causing a mismatch to the target sequence. The difference of the hybridization signals on corresponding "perfect-match" and "mis-match" spots is finally used to estimate the relative abundance of the sequence of interest. In consequence, the short probes can discriminate well between single nucleotide polymorphisms.[15-16] Affymetrix does not promote competitive hybridizations of fluorescently labelled samples. Instead, the samples are labelled with biotin. The hybridization signal is generated by a streptavidin-phycoerythrin conjugate. Streptavidin binds to the biotin moieties of the hybridized samples. The signal is amplified on the chip by the application of goat-antibodies against streptavidin and biotinylated anti-goat antibodies that in turn bind multiple further streptavidin-phycoerythrin conjugates.

Most other microarray techniques make use of fluorescent labelling, whether used for single-color or for dual-color (competitive) hybridizations. The fluorophors can either be incorporated directly during the synthesis of the cDNA or during an in-vitro transcription adding already labelled nucleotides to the reaction mixture, or indirectly by adding amino-allylated nucleotides that are subsequently coupled with free monoreactive fluorophors.

1.2 Pulmonary Hypertension

Pulmonary Hypertension (PH) is clinically defined as a mean pulmonary arterial pressure (PAP) of more than 25 mm Hg at rest and 30 mm Hg during exercise while the normal mean pulmonary artery pressure in adults is 12-16 mm Hg.[17] PH is a life threatening disease that leads without treatment after 28 month in mean to right heart insufficiency and death, histologically characterized by lumen-obliterating endothelial cell proliferation and vascular smooth muscle hypertrophy of the small precapillary pulmonary arteries.[18]

1.2.1 Historical Background

The disease was first described over 100 years ago in a patient with right heart failure whose necrosis showed no obvious reason for pulmonary arteriosclerosis.[19] In 1901, Ayerza noted the profound cyanosis associated with this disorder, and described the disorder as *cardiacos negros* but the term so-called pulmonary hypertension was coined by Dresdale and his colleagues in 1951.[20] In 1954, Dresdale *et al.* reported the first documented cases of familial primary pulmonary hypertension (PPH).[21] In 1967, an increased frequency of PPH in Europe was linked to the use of the appetite suppressant aminorex fumarate. As a result, in 1973 WHO convened an international meeting on PPH.

The frequency of PPH in the general population is estimated at 1-2 cases per million people. PPH can develop at any age; the mean age at diagnosis is 36 years.[22] PPH began surfacing through the 1970s because of the latency period found to exist

between drug use and PPH diagnosis of 4-6 years. Today familial and sporadic cases of PPH are continuously diagnosed. A delay in diagnosis results in the disease progressing to late stages without proper treatment.

There is a female excess of PPH in both adult disease (ratio women/men 1.7-3.5) and childhood familial PPH.[23] More recently, in the United States and France, several cases of PPH have been associated with the appetite suppressants, fenfluramine and dexfenfluramine. In the United States it has been estimated that 300 new cases of PPH are diagnosed each year. Apparently it also affects people of all racial and ethnic origin equally. Apart from the primary pulmonary hypertension there are several reasons for the manifestation of increased pulmonary pressure secondarily and in the context of other diseases and states. Examples are the thrombembolic disease, veno-occlusive disease or chronic hypoxia.

1.2.1.1 Classification

There are many causes and, hence, ways of classifying the pulmonary hypertension.[24] Originally, PH was classified as either primary (idiopathic) or secondary (associated with diverse cardiopulmonary and systemic diseases). However, following a World Health Organization symposium held in Evian, France in 1998, a revised classification for PH was adopted. This classification separated conditions that directly affect the pulmonary arterial tree from disorders that either predominantly affects the venous circulation or conditions that affect the pulmonary circulation by altering respiratory structure or function. Thus, while the term secondary pulmonary hypertension was abandoned, PPH remained the term of choice to define familial or sporadic disease of undetermined cause. In addition, the Evian meeting emphasized the role of functional assessment of patients with PH, and a functional assessment classification, modified from the New York Heart Association functional classification, was also adopted. The impact of these classifications is perhaps best reflected by the regulatory approval of several new drugs for PAH, recognizing the common features shared by patients with this disease processes.[25]

Shortcomings in the Evian classification, however, became clear with its application in the clinical setting, coupled with further developments in the elucidation of the

pathogenesis of PH. A revision of this classification was proposed at the third World conference on pulmonary hypertension, held in Venice in 2003: PPH has been replaced by idiopathic PAH (IPAH) or, when supported by genetic investigation, familial PAH (FPAH). The experts believed that these terms more accurately and appropriately describe our contemporary understanding and clinical perspective.[25]

1.2.1.2 Histopathology

Chronic PH is associated with structural changes in both the pulmonary vasculature and the right ventricle (figure 4). Pathological findings consistent with IPAH/FPAH were first described in autopsy specimens a century ago.[26] The pulmonary arteries are characterized by intimal fibrosis, medial hypertrophy, adventitial proliferation, obliteration of small arteries and on occasion, vasculitis or changes in the walls of the pulmonary veins.[27] A fascinating focal vascular structure, the plexiform lesion, is found in many cases of IPAH/FPAH. Plexiform lesions are not pathognomonic for IPAH/FPAH, because they are also found in cases of severe PAH associated with other diseases. The plexiform lesion resembles the renal glomerulus, and its many channels are lined with endothelial cells rich in type 3-nitric oxide (NO) synthase, factor VIII, vimentin, and the receptor for vascular endothelial growth factor.[27] In the central core of the lesion, the endothelial cells are cyclin-kinase inhibitor p27/kip1–negative cells, whereas in peripheral areas adjacent to sites of angiogenesis, p27/kip1–positive cells are present.[28] It has been proposed that plexiform lesions are a form of neoplastic lesion, reflecting a dysregulation of endothelial growth.[29] Alternatively, plexiform lesions may represent an angiogenic response to local ischemia or hypoxia, as occurs with the creation of collateral vessels associated with obstructed arteries in other vascular beds. Computerized 3D reconstructions of vessels in IPAH/FPAH demonstrate that plexigenic lesions occur distal to vascular obstructive lesions.[28]
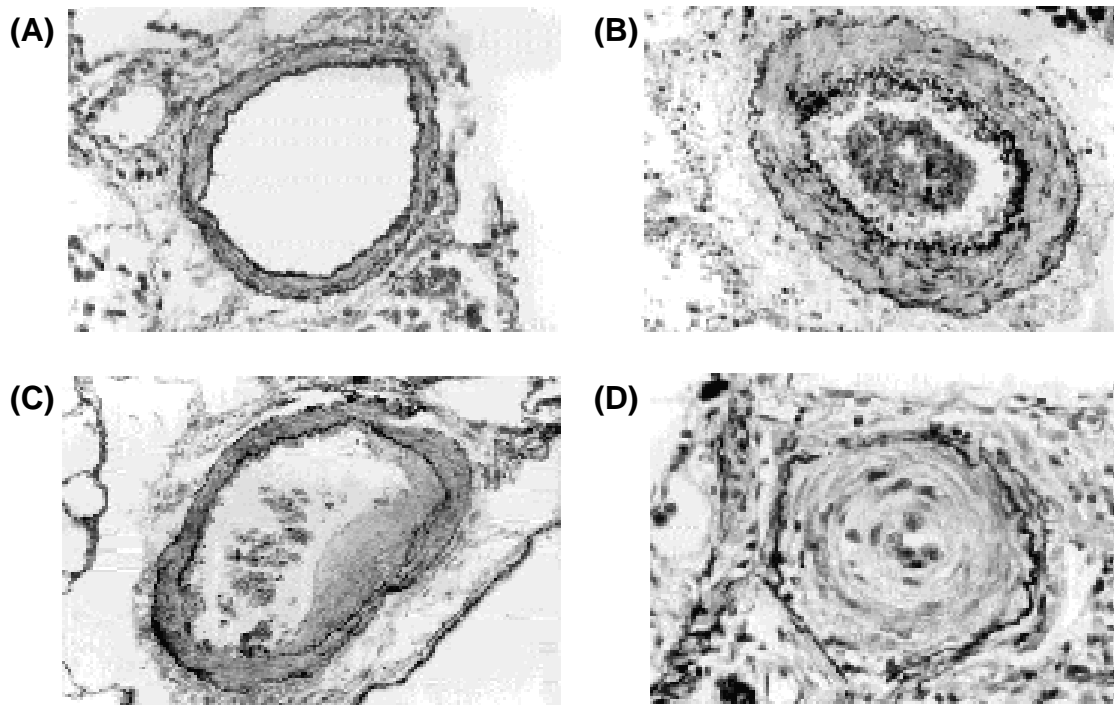
Figure 4. Photomicrography of lung section. (A) Control shows a normal small pulmonary artery with typically thin muscular wall, (B) shows a small pulmonary artery with hyperplasia of smooth muscle cells and thickening of the wall during PPH, (C) Shows fibrous intima proliferates on inner wall of small pulmonary artery, and (D) concentric laminar intima fibrosis with bands of scarred tissue build up on inner wall, substantially narrowing the blood vessel. (Picture adopted from http://www.healthnewsflash.com/conditions/primary_pulmonary_hyper-tension.php#pr).

1.2.2   Causes for Primary Pulmonary Hypertension

In a recent important advance, a genetic cause of the familial form of primary pulmonary hypertension has been discovered. Mutations in bone morphogenetic protein receptor 2 (BMPR2) have been associated with familial PAH and sporadic PPH.[30] BMPR2 is a cell signalling protein that plays a role in lung development, and the mutations found in patients with PPH are believed to reduce signalling in the BMP pathway. This, in turn, could lead to the over-proliferation of cells (figure 5).
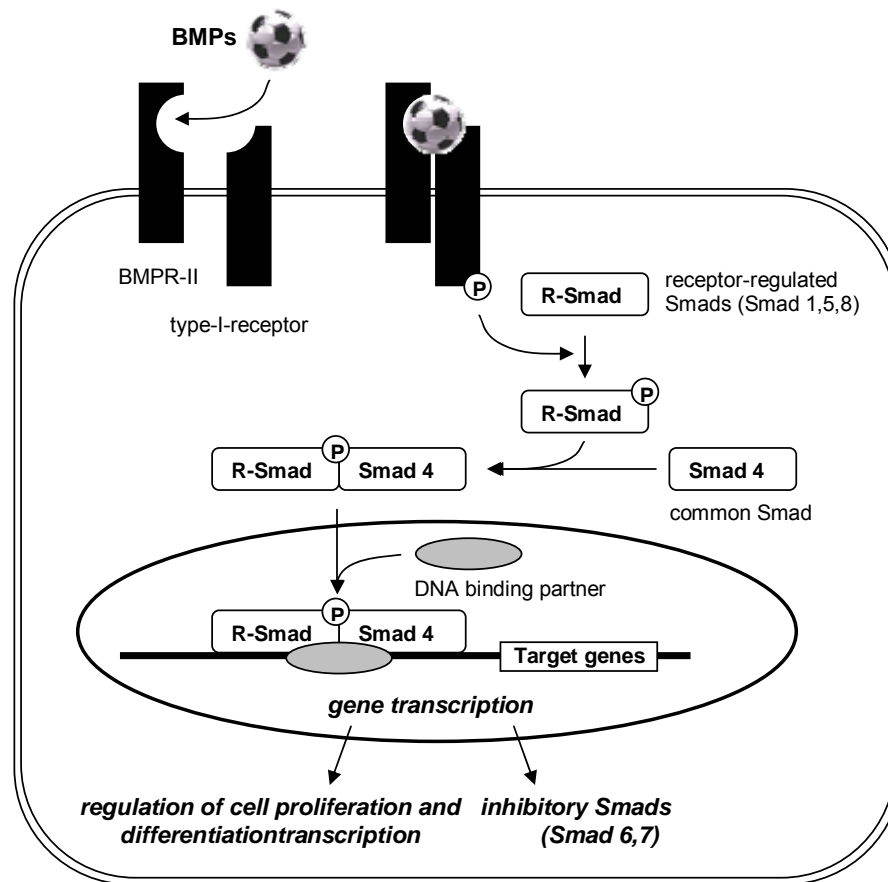
Figure 5. *BMP signalling pathway. Picture adopted from Strange JW. et al.[31]*

In pulmonary arterioles, the over-proliferation of smooth muscle cells is the characteristic of PPH, leading to progressive muscularization of normally non-muscular parts of the blood vessels, thereby allowing these newly musculated parts to vasoconstrict. This increased vasoconstriction finally leads to hypertension. It is not clear whether familial PAH is molecularly distinct from sporadic/idiopathic PAH. Sporadic cases of PAH are more common than familial cases, and their development can be associated with several things including: pregnancy, hypothyroidism, and the use of oral contraceptives, cocaine, or the appetite suppressant drugs, phentermine-fenfluramine (phen-fen) and monocrotaline extracts. People with autoimmune disease or late stage of HIV infection can also develop PAH.

1.2.3   Animal Models

Application of some toxins to the animal's lung causes inflammatory responses. In consequence of the cell injuries and the inflammatory processes, the animals develop acute or chronic PH. The best-characterized animal models for PH comprise rats treated with the alkaloid monocrotaline. Additionally, mice treated with pneumolysin, a pore-forming exotoxin of *Stretococcus pneumoniae*, developed PH as well. Further, chronic forms of PH can be induced by a low environmental oxygen tension.

1.2.3.1   Hypoxia-based Model

Exposure of mice to low levels of environmental oxygen results in alveolar hypoxia and reliably causes chronic pulmonary hypertension and morphological alterations of the precapillary pulmonary vessels. Chronic hypoxia can be induced by exposing cattles [32] or several mammalian species to normal air at hypobaric pressures or to oxygen-poor air (10 %) at normal pressure. Chronic hypoxic exposure of animals has been used for decades to induce pulmonary vascular remodelling.

1.2.3.2   Monocrotaline (MCT) Based Model

Monocrotaline is a pyrrolizidine alkaloid toxin from *Crotalaria spetabilis*.[33] It is hepatotoxic, pneumotoxic, and causes chronic pulmonary hypertension in humans and animals.[34] People are exposed to pyrrolizidine alkaloid as through consumption of herbal medicines made from pyrrolizidine alkaloid-containing plants or by ingesting food grains contaminated with seeds or other components of pyrrolizidine alkaloid-containing plants.[33]

MCT is bioactivated in the liver by cytochrome P_{450} monooxygenases to pyrrolic metabolites, which travel via the circulation to the lungs, where they cause injury by unknown mechanisms.[35] One putative metabolite of MCT is monocrotaline pyrrole (dehydromonocrotaline), a moderately reactive, bifunctional alkylating agent that produces sinusoidal endothelial cell injury, hemorrhage, fibrin deposition, and coagulative hepatic parenchymal cell oncosis in centrilobular regions of the liver.

In the rat model, systemically applied MCT induces endothelial inflammation with a structural remodelling of the lung arteries leading to pulmonary hypertension and similar histological changes like PAH in humans. The inflammatory mechanisms appear to play a significant role in some types of PH, including human types of PH.[36] The MCT rat model has become one of the most widely used animal models to study various aspects of PH.[33] Rats exposed to MCT develop an acute pulmonary vascular inflammatory reaction with subsequent remodelling including pulmonary artery smooth muscle hypertrophy, leading to a persistent severe pulmonary hypertension after 3 to 4 weeks.[37-39] This is a reproducible and well-established model of the disease which may be of value for investigating some aspects of this condition.[40] For instance, pulmonary vascular inflammation seems to play a key role in subjects developing pulmonary arterial hypertension in the context of toxic oil syndrome, autoimmune diseases, or infectious conditions.[41] Pulmonary vascular inflammation may also play a key role in a subset of patients with idiopathic pulmonary hypertension. However, the development of the medial hypertrophy revealed that it is preceded by intense metabolic activity and proliferation of the pulmonary endothelial cell layer.[41]

In the normal pulmonary circulation, a balance favouring vasodilation and inhibiting proliferation is maintained between the vasodilators like prostacyclin and nitric oxide on the one hand, and potent pulmonary vasoconstrictors like endothelin I on the other hand. In PAH, imbalances of vasodilator and vasoconstrictor agents have been implicated in both the predominance of increased vasomotor tone and the chronic remodelling of resistance vessels, including vascular smooth muscle cell growth. The balance is tilted toward the production of endothelin-I and an enhanced excretion of thromboxane metabolites has been noted.[42] Additionally, a reduced excretion of prostaglandin can be detected in the circulating blood. Moreover, enhanced activities of phosphodiesterases (PDEs), which hydrolyze the prostaglandin- and NO-induced second messengers, cAMP and cGMP, were observed in experimental conditions of pulmonary hypertension.[43]

Among the large variety of cellular functions that are orchestrated by the cAMP-dependent protein kinase A cascade, the anti-inflammatory effects caused by increased cAMP levels have attracted considerable interest both in immunological and pharmacological research. Intracellular cAMP concentrations increase as a

11

consequence of receptor-triggered adenylyl cyclase activation or by decreased activity of phosphodiesterases, which regulate the hydrolysis of cAMP and cGMP (figure 6).
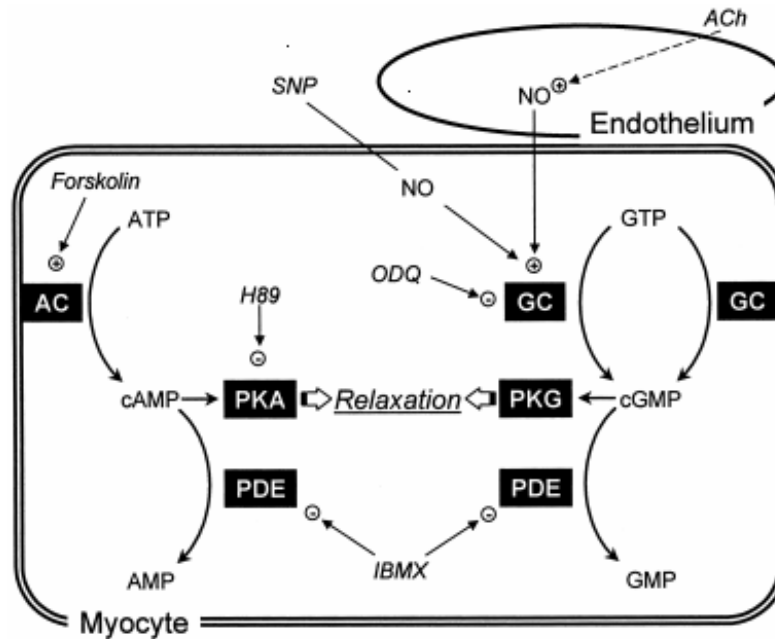
Figure 6. *Cyclic nucleotides as second messengers in the regulation of the vascular tone. cAMP is an important second messenger regulating diverse function such as cell shape, protein phosphorylation, gene transcription, etc. As much as 10 subtypes of adenylyl cyclase are capable of converting ATP to cAMP. Hydrolysis of cAMP is mediated through a class of enzymes known as PDEs. These enzymes can be classified according to their specificity for cAMP and cGMP. There exist PDEs that only hydrolyze cAMP or cGMP, as well other subtypes that hydrolyze both cyclic nucleotide and therefore limit their action. + = Stimulation; – = inhibition (Picture adopted from Uder, M. et al.).* [44]

The family of mammalian phosphodiesterases consists of at least 11 isoenzymes. Some PDEs (PDE3, PDE4 and PDE5) seem to play a role in smooth muscle relaxation.[45] In inflammatory cells, including mast cells, eosinophils, macrophages, T-lymphocytes and structural cells, PDE3, 4, and 5 are predominant.[46] Due to higher PDE3 and PDE4 concentrations in the cells, PDE3/4 inhibitors that had been proven safe were targeted as possible options for PH and asthma treatment. When PDEs are inhibited, the cellular level of cAMP increases, resulting in smooth muscle relaxation and potentiation of the bronchodilator effect of agonists. Tolafentrine, which is a

synthetic PDE 3/4 inhibitor, possesses a strong antiproliferative effects in the pulmonary circulation[47]. The reduction in the number of peripheral arteries in MCT-treated animals reflects endothelial injury and occlusion of peripheral vessels. Tolafentrine reduces the wall thickening and remodelling of intrapulmonal arteries. Moreover, a significant increase in vascularization by tolafentrine may result from vascular endothelial growth factor, which is known to be induced by cAMP-increasing agents.[48]

1.2.3.3 Pneumolysin (PLY) Model

Streptococcus pneumoniae, a gram-positive bacterium, is the most prevalent pathogen involved in community-acquired pneumonia[49], septic meningitis[50], and otitis media.[51] In the pre-antibiotic era streptococcal pneumonia or pneumococcal pneumonia had a high fatality rate, being a frequent cause of death in the elderly.

Invasive pneumococcal disease appears to depend on both pneumococcal cell wall components including peptidoglycan and lipoteichoic acid, as well as a multitude of virulence factors.[52-53] A number of pneumococcal proteins have been characterized as putative virulence factors, among them pneumolysin (PLY), the neuraminidases A and B, and hyaluronidase[54] that appear to be involved in the pathogenesis of meningitis and other related diseases. Pneumolysin is involved in inflammatory processes, activating neutrophils/macrophages and the complement system.[55] This effect may participate in the pathogenesis of septic organ failure and the host response may critically depend on the compartmentalization and amount of toxin release.

PLY is a cytoplasmic 53-kDa protein that belongs to a group of thiol-activated cholesterol-dependent cytolysins and interacts with its cholesterol receptor on target cells, leading to pneumolysin insertion into target-cell membranes and subsequently to pore formation and cell lyses.[56] PLY differs from others in this family because it lacks the N-terminal signal sequence that would facilitate its transport out of the cytoplasm. Instead, it is thought that the toxin is released from the pneumococcal cytoplasm via the enzyme autolysin LytA, which induces cell wall degradation and the release of cytoplasmic contents. The crystal structure of one member of the family, perfringolysin

has been solved by X-ray crystallography, by the group of Mike Parker in Melbourne (figure 7).
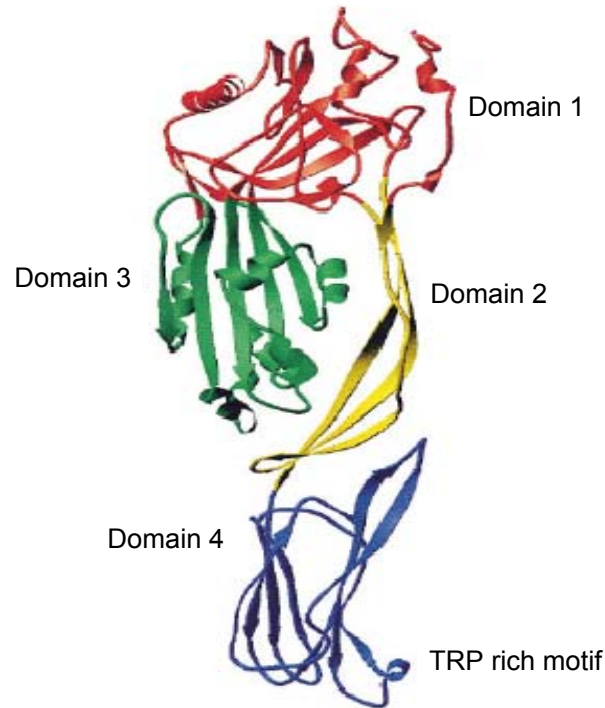
Figure 7. Protein Structure of Perfringolysin. It contains of 4 distinct domains indicated by different colors. These domains involved for cell binding, oligomerization, and pore formation processes. (Picture taken from Jamie Rossjohn et al.). [57]

By pore-formation PLY has the capacity to damage the extracellular matrix or the plasma membrane of eukaryotic cells. The damage not only may result in the direct lysis of cells but also can facilitate bacterial spread through tissues. Toxins that mediate this cellular damage do so by either enzymatic hydrolysis or pore formation. The concept of membrane damage as an effector mechanism of bacterial exotoxins arose during the 1970s through the work on α-toxin by Freer *et al*. 1968 and, subsequently, Thelestam and Molby (1975). These studies generated the idea that staphylococcal α-toxin produced permeability defect in membranes. The α-toxin is cytolytic to a variety of cell types, including human monocytes, lymphocytes, erythrocytes, platelets, and endothelial cells.[58]

The molecular mechanism of the damage of cellular membranes by the α-toxin comprises several sequential events (figure 8). When *S. pneumoniae* cells burst, pneumolysin is released and binds to cholesterol in cell membranes by either unidentified high-affinity receptors or through nonspecific absorption to substances such as phosphotidylcholine or cholesterol on the lipid bilayer.[58] Second, membrane-bound protomers oligomerize and form arc and ring structures (pores). Third, the heptamer undergoes a series of conformational changes that create the stem domain of the toxin, which is then inserted into the membrane.

The α-toxin pore allows the influx and efflux of small molecules and ions that eventually lead to swelling and death of nucleated cells. Moreover, pore formation has also been shown to trigger secondary events include endonuclease activation, increased platelet exocytosis, release of cytokines and inflammatory mediators, and production of eicosanoids.[58]
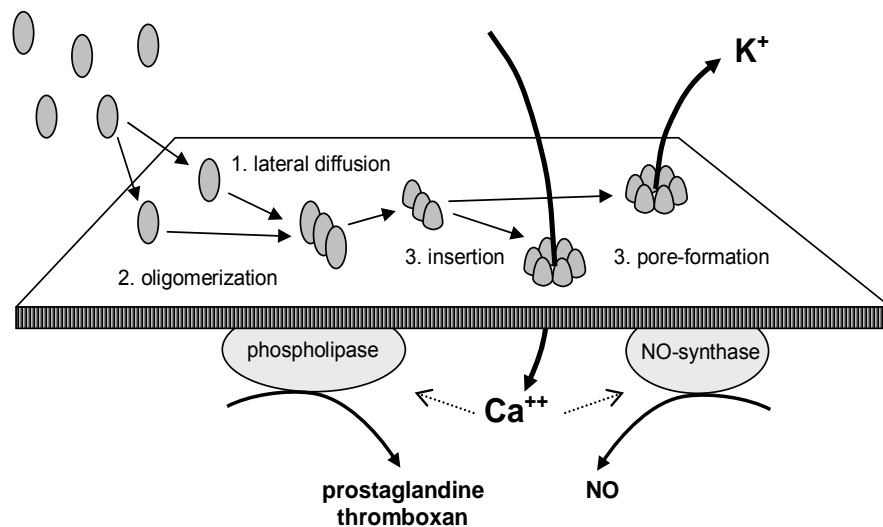
Figure 8. Schematic of the mechanism of pore formation by pneumolysin. The toxin is secreted as a monomer (left) and incorporated in the cell membrane of its target cells. The transmembrane pores are formed in the membrane after ologomerization. The pores are permissible for different ions. The pore-induced ion fluxes activate target cells most likely by an increased intracellular Ca^{++} concentration, stimulating for example the production of nitric oxide or leukotrienes.

2   Aim of this Work

This thesis consists of two parts.

The first part focuses on establishing a reliable platform for microarray experiments. It shows the comparison of different protocols for sample preparation, sample labelling and competitive hybridization on cDNA- and oligonucleotide-spotted microarrays. Various methods and important parameters are optimized, in particular RNA extraction, RNA preamplification, direct and indirect labelling, and slide processing (preprocessing, hybridization, and washing). Particular importance is addressed to the comparison of different preamplification protocols that allow the use of trace amounts of sample material for microarray analyses.

The second part shows the application of different array technologies for gene expression profiling to two important models of pulmonary hypertension. Affymetrix GeneChips™ are utilized to reveal characteristic changes in gene expression patterns of pneumolysin-induced pulmonary hypertension in mice, whereas cDNA-macroarrays and oligonucleotide-spotted microarrays were used to study the gene expression in monocrotaline-induced and tolafentrine-attenuted pulmonary hypertension in rats.

3   Materials

3.1   Animals

Male Sprague-Dawley rats (Charles River, Sulzfeld, Germany)

Female BALB/c mice (Charles River, Sulzfeld, Germany)

3.2   DNA Microarrays

Expression arrays were used for expression profiling of rat and mouse samples. The arrays were spotted with either cDNAs ("cDNA") or with gene-specific oligodeoxynucleotides ("oligo").

Table 1. Expression arrays.

Organism	Matrix	Probes	Number of Spots	Name	Supplier
rattus norwegicus	nylon	cDNA	1176	Atlas Rat 1.2	BD Siosciences, Heidelberg, Germany
mus musculus	glass	cDNA	20000 2 x spotted	Mouse 20K, Lion	DKFZ, Heidelberg, Germany
mus musculus	glass	oligo (50mer)	10000	Mouse 10K	MWG-Biotech, Ebersberg, Germany
mus musculus	glass	oligo (60mer)	22000	Mouse 22K	Agilent Technologies, Waldbronn, Germany
mus musculus	glass	oligo (25mer)	36000	MG U74A09	Affymetrix, Santa Clara, CA, USA

3.3 Instruments

Table 2. Instruments.

Instrument	Supplier
GeneTAC Hybridization station	PerkinElmer, Applied Biosystems, Foster City, USA
GenePix 4100A scanner	Axon Instruments, Union City, CA, USA
Bioanalyzer 2100	Agilent Technologies, Waldbronn, Germany
ND-1000 UV spectrophotometer	NanoDrop, Montchanin, USA
ABI 7700 Sequence Detector	PerkinElmer, Applied Biosystems, Foster City, USA
Icycler	Bio-Rad, Munich, Germany
Touch Down hot Lid PCR cyler	Hybaid, Heidelberg, Germany
TRIO Thermoblock	Biometra, Göttingen, Germany
Liquid scintillization counter	Hidex, Turku, Finnland
Typhoon phsphoimager system	Amersham Biosciences, Freiburg, Germany

3.4 Chemicals and Biochemicals

Table 3. Chemicals and Biochemicals.

Chemical	Supplier
PeqGOLD^{TM} TriFast solution	peqlab, Erlangen, Germany
GiTC (4M 25mM Na-3-citrate: 0.5% laurylsarcosin, 100mM Tris/Hcl)	Sigma, Taufkirchen, Germany
β-mercaptoethanol (98%)	Sigma, Taufkirchen, Germany
Phenol saturated with 0.1 M citrate Buffer, pH 4.3 +/- 0.2	Sigma, Taufkirchen, Germany
$CHCl_3$ (99%)	Sigma, Taufkirchen, Germany
C_3H_8O(99%)	Sigma, Taufkirchen, Germany
NaOAc (2M, pH 4.5)	Sigma, Taufkirchen, Germany
100% ethanol	Sigma, Taufkirchen, Germany
NaOH (1M)	Merck,Darmstadt, Germany
HCl (1M)	Merck,Darmstadt, Germany
TE (pH 7.5)	Sigma, Taufkirchen, Germany

MCT (20 mg/ml)	Sigma, Deishofen, Germany
100% ethanol	Merk, Darmstadt, Germany
Agrose (Topvision^{TM})	MBI Fermentas, Walldorf Baden, Germany
Ethidium Bromide (10 mg/ml)	Carl Roth, Karlsruhe, Germany
dATP, dCTP, dGTP and dTTP, (100 mM)	Amersham Biosciences, Freiburg, Germany
Cy5 dCTP (1mM)	Amersham Biosciences, Freiburg, Germany
Cy3 dCTP (1mM)	Amersham Biosciences, Freiburg, Germany
Cy3 monofunctional reactive dye	Amersham Biosciences, Freiburg, Germany
Cy5 monofunctional reactive dye	Amersham Biosciences, Freiburg, Germany
Cy3 UTP (1mM)	PerkinElmer, Boston, USA
Cy5 UTP (1mM)	PerkinElmer, Boston, USA
Biotin-11 CTP	PerkinElmer, Boston, USA
Biotin-16 UTP	PerkinElmer, Boston, USA
MgCl$_2$ (25 mmol/L)	PerkinElmer, Weiterstadt, Germany
10X PCR buffer	PerkinElmer, Weiterstadt, Germany
Salmon Sperm DNA	Sigma, Taufkirchen, Germany
Bovine Serum Albumin (50 mg/ml)	Invitrogen, Karlsruhe, Germany
ULTRAhyb^{TM} buffer	Ambion, Dresden, Germany
SDS 99%	Sigma
NaCl	Sigma
EDTA	Sigma
Boric acid	Merk
α-^{32}P-dATP	Amersham Biosciences, Freiburg, Germany

3.5   Buffers and Solutions

<u>1 M Tris-HCl stock</u>

Tris or TRIZMA base - 60.55 g

Milli-Q water - 400 ml

The pH was adjusted with conc. HCl to 7.5.

Volume was adjusted to 500 ml with Milli-Q water.

<u>0.5 M EDTA stock</u>

EDTA - 93.05 g

Milli-Q water - 400 ml

The pH was adjusted with NaOH pellets to 7.5.

Volume was adjusted to 500 ml with Milli-Q water.

<u>1 M Sodium citrate stock</u>

Sodium citrate - 29.4 g

Volume was adjusted to 100 ml with Milli-Q water.

<u>4M GTC</u>

GTC - 47.3 g

25 mM Sodium citrate - 2.5 ml from 1 M stock

0.5% N-lauroyl sarcosine - 0.5 g

100 mM Tris - 1.21 g

Volume was adjusted to 100 ml with RNase-free water.

<u>2M NaOAc</u>

Sodium acetate - 54.4 g

Volume was adjusted to 100 ml with Milli-Q water.

The pH was adjusted with 100% acetic acid (Merk) to 4.5.

<u>TE</u> (10 mM Tris, 1.0 mM EDTA, pH7.5)

Tris- stock (1M, pH 7.5) - 1 ml

EDTA-stock (0.5M, pH 7.5) - 200 µl

Volume was adjusted to 100 ml with Milli-Q water.

<u>Saline citrate buffer (SSC)</u> 20X

NaCl - 175 g

Sodium citrate - 88 g

Milli-Q water - 900 ml

pH was adjusted to 7.0 with HCl and volume was and adjusted to 1 liter.

<u>10% SDS</u>

SDS – 10 g

Volume was adjusted to 100 ml with distilled water.

3.6 Oligodeoxynucleotides

Random hexamers (50µM) were obtained from Applied Biosystems, Darmstadt, Germany, Oligo-dT primer (12-18 nt, 0.5µg/µl) were bought from Eurogentec, Searing, Belgium. Primers were ordered from MWG, Ebersberg, Germany.

Table 4. *Primers.*

Targe gene [1]	Genbank Accs.No.	Sequence 5'→3'	Length (nt)	Amplicon Length (bp)
mGAPDH-FP	NM_001001303	GTGATGGGTGTGAACCACGAG	21	121
mGAPDH-RP		CCAACAATGCCAAAGTTGTCA	21	
mGAPDH-TM-Probe		**GTGCAGGATGCATTGCTGACAATCTTGA**	28	
rPBGD-FP	BC088162	ATGTCCGGTAACGGCGGC	18	139
rPBGD-RP		GGTACAAGGTTTTCAGCATTCG	22	
rPBGD-TM-Probe		**CCAGCTGACTCTTCCGGGTGC CCAC**	25	
mGAPDH-e-3'UTR-FP	NM_001001303	ACAGGGTGGTGGACCTCATG	20	102
mGAPDH -e-3'UTR-RP		GTTGGGATAGGGCCTCTCTTG	21	

[1] the first letter indicates the organism: r = rattus norwegicus, and m = mus musculus.

3.7 Enzymes

Table 5. *Enzymes.*

Chemical	Supplier
CyScribe reverse transcriptase (100U/µl)	Amersham Biosciences, Freiburg, Germany
DNase Set (50) (1500U)	Qiagen, Hilden, Germany
DNA polymerase I (10U/µl)	Invitrogen, Karlsruhe, Germany
RNase Inhibitor (20 U/µl)	Applied Biosystems, Darmstadt, Germany
MuLV Reverse Transcriptase 50 U/µl	Applied Biosystems, Darmstadt, Germany

M-MLV Reverse Transcriptase, RNase H Minus, Point Mutant (200 U/µl)	Promega, Madison, USA
SuperScript™ II RNase H ⁻Reverse Transcriptase, 200U/µl, first and second strand buffers	Invitrogen, Karlsruhe, Germany
RNAseout, 40 U/µl	Invitrogen, Karlsruhe, Germany
E.coli DNA ligase, 10 U/µl	Invitrogen, Karlsruhe, Germany
E.coli DNA Polymerase I, 10 U/µl	Invitrogen, Karlsruhe, Germany
RNAse H, 2 U/µl	Invitrogen, Karlsruhe, Germany
Proteinase K, 10 mg/ml	Sigma-Aldrich, Taufkirchen, Germany
T4-DNA Polymerase, 5 U/µl	Invitrogen, Karlsruhe, Germany
RNAse, DNAse free, 20 mg/ml	Invitrogen, Karlsruhe, Germany
Klenow Polymerase, 2 U/µl	Roche diagonstics, Mannheim, Germany
Taq DNA-Polymerase, 5 U/µl	Applied Biosystems, Brunnenweg, Germany

3.8   Kits

Table 6. *Kits.*

Chemical	Supplier
RNeasy Mini	Qiagen, Hilden, Germany
Oligotex mRNA Mini	Qiagen, Hilden, Germany
SMART Fluorescent Probe Amplification	BD Biosciences, Heidelberg, Germany
RiboAmp® RNA Amplification	Arcturus, Mörfelden-Walldorf, Germany
RiboMax T7	Promega, Mannheim, Germany
CyScribe First Strand cDNA Labelling	Amersham Biosciences, Freiburg, Germany
Fluoroscript labelling	Invitrogen, Karlsruhe, Germany
Ominiscript® RT	Qiagen, Hilden, Germany
Microcon columns YM-30 and YM-50	Millipore, Schwalbach, Germany
QIAquick PCR Purification	Qiagen, Hilden, Germany
RNA 6000 Nano Chips	Agilent Technologies, Waldbronn, Germany
qPCR^{TM} Mastermix	Eurogentec, Seraing, Belgium
qPCR^{TM} Mastermix for SYBR® Green I	Eurogentec, Seraing, Belgium
Atlas^{TM} Nylon rat 1.2	Clontech: BD Biosciences, Heidelberg, Germany

3.9 Fragment Length Standards

RNA 6000 Ladder (0.2, 0.5, 1.0, 2.0, 4.0 and 6.0 kb) (Agilent Technologies, Waldbronn, Germany)

4 Methods

4.1 Preparation of Total RNA

The quality of RNA has a strong impact on the validity and reliability of the microarray experiment. Thus, it is essential to take all reasonable precautions and quality checks when preparing the samples for microarray experiments. Apart from the classical methods for RNA extraction, many commercial kits are available.

4.1.1 RNA Extraction with GTC-Phenol-Chloroform

Total cellular RNA was isolated from 50 mg homogenized lung tissue following the protocol of Chomczynski *et al.*[59] Guanidine isothiocyanate (GTC)/phenol/chloroform based RNA extraction methods are very popular because they require much less time than traditional methods (e.g., $CsCl_2$ ultracentrifugation). The GTC salt denatures the cellular proteins and inactivates RNases to ensure isolation of intact RNA.

The lung tissue was fixed on the Tissue-Tek® and then 10 μm thin sections were cut in a tissue cryostat. The sections were collected in 1.5 ml Eppendorf tubes and homogenized by disrupting in 1000 μl of 4 M GTC buffer using a disposable syringe and 20 G sterilized needles. The Phase Lock Gel tubes (Heavy type, 15 ml, Eppendorf) were pre-spun for 2 min at 5,300xg. Afterwards, lysed material, 700 μl phenol pH 4.5, 200 μl chloroform and 100 μl 2M NaOAc were added and vortexed. The mixture was centrifuged at 5,300xg for 20 min at 4°C. Upper phase was removed carefully and collected into fresh 1.5 ml Eppendorf tubes. For the RNA precipitation, 600 μl of cold isopropanol was added to the supernatant and incubated for 2 hours at -20°C. Samples were centrifuged at 14,000xg for 15 min at 4°C. The pellets were washed with 75 % cold ethanol and air-dried. Finally, RNA was dissolved in 20 μl RNase free water.

4.1.2   RNA Extraction by TriFast™ / DNase Digestion / RNeasy

Fifty mg tissue were sliced as mentioned 4.1.1 and was lysed in 1000 μl TriFast™ for 10 min at room temperature. The lysed mixture was centrifuged for 5 min at 10,000xg, the upper phase was transferred into a new 1.5 ml Eppendorf tube. 200 μl chloroform were added, vortexed and incubated for 10 min on ice. After this, the samples were centrifuged for 15 sec at 16,000xg at 4°C. The upper phases were transferred carefully into fresh 1.5 ml Eppendorf tubes and mixed with the same volume of 75% chilled ethanol. Subsequent DNAse digestion and RNA purification was done using an RNeasy Miniprep column according to the manufactures instructions.

4.1.3   RNA Extraction with the RNeasy Kit

The basic principle of the RNeasy column technology is a combination of the selective binding properties of a silica gel-based membrane with the speed of microspin technology. 30 mg of lung tissue from the mice were used for the extraction. RNA was isolated and purified as per the instruction given for the Qiagen RNeasy Miniprep kit.

4.1.4   Quality and Quantity Measurement

RNA quality was analysed by microcapillary electrophoresis on Agilent LabChip®. For the Agilent LabChip analysis, 1μl of total RNA solution was loaded on RNA 6000 Nano Chip® and by following the steps given in the Agilent manual. The electropherograms of high-quality RNA show clear peaks for the 18S and 28S ribosomal RNAs. The electropherograms were checked for the absence of high-molecular nucleic acids that indicate contaminations with DNA.

The total RNA quantification and purity was determined with a NanoDrop ND-1000 spectrophotometer. The quantity of the isolated RNA was calculated from the absorbance at 260 nm and the purity was determined by the ratio OD_{260}/OD_{280}. Purity was considered good when the ratio was greater than 1.8. Low absorbance at 230 nm indicates the absence of salt.

4.2   Preparation of mRNA

The preparation of mRNA was performed using the oligotex mRNA extraction kit. 25 µg total RNA were introduced to the mRNA extraction. Messenger RNA was purified as per the instruction given on mRNA mini kit from Qiagen.

4.3   RNA Amplification

Experiments involving glass microarrays typically require at least 20 µg of total RNA for cDNA labelling and subsequent hybridization. However, such amounts of RNA are not available from small precious samples obtained from laser microdissections or needle biopsies. However, small amounts of RNA can be preamplified to produce sufficient material for microarray experiments. The commonly applied preamplification techniques are:

      (a) T7-IVT (1-2 rounds) linear amplification [60-61] and

      (b) PCR-based exponential amplification [62-63]

4.3.1   T7-Based RNA Preamplification (T7-IVT)

In 1990, van Gelder *et al.* described a protocol for linear RNA amplification from limited quantities of cDNA. Based on *In-vitro* transcription using T7-RNA polymerase, they were able to amplify RNA from heterogeneous populations by a factor of 10^3. Using this approach and by performing two rounds of linear RNA amplification, Eberwine *et al.* were able to profile the gene expression in single live neurons. [64]

Recently, a linear RNA amplification kit was developed (RiboAmp®, Arcturus) to amplify RNA from very small amounts of material. Using 2-3 µg RNA, one round of T7-IVT is argued to allow for a 1,000-fold amplification of mRNA, while two rounds shall permit a million-fold amplification of the mRNA.

The amplification workflow is shown in figure 9. The procedure consists of reverse transcription with an oligo-dT primer linked to a T7-promoter sequence. Afterwards,

double stranded DNA is synthesized. Finally this DNA is then used as a template for the *In-vitro* transcription by T7 RNA polymerase. By providing labelled ribonucleotides in the reaction mixture, labelled aRNA is produced that can be used directly in subsequent hybridizations.
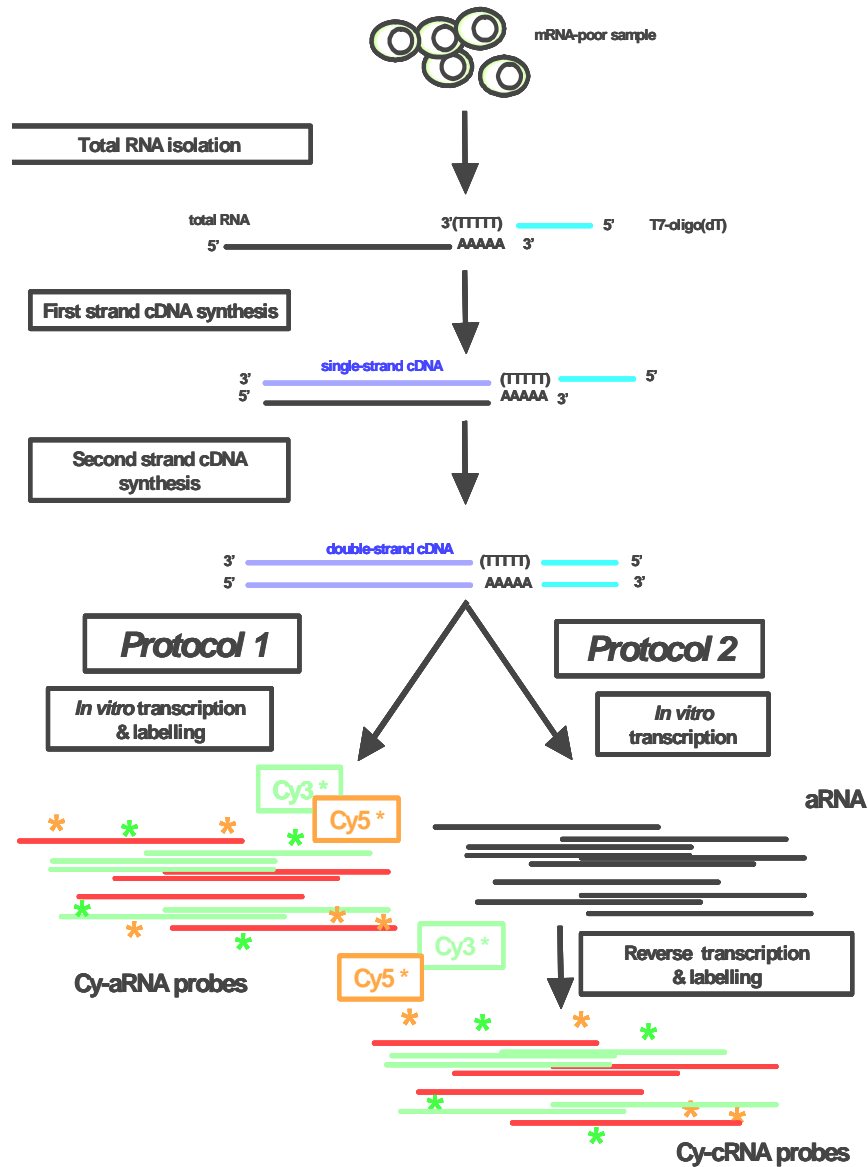
Figure 9. *Flow chart for the amplification and direct labelling method following the Acturus protocol (Picture adopted from http://arrays image. free.fr/The%20aRNA%20amplification.htm).*

Starting with 50 ng total RNA from mice kidney, two rounds of T7-based RNA amplification were performed in triplicate using the Acturus kit. After the first strand cDNA synthesis, 6 µl of each reaction were taken off to serve as unamplified reference sample for the subsequent real-time PCR analyses. After preamplification, 4 µl aRNA each were reverse transcribed in 20 µl reactions. Each 6 µl cDNA were then used for real-time PCR analysis to compare unamplified and amplified material to calculate the amplification factors for specific target sequences.

4.3.2   SMART™ based RNA Preamplification

Alternatively, SMART™ (switching mechanism at the 5' end of the RNA transcript) based RNA amplification is a PCR-based method suggested for producing high quality cDNA from nanogram quantities total RNA.[65] The procedure is shown in figure 10. The amplification method consists of reverse transcription with a modified oligo-dT primer (SMART™ CDS Primer IIA) to initiate the first strand synthesis reaction. When reverse transcriptase reaches the 5' end of the RNA, the enzyme's terminal transferase activity adds a few additional nucleotides, primarily deoxycytidine, to the 3' end of the cDNA. The next primer, SMART™ II, is an oligonucleotide with an oligo-dG sequence at its 3' end to hybridize to the deoxycytidine stretch, creating an extended template for the reverse transcription. The reverse transcriptase then switches templates and continues replicating to the end of the oligonucleotide. The full-length single stranded cDNA contains sequences that are complementary to the BD SMART II A oligonucleotide. The BD SMART anchor sequences are then used as universal priming sites for full-length cDNA amplification.
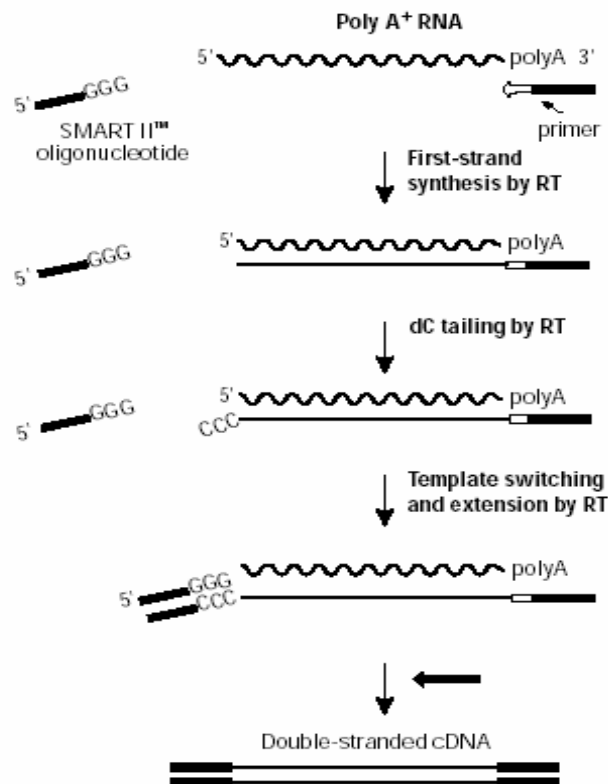
Figure 10. *Flow chart shows the cDNA synthesis and amplification method (BD Atlas SMART™ fluorescent Probe Amplification Kit).*

For comparison of T7 and SMART™ based pre-amplification, SMART™ amplification was performed six times starting with 50 ng total RNA from mice kidney and liver. The preamplification was carried out using the SMART kit (Clontech) following the kit instructions. After the first strand synthesis, 6 µl of cDNA were taken off from each reaction to serve as the unamplified reference sample in the subsequent real-time PCR. Finally, dscDNA was purified with the QIAquick PCR Purification Kit. Each 6 µl dscDNA were then used for real-time PCR analysis to compare unamplified and amplified material to calculate the amplification factor.

4.4　cDNA Synthesis by Reverse Transcription

cDNA synthesis was performed using 1-2 µg RNA. The RNA was redissolved in RNase free water to a volume of 10.5 µl. Samples were incubated for 10 min at 70°C for RNA denaturing and then rapidly cooled on ice. For cDNA synthesis, a mastermix was prepared using 4 µl MgCl$_2$ (25 mmol/L), 2 µl 10X PCR buffer II, 1 µl dNTP (10 mmol/L each), 1 µl random hexamers (50 µmol/L), 0.5 µl RNase inhibitor (10 U), and 1 µl of MuLV (50 U). For the first-strand sythesis, the reactions were incubated for 10 min at 20°C, 60 min at 43°C, and 5 min at 95°C.

4.5　Real-time Quantitative PCR

Real-time quantitative PCR for PBGD and GAPDH were performed using the ABI 7700 sequence detection system. Each 50 µl-reaction contained 25 µl (2x) TaqMan Universal Master Mix supplemented by 4.5 µl forward and reverse primers (10 pmol/µl), 1 µl dual-labelled fluorogenic probe (10 pmol/µl), 2 µl cDNA sample and 13 µl water. The cycling protocol was:

1x	50°C, 2 min
1x	95°C, 6 min
45x	95°C, 20 sec
	60°C, 30 sec
	73°C, 30 sec

Whereas for the 3' UTR-GAPDH, real-time PCR was performed using SYBR® Green I. Each 50 µl-reaction contained 25 µl (2X) PCR reaction buffer, 1 µl forward and reverse primers (200 nM), 1.5 µl of SYBR® green, 2 µl cDNA sample and 19.5 µl water.

The cycling protocol was:

1X	95°C, 6 min
45X	95°C, 20 sec
	60°C, 30 sec

72°C, 30 sec with hold 60

95°C, 0.15 sec

40°C, 1 min

The data was acquired after the extension phase at 73°C. Amplification curves were evaluated using the instrument's software (SDS version 1.7) according to the analysis standards given in the manual. The crossing point data (Ct values) were exported to spread sheet software (Excel) for further analysis.

The relative concentration of the target sequence in relation to the reference was expressed as $2^{\Delta Ct}$ where ΔCt is the difference between the Ct values of the samples being compared.[66]

4.6 DNA-Arrays

4.6.1 Nylon Membranes

4.6.1.1 Labelling: Generation of Radioactive Labelled cDNA

6 µg total RNA were reverse transcribed by adding 1.2 µl CDS primer (Atlas™ Nylon arrays rat 1.2) and incubation for 5 min at 70°C. Reactions were then incubated for 10 min at room temperature. The master mix supplied with the Atlas™ Nylon arrays rat 1.2 kit for four samples were prepared by adding following ingredients: 20 µl 5X buffer, 4.5 µl dNTP, 14 µl α-^{32}P-dATP, 2.0 µl DTT (0.5 M) and 4.0 µl M-MLV reverse transcriptase. 11 µl master mix were distributed to each sample. Afterwards, the reaction mix was incubated for 1 hr at 42°C. The reaction was terminated by heating to 70°C for 15 min. Radioactively labelled cDNAs were purified and eluted in 100 µl of elution buffer (supplied with Atlas™ Nylon arrays rat 1.2 kit). The activity was measured with a liquid scintillization counter (Hidex).

4.6.1.2 Hybridization

The purified α-^{32}P-labelled cDNA in elution buffer were hybridized on Rat 1.2 Atlas™ cDNA arrays nylon filters with 1,176 spotted cDNAs. Hybridization was carried out at 68°C overnight. The filters were washed according to the manual.

4.6.1.3 Scanning

Filters were wrapped in plastic and exposed for 4-7 days to imaging plates (Fuji Photo Film) in a lead sheathing. The film was read out with a phosphoimager system.

4.6.1.4 Analysis

Raw data were collected using the AtlasImage™ 2.0 software. Values of spot intensities were adjusted by a global normalization using the sum method provided by the software. The mean global background was subtracted from the spot intensities.

The $\log_2$-intensity values were normalized for each membrane by a Z-transformation. The normalized log-values were transformed back into intensity values ("Z"). Using the pair of Z values for the two spots on corresponding membranes, the value for the adjusted difference of the intensities is calculated by $D=(Z_2-Z_1) / \max (Z_1,Z_2)$, where $\max (Z_1,Z_2)$ is the greater one of the values Z_1 and Z_2. The codomain for the adjusted difference is limited in the range of -1 to $+1$. The Z values are not defined for background-corrected intensities smaller or equal to zero. It exist defined limiting values (i.e., the limits of the codomain) for the adjusted difference for the case that only one of the Z values is not defined, assuming a limiting intensity values of zero. Only when both of the intensity values are zero, the adjusted difference cannot be calculated. Genes were considered to be differentially expressed when both of the following criteria were fulfilled:

> $p \leq 0.10$ of a one sample t-test with H_o: D=0 and H1: D $\neq$ 0 and
> $|D| \geq 0.30$ (corresponding to a fold-change of ≥ 1.4)

4.6.2 Glass Microarrays

4.6.2.1 Labelling: Generation of CyDye-Labelled cDNA by RT

The following protocols describe RNA labelling with Cy3 and Cy5 dyes using four different reverse transcriptase enzymes, see table 7 a while table 7 b show steps for direct labelling using Klenow DNA polymerase.

Table 7. (a) *Pipetting plan for target labelling during RT.*

	Amersham CyScribe	Invitrogen Fluoroscript	Qiagen Ominiscript	Invitrogen Superscript II
RNA (25µg)	10	4	12	17
Oligo dT (µl)	1	1	0.5	1.5
Volume (µl)	11	5	12.5	18.5
Step 1	70°C, 5' RT, 10'	70°C, Ice, 10'	-	65°C, 10' RT, 10'
5X Buffer (µl)	4	4	-	8
10X Buffer	-	-	2	-
0.1M DTT (µl)	2	2	-	4
dCTP nucleotide Mix	1	-	-	-
dNTP (5mM dATP, dGTP, dTTP, 2 mM dCTP) (µl)	-	1	0.4	4
1 mM Cy3/Cy5 dCTP	1	2	2	4
RNAse-inhibitor (40U/µl)	-		1.0	-
Enzyme	1	1	1.5	1.5
Water	-	5	0.6	-
Total Volume (µl)	20	20	20	40
Step 2	42°C, 90'	50°C, 60'	37°C, 90' 95°C, 10'	39°C, 120'
200mM EDTA (µl)	-	2	-	-
2.5 M NaOH (µl)	2	-	-	-
1M NaOH (µl)	-	2[1]	-	10[2]
2M HEPES (µl)	10[3]	-	-	-

	Amersham CyScribe	Invitrogen Fluoroscript	Qiagen Ominiscript	Invitrogen Superscript II
TE (pH 7.5)	-	1	-	200
1M HCL	-	2	-	10
1MTris/HCL pH 5 (µl)	-	1	-	-

[1] following incubation for 10' at 70°C

[2] following incubation for 10' at 65°C

[3] following incubation for 5' at 37°C

(b) *Direct labelling with Klenow DNA polymerase.*

dscDNA (2µg) (µl)	10
Random hexamer @ 5mg/ml (µl)	2
Mili Q water (µl)	8
Tolal volume (µl)	20
Step 1	95°C, 5'; ice, 5'
10X Klenow buffer	4
dNTP mix (5mM dATP, dGTP, dTTP, 2 mM dCTP) (µl)	5
1mM Cy3 or Cy5-dCTP (µl)	2
Klenow polymerase (µl)	1.5
Mili Q water (µl)	7.5
Adjusted total volume (µl)	20
Step 2	37°C, 2 hrs
0.5 M EDTA (µl)	5

After the labelling reaction, labelled cDNA was purified with the PCR Purification Kit according to the kit protocol.

4.6.2.2 Labelling: Generation of CyDye-Labelled aRNA by T7-IVT

Each two samples of 50 ng total RNA from mice kidney and liver were amplified by T7-IVT as described in section 4.3.1. aRNA from kidney and liver (n=2) were labelled with Cy5 and Cy3 dyes as follows: 4 µl IVT buffer, 6 µl IVT master mix, 2 µl IVT enzyme, and 1.2 µl Cy5/Cy3-UTP (0.50 mM) mix were added during the 2nd round IVT process

in a total reaction volume of 24 µl. The amplification and labelling reaction together were incubated for 4 h at 42°C. Finally, the labelled aRNA was purified in 30 µl using the columns provided with the kit.

4.6.2.3 Labelling: Generation of CyDye-Labelled dscDNA by SMART™

Each two samples of 50 ng total RNA from mice kidney and liver (n=2) were introduced to SMART™ based amplification with 15 cycles as described in section 4.3.2. The samples (dscDNA) were finally purified with the QIAquick PCR Purification Kit. The purified dscDNA was labelled following the kit protocol. Briefly, this indirect labelling procedure is performed in two steps:

The first step produces aminoallylated DNA: 500 ng dscDNA were diluted in 76 µl of sterile water. A reaction mix composed of 10 µl 10X random primer mix (N-18), 2 µl 10X Labelling dNTP Mix, 10 µl 10X BD Advantage™ 2 PCR Buffer and 2 µl 50X BD Advantage™ 2 polymerase Mix were added to get a final volume of 100 µl. The PCR reactions were performed using the following programe: 95°C 5 min, 3 cycles: 94°C 1 min, 25°C 1 min 30 sec, 50°C 10 min, 68°C 5 min. The reactions were terminated by adding 0.5 µl 0.5 M EDTA (pH 8.0). After 10 µl quick clean resin solution were added, the PCR products were purified through 0.22 µm spin filters. The supernatant from each reaction was collected after centrifugation. For precipitation, 11 µl of 3M NaOAc together with 275 µl 100% ethanol were added and incubated for 1 hr at -20°C. The Pellets were washed with 70% ethanol and finally dissolved in 10 µl 2X fluorescence labelling buffer.

The second step couples the monoreactive dyes: 5 mM fluorescent dye stock was prepared by adding 45 µl DMSO directly to the Cy3 and Cy5 reactive dye. Afterwards, 10 µl of the DMSO/dye mixture were added to the aminoallylated cDNA sample and incubated for 30 min at room temperature in the dark. 2 µl of 3M NaOAc together with 50 µl 100% ethanol were added and incubated for 2 hr at -20°C to precipitate the cDNA. The pellets were washed with 70% ethanol and dissolved in 100 µl nuclease free water. Finally, the samples were purified with the QIAquick PCR Purification Kit.

4.6.2.4 Quality and Quantity Control of Labelled Products

For all labelled samples, CyDyes-labelled products quality and quantity were measured on nanodrop spectrophotometer. The quality of the labelling was estimated by the shape of the absorbance spectra (figure 11) and by the incorporation rate of fluorescent molecules.
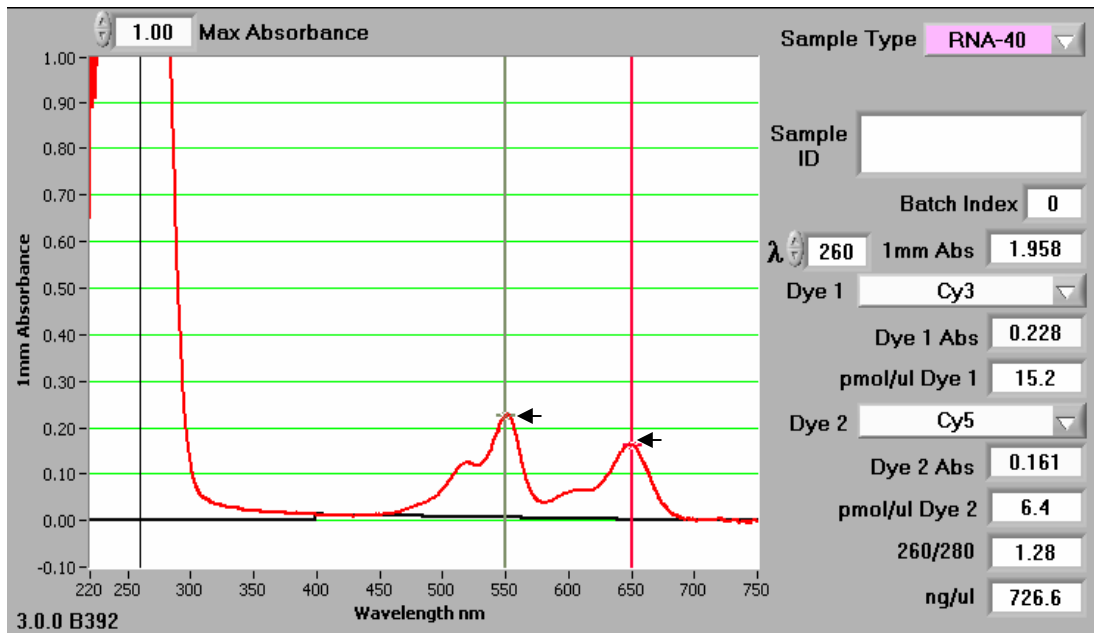
Figure 11. *OD-Spectrum of a mixture of Cy3- and Cy5-labelled cDNAs (Screenshot taken from the Nanodrop software). The peak heights at 550 nm and 650 nm correspond to the amount of Cy3 and Cy5, respectively.*

The frequencies of incorporation (FOI) in CyDye molecules per kb were calculated from the measured absorbance values by the following formulas:

for Cy3: OD_{550} / OD_{260} x 58.5

for Cy5: OD_{650} / OD_{260} x 35.1

4.6.2.5 Slide Preprocessing, Hybridization and Washing

Typically, cDNA spotted slides from the DKFZ need to be prewashed before hybridization. The slides were prewashed by dipping the slides for 2 min each into

1. 0.2 % SDS
2. Double distilled water (RT)
3. Double distilled water (95°C)
4. 100% ethanol

Finally, slides were dried by with compressed air or by centrifugation.

For the mouse 10K and rat 10K oligonucleotide-spotted glass slides, 25 pmol each Cy3 and Cy5 labelled sample were pooled. The volume of the pooled samples was adjusted to 15 µl. The hybridization buffer was preheated to 42°C before the labelled samples were added and the complete mix was then first incubated for another 3 min at 42°C, then for 3 min at 95°C, and finally for 3 min at 4°C. The hybridization was carried out at 42°C for 16 h in the PerkinElmer hybridization station with enabled agitation. After hybridization, the slides were either washed automatically in the station or removed and washed manually. The protocol for machine washing is shown in table 8.

Table 8. *Machine washing protocol.*

Buffers	Flush (µl)	Cycle numbers	Temp. (°C)	Time (sec)	Hold
2X SSC, 0.1% SDS	500	3X	42	30	2'
1X SSC	500	3X	25	30	2'
0.5X SSC	500	2X	25	30	2''

The manual washing was done by dipping the slides one by one into 200 ml of buffer 1 (2X SSC, 0.1% SDS), buffer 2 (1X SSC), and buffer 3 (0.5X SSC) for 5 min each. Slides were dried using centrifugation and scanned.

4.6.2.6 Tests to minimize unspecific fluorescence

To minimize the high fluorescence background on the slides, following parameters were tested:

1) Buffers

Two slides from each i.e. cDNA (DKFZ) spotted and Oligospotted (MWG), were tested in a three different series of set of buffers (see section 5.1.4.1). Slides were manually washed and were dried by centrifugation.

2) Ethanol brands

Three normal glass slides were dipped in a 200 ml of two different brands of ethanol. Slides were dried by centrifugation.

3) Canned and compressed air

Six normal glass slides were dipped in 200 ml of double distilled water. Three slides each were dried with canned air and by comperssed air, respectively.

4) Washing

Several slides were washed manually as well as automatically. The scans were compared.

4.6.2.7 Scanning

All hybridized arrays were scanned at a resolution of 10-µm utilizing an Axon 4100A GenePix scanner. The gain settings for the photomutiplier tubes were adjusted to use the entire dynamic range of the instrument and to get comparable fluorescence yield in both channels. Images of Cy3 and Cy5 signals were recorded as 2 layer 16bit TIFF-files and analysed using GenePix Pro 5.0.

4.6.2.8 Analysis

Spots that showed artefacts such as irregularities or spots covered by dust particles were flagged "bad" and so removed from further analysis. For all data, the local background was subtracted from the intensity values of each spot on the array. The data were analysed using R 1.9.1 and the "limma" package.[67-70]

Spots were weighted by foreground/background – ratio, homogeneity, and saturation. Sigmoid functions were designed to get weighting-factors between 0.0 (bad) and 1.0 (good) depending on the quality criteria (see figure 12)
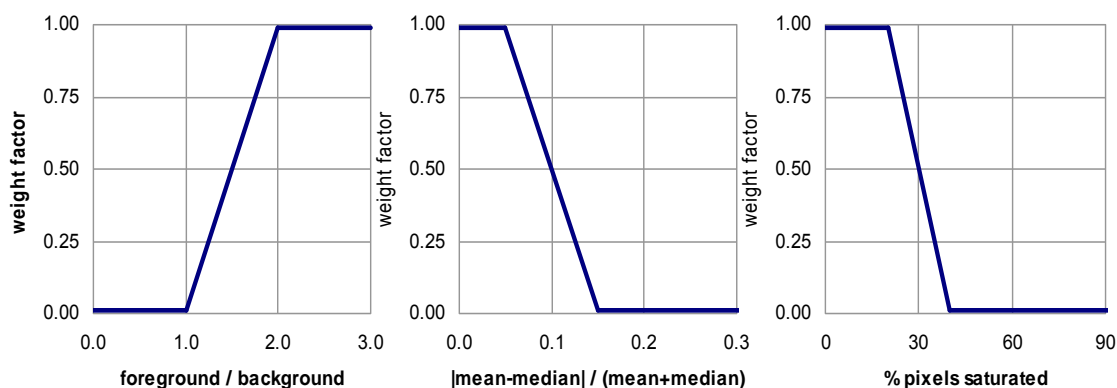
Figure 12. *Spot weight functions use for microarray analysis.* **Left:** *relative signal intensity,* **middle:** *spot homogeneity,* **right:** *saturation.*

Factors were calculated for each channel individually and the smaller factor was taken for subsequent calculations. The final weighting factor was the product of the three quality-specific factors.

An 'MA-plot', as described in Dudoit *et al.*,[71] is used to represent the data. R and G values are the mean of the foreground intensity minus median of the background intensity at 535 nm (Cy3) and 635 nm (Cy5). M values express the log fold-change or log ratio ($M = \log_2(R/G)$), whereas A values represent the average log intensity ($A = \frac{1}{2} \cdot \log_2(R \cdot G)$). MA-plots are helpful to identify intensity-dependent artifacts. Although MA-plots are straight-forward, the very high correlation between the two channel intensities always dominates the plot making the more interesting features of the plot difficult to discern. It also displays the important relationship between differential expression and intensity that is used in later analysis steps.

The data were corrected for intensity dependent artifacts by subtracting a weighted LOESS function (locally weighted scatter plot smother).[72] The effect of the LOESS correction is shown in figure 13.
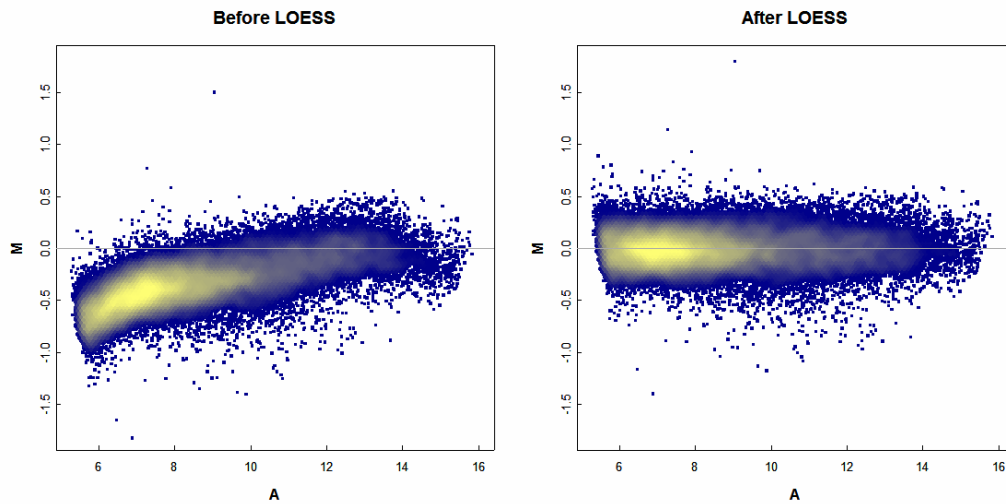
Figure 13. *An MA-plot. An example shows distribution of expression values before and after loess correction.*

After the LOESS correction has been performed, the corrected expression values were averaged over the technical and biological replicates using the linear model fit of the "limma" package.[73] The probability of differential expression was estimated using the Bayesian approach with a fraction of 0.1% of the genes being estimated to be truly differentially expressed. Genes were considered to be differentially expressed (selected) when the Bayesian odds-ratio was greater than 1.

4.6.3 Affymetrix GeneChips

4.6.3.1 Labelling: Generation of Biotinylated cRNA

From each *in-vivo* (IT and IV) and *ex-vivo* (IT and IV) group, 15 µg total RNA were amplified by T7-based RNA preamplification and labelled with biotin using the Affymetrix target labelling protocol (see figure 14).

Eukaryotic Target Labeling for GeneChip® Probe Arrays
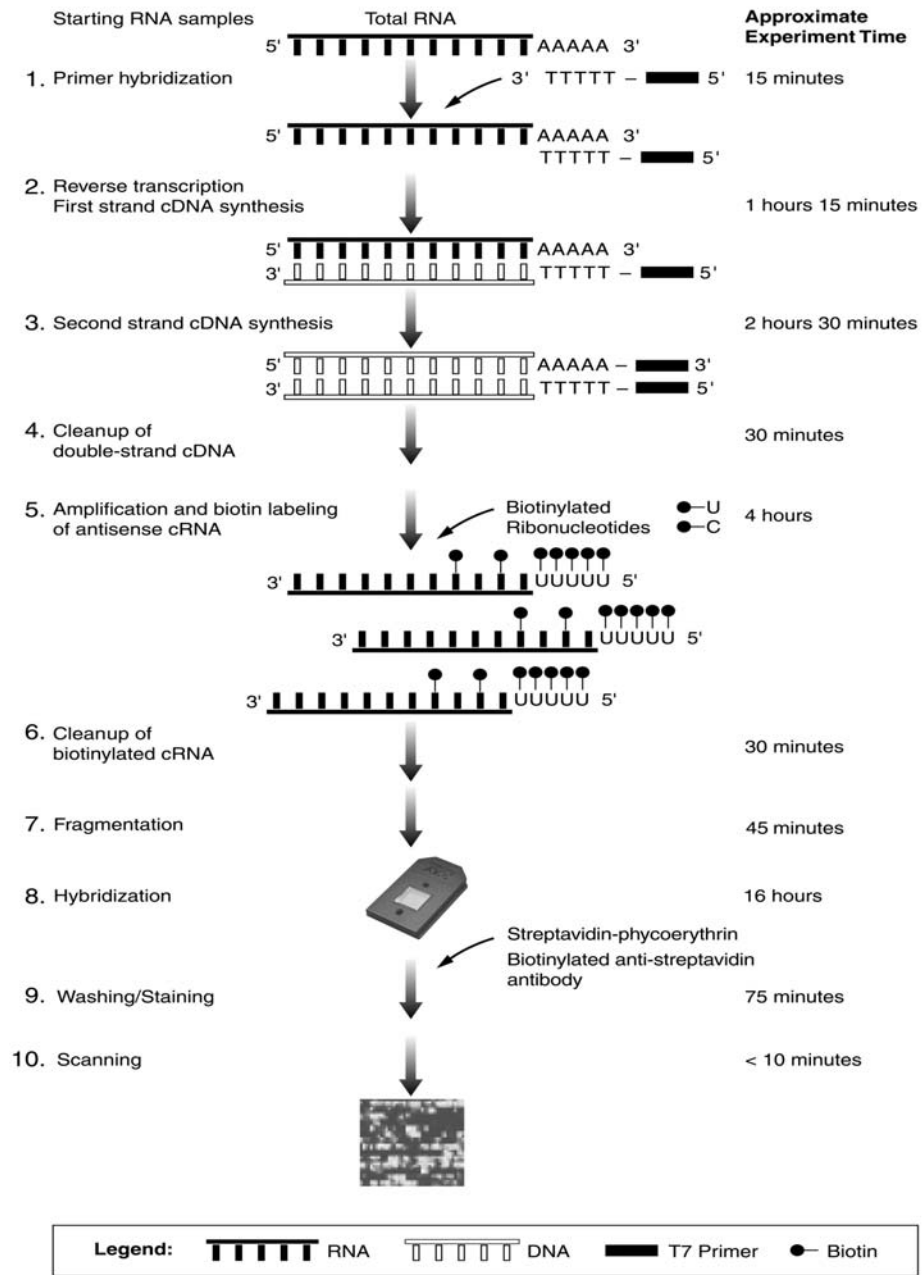
Figure 14. Target amplification and labelling procedure (Picture taken from www.affymetrix.com)

4.6.3.2 Hybridization, Scanning and Analysis

cRNA quality and quantification were measured on nanodrop spectrophotometer as described in section 4.6.2.4. Hybridization, scanning and data analysis were done at Max-von-Pettenkofer Institute, München by R. Hoffmann. Cluster analysis on the analysed data was performed using the dChip software.[74]

4.7 Animal Models

4.7.1 Monocrotaline Rat Model

All preparations were done at the laboratory of PD Dr. R. Schermuly, Department of Internal Medicine, University of Giessen, Lung Center. Male Sprague-Dawley rats weighing 300–450 g were used in the study. MCT was dissolved in 3 ml of 1N HCl, the pH was adjusted to 7.4 with 2 ml of 1N NaOH. 600 ml solution was given in a single subcutaneous injection (60 mg/kg) to male rats. Three groups with 3 animals per group were studied for chronic aspects:

1) $Control_{28}$: control animals treated with isotonic saline were kept for a period of 28 days

2) MCT_{28}: animals treated with MCT were kept for a period of 28 days;

3) MCT_{28} / $tolafentrine_{14-28}$: like group 2 but were additionally treated with tolafentine from day 14-28;

4) $Tola_{14}$: animals treated with tolafentrine for a period of 14 days.

The animals of the $control_{28}$ and $tola_{14}$ groups were first anesthetized with fentanyl and metedomidine (300 and 300 µg/kg IP) and then subjected to the implantation of the mini pump in the dorsal subcutaneous region. This allowed a continuous application of NaCl (for control group) or 5 mg/ml tolafentrine per day, respectively. After 4 weeks, the rats were anesthetized with sodium pentobarbital (50 mg/kg, ip). The lungs were perfused, harvested and immediately stored in liquid nitrogen.

4.7.2 Pneumolysin Mice Models

4.7.2.1 Pneumolysin Animal Model

Female 8-12 weeks old BALB/c mice between were used for all the experiments. The animals were prepared by the group of PD Dr. U. Maus, Department of Internal Medicine, University of Giessen, Lung Center. Three mice each were instilled with 200 ng pneumolysin via intratracheally (IT) or intravenously (IV), respectively. Two untreated mice served as control. After 24 h, the mice were anesthetized. The lungs were perfused with Hank's balanced salt medium (HBSS) free of calcium and magnesium and harvested from the animals. IT treatment of PLY resulted in severe illness and respiratory distress. Systemic (IV) PLY application showed no effect on the health state.

4.7.2.2 Pneumolysin Organ Model

All isolated lung preparations were done at the laboratory PD Dr. N. Weissmann, Department of Internal Medicine, University of Giessen, Lung Center. Three lungs each were instilled for 2 hrs with 200 ng pneumolysin via IT or IV, respectively. Two untreated organs served as a control. Lungs were ventilated and perfused artificially.

5 Results

5.1 Technical Aspects

5.1.1 RNA Extraction Methods

Preparation of high quality RNA is the first and one of the most critical steps in performing microarray experiments successfully. Several methods can be employed to extract RNA from tissue and cells,[75-78] and for most of them kits are available. Three methods were tested to compare their reliability as well as the yields, qualities and purities of the isolated RNAs. Table 9 shows the results of the three different extraction methods tested.

Table 9. *Results of different RNA extraction methods.*

	GTC based	RNeasy column	Trifast/column/DNase
Tissue	Rat lung	Rat lung	Rat lung
Tissue introduced	50 mg	30 mg	60 mg
Total isolation time	5 h	30 min	4 h
Number of repetitions	4	3	4
OD_{260} / OD_{280}	2.0	1.6	2.0
RNA yield total[1]	~35 µg	~20 µg	~100 µg
RNA yield µg/mg tissue	0.7	0.7	1.7

[1] an average amount was calculated for each methods.
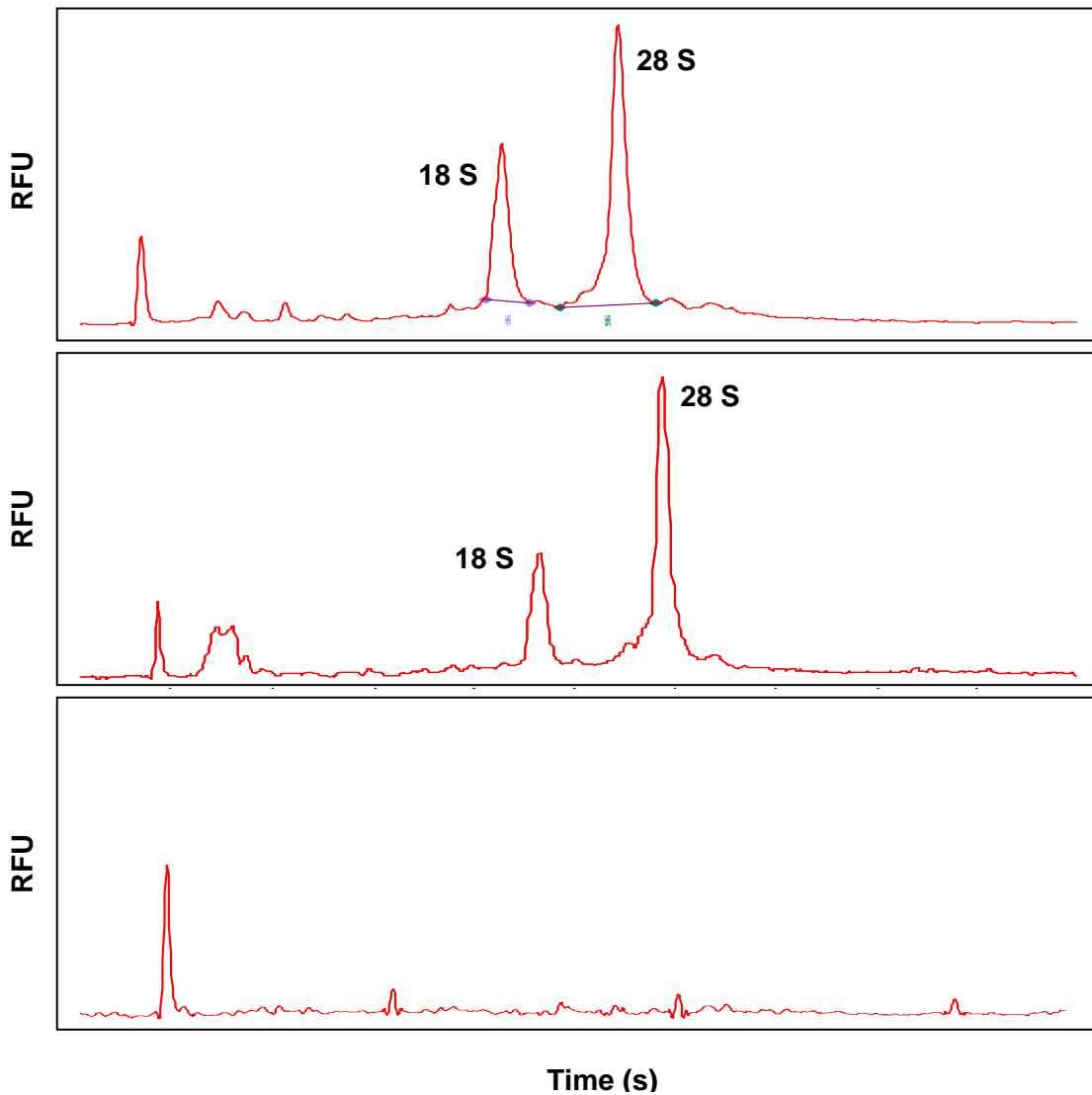
Figure 15. *Microcapillary electropherograms of isolated RNAs.* ***Top:*** *GTC-method,* ***middle:*** *Trifast/column/DNAse-method,* ***bottom:*** *RNeasy column-method. RFU: relative fluorescence units.*

The integrity of the RNA was estimated from the peaks of the 28S and 18S rRNAs in the electropherograms (figure 15). The integrity of RNA isolated with both the GTC– and the Trifast/column/DNase-method were comparably good whereas the RNA isolated with the RNeasy column seemed to be highly degraded.

5.1.2 Reverse Transcriptases for Direct RNA Labelling

For RNA labelling, many protocols as well as commercial kits are available.[79] To obtain labelled single strand cDNA, RNA is usually reverse transcribed in the precence of Cy-labelled deoxynucleotides. More than 20 pmol fluorescently labelled cDNA with more than 10 labelled nucleotides per 1000 nucleotides are required to get acceptable fluorescence signals on high-density microarrays.[80] The yield of a labelled sample depends on fidelity of the reverse transcriptase to synthesize cDNA and to incorporate dye-coupled nucleotides. Four different reverse transcriptases were tested for their suitability to generate labelled cDNA (figure 16).
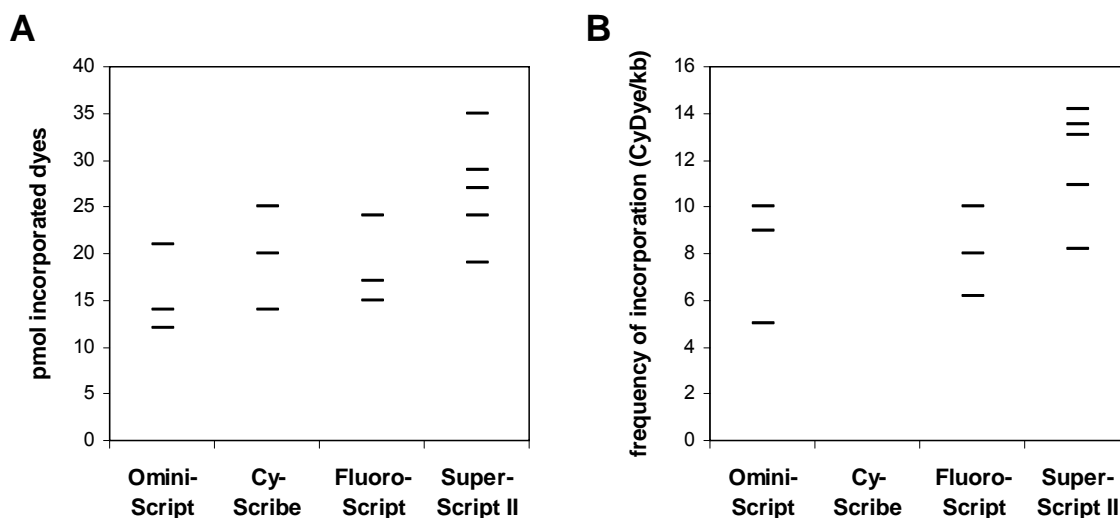
Figure 16. *Labelling performances of different reverse transcriptases.* ***(A)*** *Yields of incorporated dye.* ***(B)*** *Frequencies of incorporation.*

The yield of incorporated dyes was between 10 and 35 pmol, the values for the FOI ranges between 5 and 15 dye molecules per kb. The FOI was not determined for the CyScribe™ enzyme because the protocol includes the addition of carrier nucleic acids that mask the cDNA, hence the FOI cannot be calculated. All enzymes perfomed comparably well, but SuperScript II enzyme resulted in slightly higher values.

5.1.3   Direct and Indirect Labelling

Protocols for direct and indirect labelling were compared to investigate which method results in a higher incorporation rate, and thus, a higher yield of fluorescence. 2 µg dscDNA were introduced i) for the direct labelling using Klenow DNA polymerase (n=3) and ii) for indirect labelling (n=3) using Super SMART™ kit (with the *Taq* DNA polymerase).
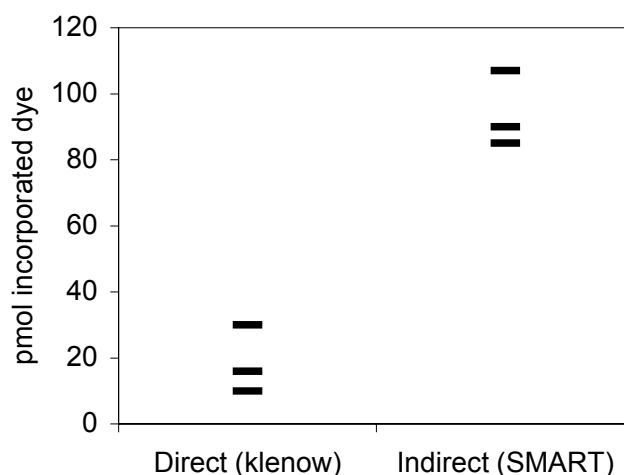
Figure 17. *Comparison of direct and indirect labelling protocols.*

Indirect labelling with the SMART™ kit turned out to be more productive than the direct labelling method (figure 17). With the indirect method on average ~90 pmol dye mulecules were incorporated in the products per reaction. The direct labelling using Klenow DNA polymerase yielded an average of ~19 pmol incorporated dye molecules. The average FOIs were ~11 CyDyes/kb for the indirect labelling and ~7.5 CyDyes/kb for the direct labelling.

5.1.4   Optimization of Hybridization and Washing

A number of factors, e.g., contaminating fluorescent particles, SDS, and temperature, can affect the hybridization and may contribute to high fluorescence background (see figure 18) that can impair the results of microarray experiments.
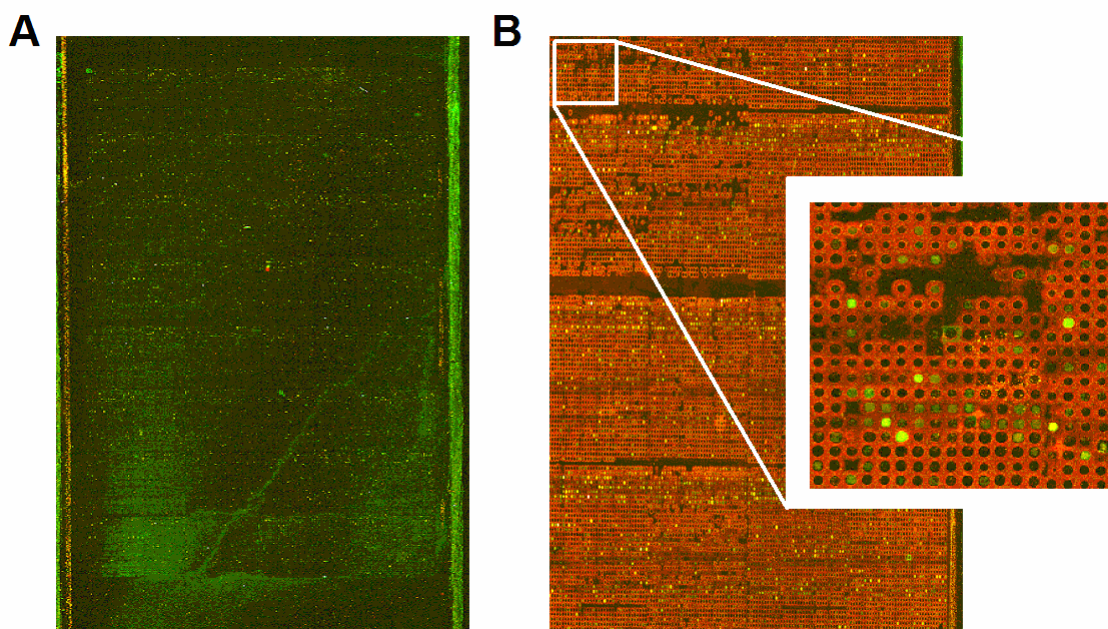
Figure 18. *High background. Mouse cDNA slides show high fluorescence background at 550 nm* **(A)** *and at 650 nm* **(B)**.

5.1.4.1 Buffer Test

Following buffers tests (table 10) were performed in order to select the reliable set of wash buffer.

Table 10. *Buffers tests.*

	Buffer 1	Buffer 2	Buffer 3	Green fluorescency observed
[D]Test 1	0.5X SSC, 0.1% SDS for 5'	0.05X SSC, 0.1% SDS for 5'	0.05X SSC for 5'	Yes
[D]Test 2	2X SSC, 0.2% SDS for 5'	2X SSC for 5'	0.2X SSC for 5'	Yes
[D+M]Test 3	2X SSC, 0.1% SDS for 5'	1X SSC for 5'	0.5X SSC for 5'	No

[D] Performed with DKFZ only

[D+M] Performed with DKFZ and MWG

Using slides from cDNA spotted from DKFZ and oligospotted from MWG, test 3 did not show green fluorescency smear on to the slides while using slides from DKFZ, test 1 and 2 showed fluorescency.

5.1.4.2 Influence of Ethanol

cDNA glass slides need to be treated with a series of washing steps before hybridization including a last incubation step with 100% ethanol to dry the slides. Ethanol has been discussed as a source of unspecific fluorescence.[81]
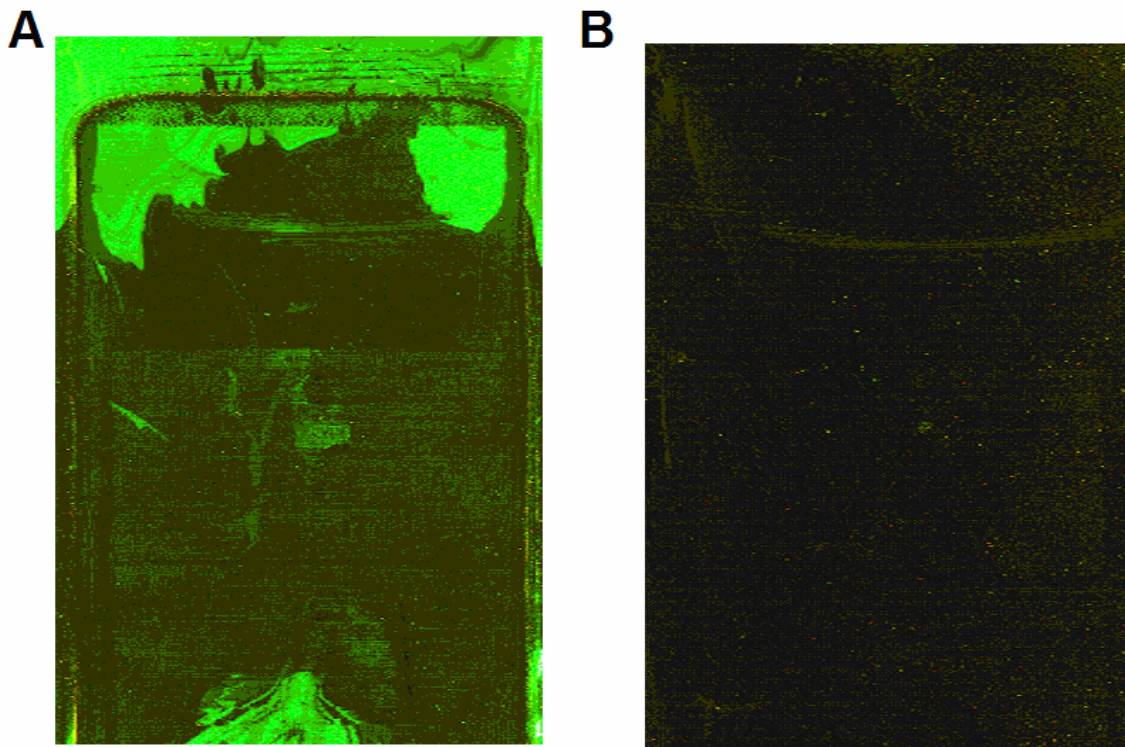
Figure 19. Influence of ethanol brand. Test slides with (A) ethanol from Merck and (B) ethanol from Sigma-Aldrich.

Three test slides each were dipped in 100% ethanol from Merck and from Sigma-Aldrich, respectively. The slides were dried and scanned. The slides dipped in the ethanol from Merck show a bright background fluorescence in the Cy3 channel (green) on the slides (figure 19 a), whereas the scans of the slides treated with the ethanol from Sigma-Aldrich did not show green smear at all (figure 19 b).

5.1.4.3 Influence of Canned Air

The slides have to be dried after washing. Using canned air for this purpose resulted in a remarkable increase in green background fluorescence (figure 20 a), whereas slides dried by compressed air (figure 20 b) or by centrifugation did not show any background fluorescence.
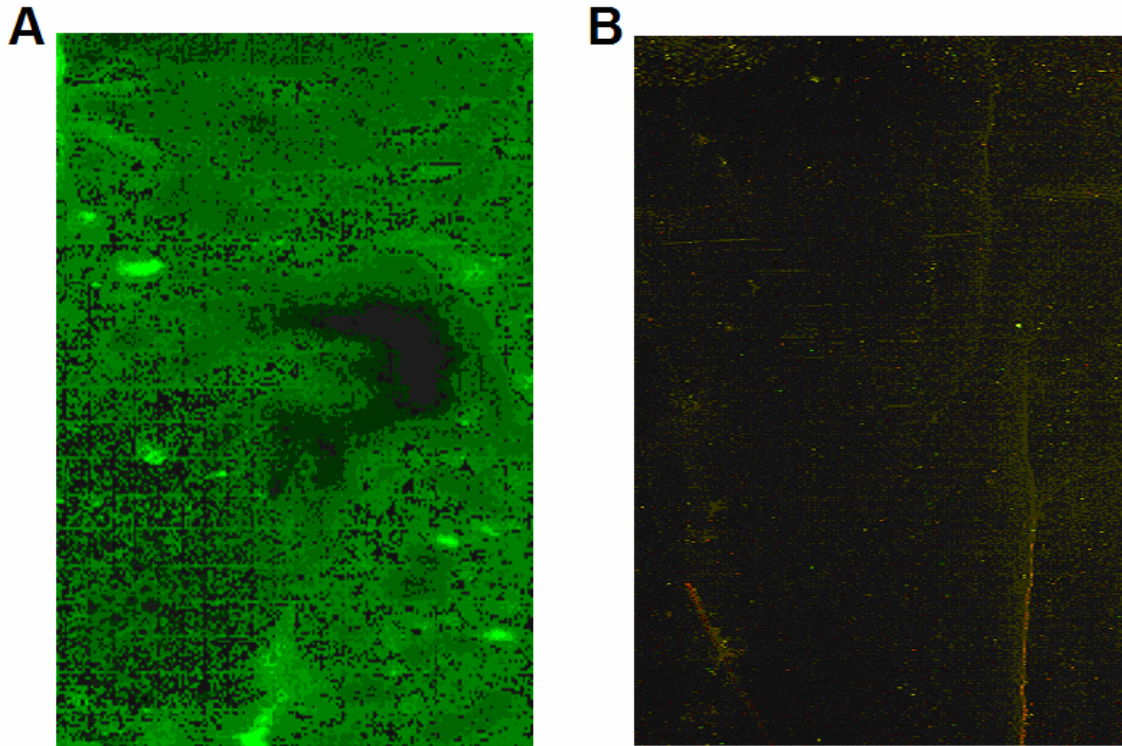
Figure 20. Influence of canned air. After drying (A) with canned air and (B) with compressed air.

Interestingly, background fluorescence was observed only when canned air was sprayed on **wet** slides. Excessively spraying of canned air on **dry** slides did not result in background fluorescence.

5.1.4.4 Influence of the Washing Procedure

The purpose of stringency washing is to minimize the background by removing hybridization buffer and unhybridized or wrongly hybridized labelled cDNA. The slides were washed in a series of buffers initially with low-stringency wash buffer (2XSSC;

0.2%SDS), then with high-stringency wash buffer (1X SSC), and finally with post-wash buffer (0.5% SSC).
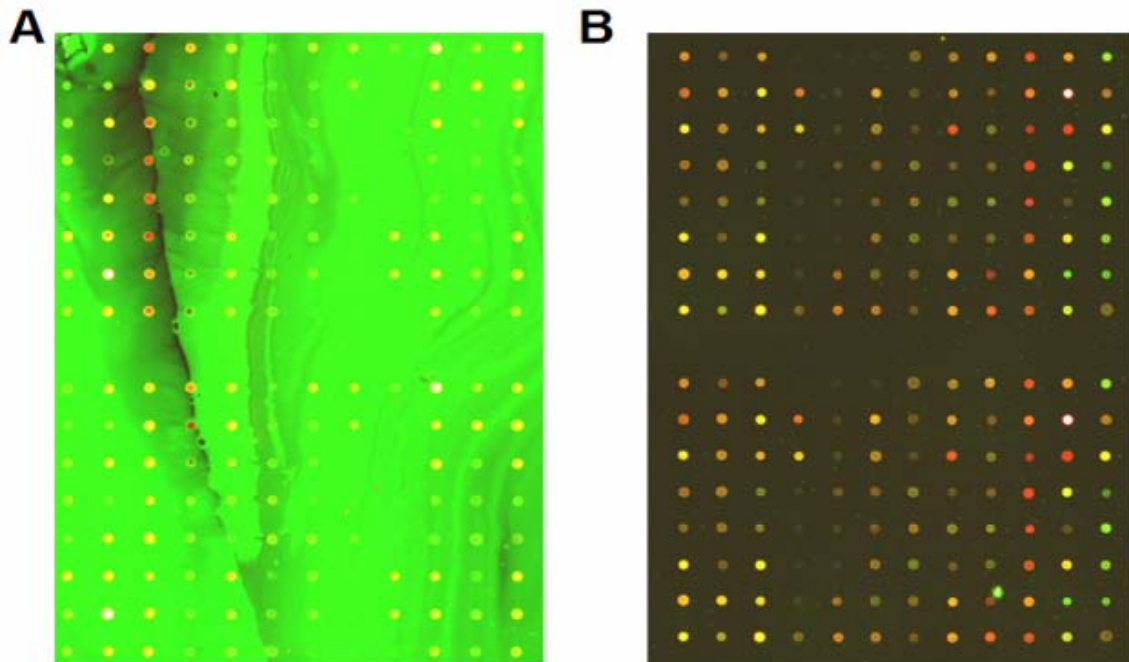
Figure 21. MWG test slides. Scanned images after *(A)* machine-washing and *(B)* manual washing.

The glass slides washed in the PerkinElmer hybridization station (as described in section 4.6.2.5) showed unexpected high green fluorescence background masking almost all gene signal intensities (figure 21 a). In contrast, manually washing by quickly transferring them into a series of buffers resulted in clean slides with almost no background fluorescence (figure 21 b).

5.1.5 Quality of cDNA Spotted and Oligonucleotide Spotted Glass Arrays

After optimization of slide-washing and slide-drying parameters, next aim was to compare cDNA versus oligonucleotide spotted slide quality in terms of reliability and reproducibility. For such comparison we used slides from three different companies:

(a) DKFZ (40K Mouse) cDNA spotted

(b)   MWG (10K Rat, 10K Mouse) oligospotted
(c)   Agilent (22K Mouse) oligospotted

In all experiments, cDNA containing 25 pmol of incorporated Cy3 and Cy5 molecules were hybridized.
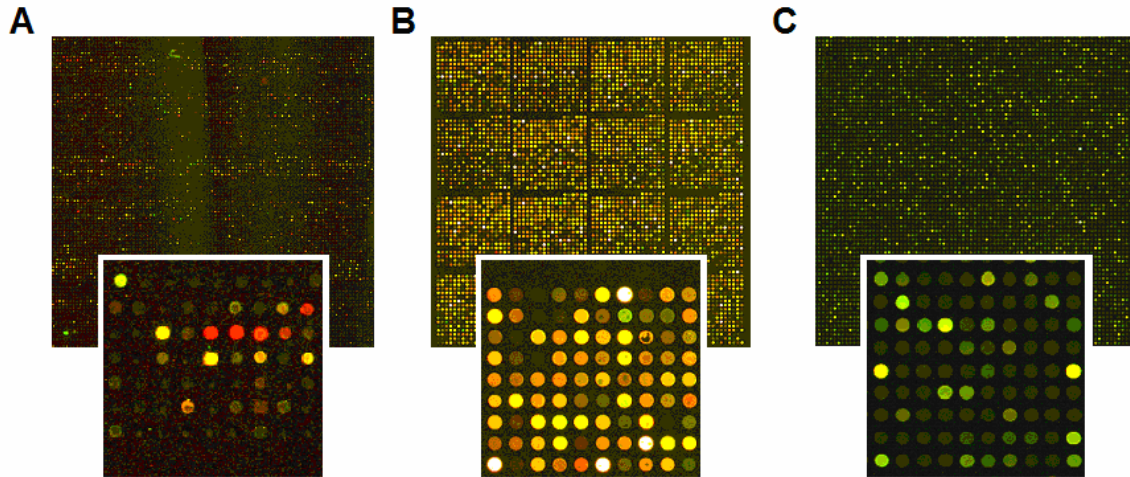
Figure 22. *Survey and spot details of different microarray slides. **(A)** DKFZ cDNA 20K in duplicate (=40K) spotted array. **(B)** MWG 10K oligospotted array. **(C)** Agilent 22K oligospotted array.*

Hybridization was performed for 16 hours on the PerkinElmer hybridization station (DKFZ cDNA-spotted slides at 42°C, oligo-spotted slides from MWG at 42°C, oligo-spotted slides from Agilent at 42°C). Slides were scanned with the Axon scanner. The DKFZ slides (figure 22 a) suffer high background and irregular spot morphologies. In contrast, the MWG and Agilent slides (figure 22 b, c) showed less background and had regular, homogenous spots.

Slide quality was analysed on the basis of: i) signal-to-noise ratios, ii) standard deviations of the within-spot ratios, and iii) spot morphology (homogeneity i.e. the relative difference of mean to median spot intensity is a good measure for homogeneity) (figure 23).
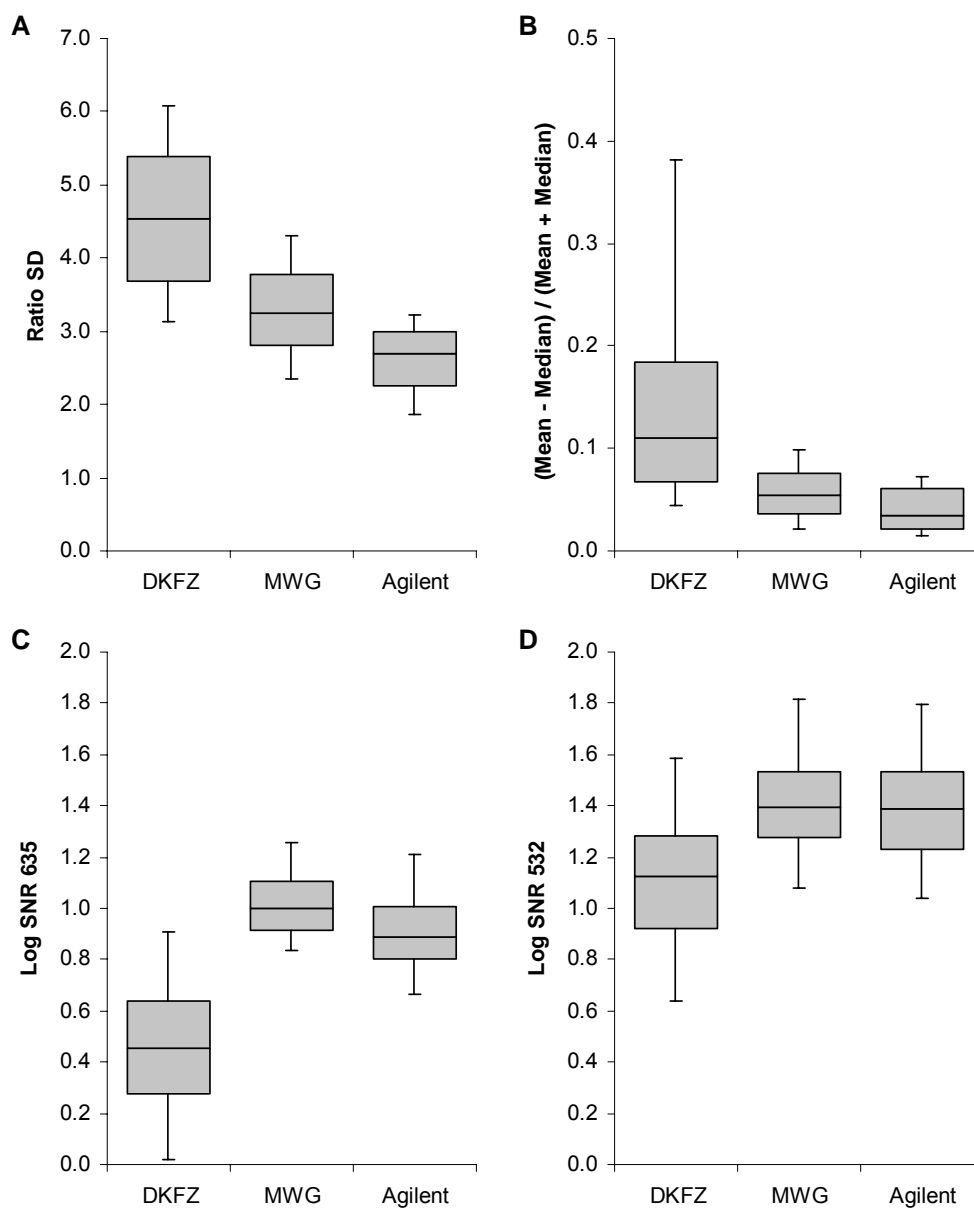
Figure 23. *Quantitative results of the slide quality measures. All Diagrams show the median and center 50% of the values for one representative slide. The whiskers include the center 90% of the values. (**A**) Ratio-SD: For each spot on the slide, the standard deviation of the log-ratios of red and green signal intensities for each pixel was calculated. (**B**) Normalized difference of the mean and the median of the foreground intensity (both channels averaged) of the spots. Deviation from zero indicates inhomogeneous intensity distributions whitin the spots. (**C**) And (**D**) Logarithms of the signal-to-noise ratios (SNR = foreground / background intensity) for each channel.*

5.1.6 Preamplification

The requirement of a large amount of high-quality RNA is a major limiting factor for microarray experiments using RNA from biopsies or from laser microdissection. An average microarray experiment requires about 20 µg of total RNA for cDNA labelling and subsequent hybridization.[82-83] However, microdissected cells and small biopsied do not yield such amounts. Several different approaches for RNA preamplification have been described and applied for microarray studies. Especially for the combination of laser microdissection and microarrays, low amounts of RNA have to be preamplified.[84] Therefore, we compared the yields and biases of the T7-IVT and SMART™ using limited starting material (~50 ng total RNA).

5.1.6.1 Assessment of Product Length

Quantitative real-time PCR was performed on aliquots of the samples before (reference) and after preamplification to determine the amplification factors of three target sequences with different distances to the poly-A-tails. The analysed target sequences are 3'UTR-GAPDH, GAPDH and PBGD with 200 bp, 700 bp, and 1400 bp distance to the poly-A-tail. The results are given in table 11 and figure 24.

Table 11. Quantitative PCR results of the preamplification experiments. The values are rounded to 2 significant digits.

Target (3'-distance [bp])	SMART		T7	
	12 cycles	**24 cycles**	**2 rounds**	
GAPDH 3'-UTR (200)	10.5 ± 2.3 (7.9..13)	16.2 ± 3.2 (13..19)	9.8 ± 0.9 (7.6..12)	ΔCt mean ± sd (90%-CI)[1]
	1500 (230..9500)	75000 (8980..625838)	870 (200..3900)	factor mean[2] (90%-CI)
GAPDH (700)	6.8 ± 0.8 (5.8..7.8)	13 ± 1.4 (12..14)	7 ± 0.4 (6.1..7.9)	ΔCt mean ± sd (90%-CI)
	120 (58..230)	8500 (3300..22000)	130 (67..250)	factor mean (90%-CI)
PBGD (1400)	11.8 ± 1.8 (8.8..15)	17.6 ± 1 (16.0..19.3)	2.8 ± 0.7 (1.0..4.6)	ΔCt mean ± sd (90%-CI)
	3500 (460..28000)	200000 (65000..650000)	7 (2..24)	factor mean (90%-CI)
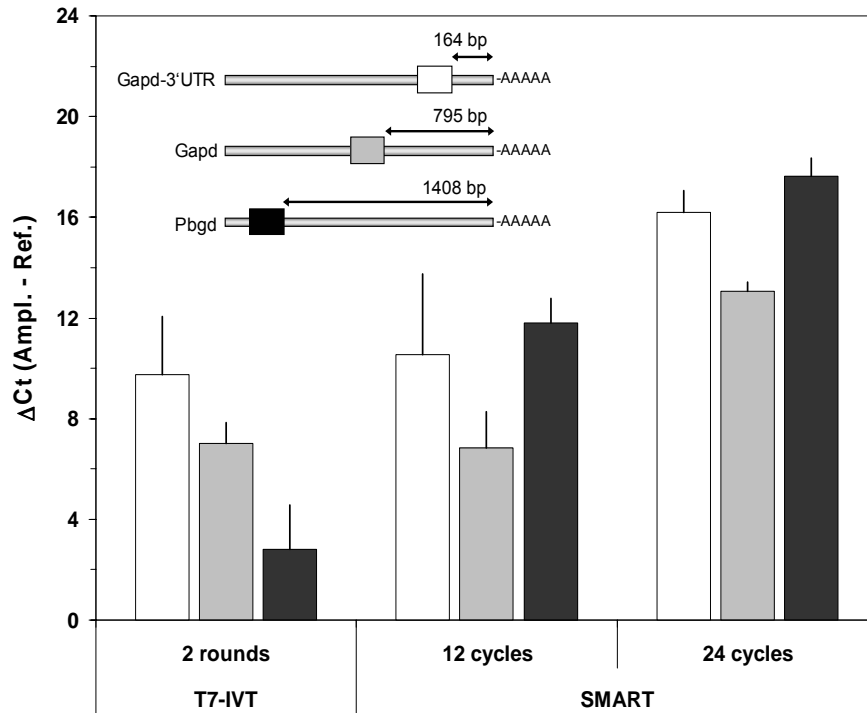
Figure 24. *Quantitative PCR results of the preamplification experiments. Mean ΔCt values (unamplified – amplified) for 3'UTR-GAPDH, GAPDH and PBGD, showing the comparison between 2 rounds of T7 and SMART™ (12 and 24 cycles) based amplification. The error bars indicate the standard deviation (n=3..5). Inlet: positions of the target sequences within the analysed transcripts.*

Mean ΔCt values for 3'UTR-GAPDH and GAPDH with 12 cycles and two rounds of T7-IVT were comparable within the margins of error (table 11). However, the PBGD target sequence that was positioned 1400 bp away from the poly-A tail was efficiently amplified by SMART™, whereas T7-IVT almost failed to amplify this sequence. The expected ΔCt values for the SMART™ amplification are the number of amplification cycles performed (i.e., 12 and 24, respectively). After 12 cycles of SMART™ amplification, the expected ΔCt was reached for 3'-GAPDH and for PBGD, whereas the ΔCt value obtained for GAPDH was considerable lower (90%-CI: 6..9, see table 11).

Furthermore, an increase of the number of amplification cycles to 24 resulted in a further increase of the amount of product. However, all ΔCt values for 24 cycles SMART™ were significantly lower than the ideally expected value of 24, indicating that the amplification reaction was already reaching the plateau phase. Notably, the relative differences of the amplification factors of the different target sequences are similar to those after 12 cycles of SMART™.

5.1.6.2 Comparison of Preamplification Techniques for Expression Profiling using DNA-microarrays

To assess which preamplification technique is more suitable for expression profiling using DNA microarrays with limited material, both techniques (SMART™ and T7-IVT) were compared. Potential amplification bias was estimated by the comparison to directly labelled cDNA from unamplified RNA as reference. 50 ng total RNA from each mouse liver and kidney were introduced using T7-IVT (2 rounds) and SMART™ (15 cycles) techniques. Two rounds of T7-IVT and 15 cycles SMART™ yielded about 50 µg aRNA with ~2000 pmol dyes and 1.5-2.0 µg dscDNA with ~40 pmol dyes, respectively. The introductory amount of sample used for expression profiling was adjusted to 25 pmol each Cy3 and Cy5 incorporated dyes. Labelled samples were hybridized on mouse 10K 50mer oligonucleotide microarrays. The whole procedure including preamplification, labelling, and hybridization was done twice to get results for two completely independent experiments.
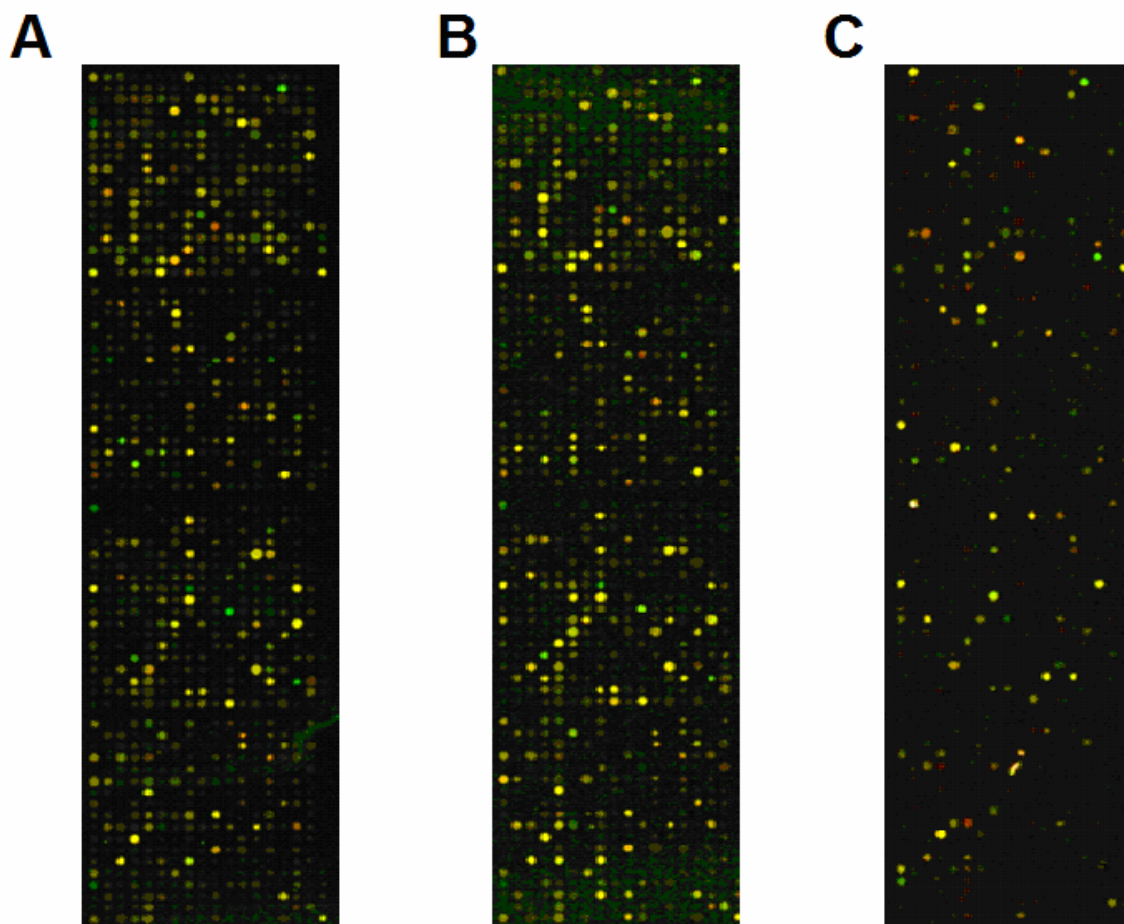
Figure 25. Comparison of microarray images. Labelled samples from mouse kidney and liver were hybridized on 10K mouse arrays from MWG. (A) Reference (unamplified), (B) SMART™ (15 cycles) and (C) T7-IVT (2 rounds).

A representative area of the scanned images (figure 25) provides a first hint that the expression profile after SMART™ is more comparable to the reference than after T7-IVT. Although the same amount of fluorescence was used for all hybridizations, many spots were missing after T7-IVT.

The reproducibility of the preamplification was estimated by a comparison of the expression profiles obtained from the two independent experiments. A direct comparison of the M values (log$_2$ ratios liver vs. kidney) for all features on the slides for the same method (reference, SMART, and T7-IVT) is shown in figure 26.
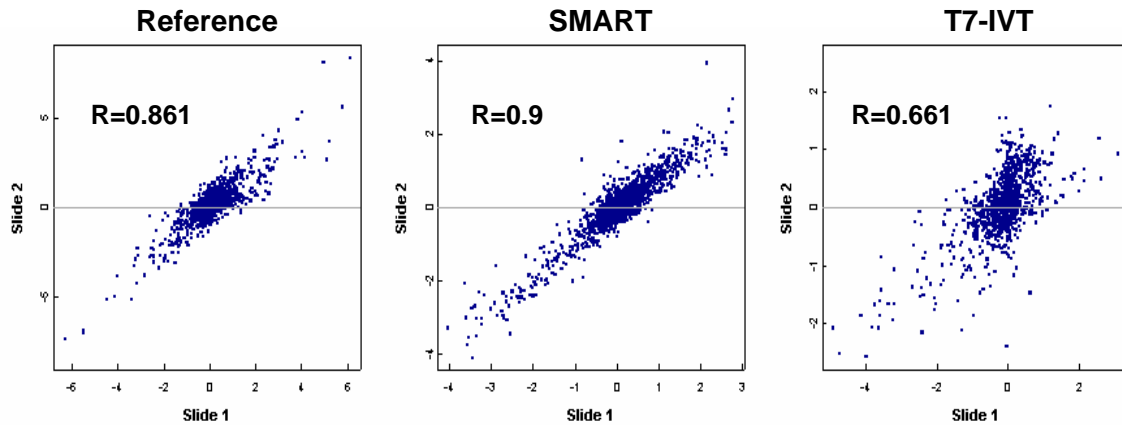
Figure 26. *Scatter plots of the M values of slide 1 versus slide 2. R=Pearson's coefficient of correlation.*

Spots with weight factors greater than 0.75 were considered for further analysis. Intra-assay comparison was assessed by the Pearson's correlation coefficient (R^2) of the M values of the two slides for each method. The within-method correlation coefficients for reference (R=0.87) and SMART™ (R=0.9) were comparably well, whereas the value of R for T7-IVT was clearly lower (R=0.66).

To analyse the correlation of the M values between the preamplification methods, the M values of the two independent experiments within each method were averaged. The scatterplots for the comparison of either amplification method with the reference are shown in figure 27. The values obtained for Pearson's correlation coefficient were 0.92 for SMART™ and 0.68 for T7-IVT. The observed dynamic range of differential expression (=range of M values) seems to be limited.

SMART versus Reference   **T7-IVT versus Reference**

R=0.852   R=0.536
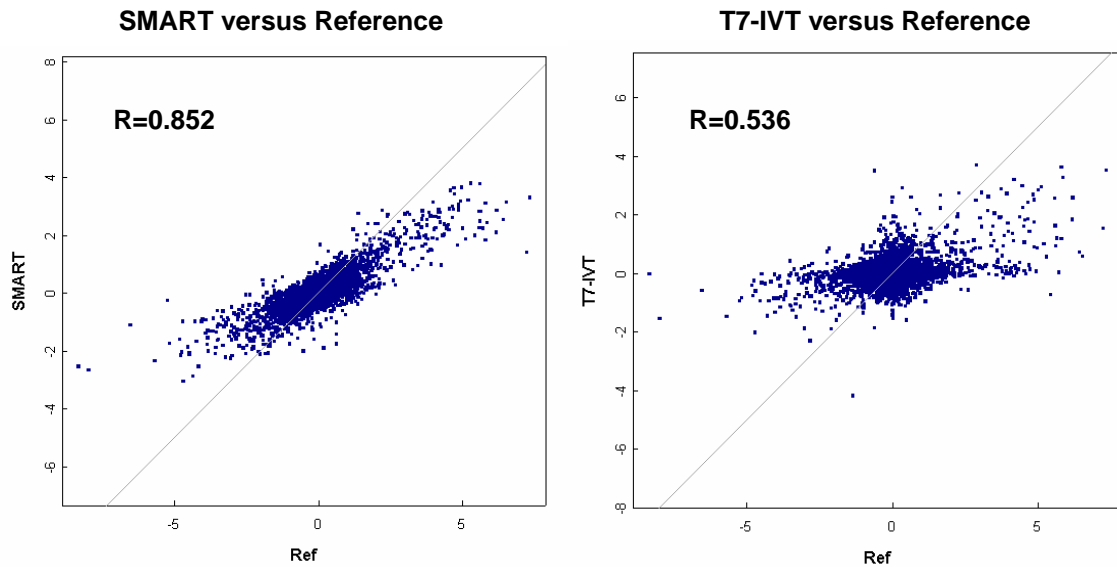
*Figure 27. Scatter plots for the M values. **Left:** SMART™ versus reference and **right:** T7-IVT (2 rounds) versus reference.*

Figure 28 shows the M/A-scatterplots for the averaged data of the two slides per group. Using the odds ratio for M≠0 and the absolute average M value as selection criteria, 57 genes are selected in the reference, 316 are selected for SMART™, and 62 genes are selected for T7-IVT (red points in figure 28). In "real" experiments, these selections would indicate the genes considered as differentially expressed.

Ref   **SMART**   **T7-IVT**
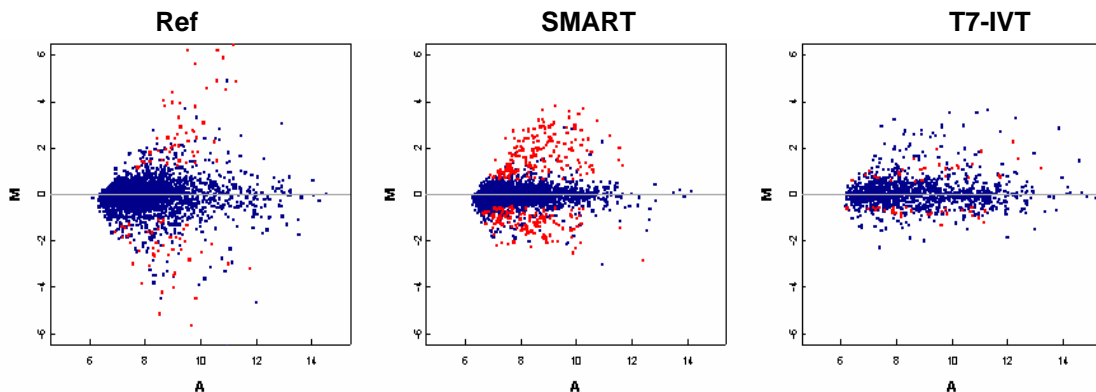
Figure 28. M/A-Scatterplots for the averages. Red: genes with an odds-ratio for M≠0 greater than 1 and |M| greater than 1 that were selected as differentially expressed.

The Venn diagram in figure 29 (left side) shows that 41 selected genes were common in reference and SMART, 2 selected genes were common in reference and IVT, 10 in

59

SMART and IVT and none of the selected genes were common in reference, SMART and IVT, respectively. The selected genes were validated using the information about their differential expression between liver and kidney in the two public databases.[85] The sets of genes listed in the databases were not identical. The differential expression of those genes listed in both the databases was assigned similarly in both databases. The results are shown in figure 29 (right side).
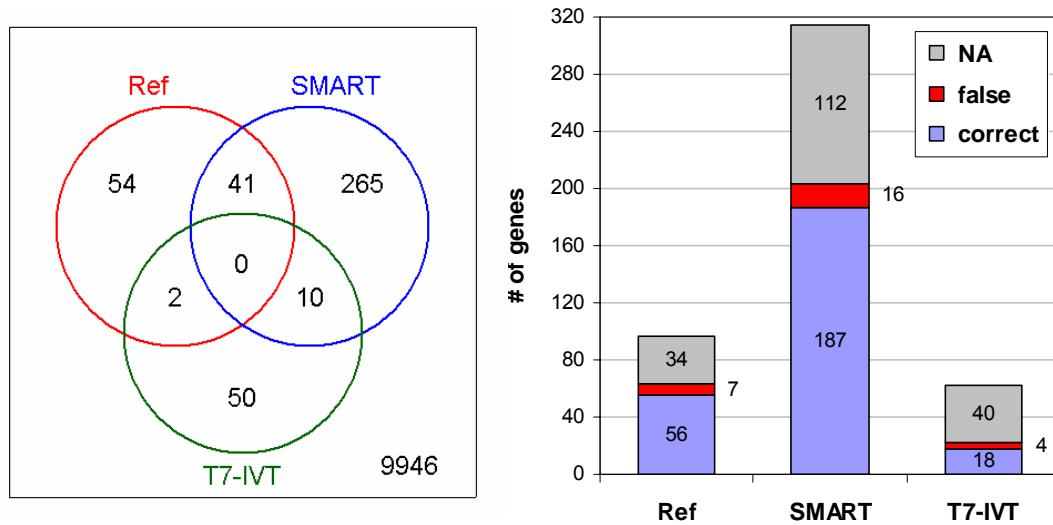
Figure 29. *Venn diagrams and* **number of selected genes found in databases.** *Ref = Reference; NA = not assigned as differentially expressed or not present in the databases.* **Blue:** *number of correctly selected genes (present in the databases and correctly assigned in differential expression);* **red:** *number of falsely selected genes (present in the databases but with the opposite differential expression);* **gray:** *number of selected genes not present in the databases.*

As figure 29 (right one) shows for the reference experiment with unamplified RNA, out of 97 significantly regulated genes, 56 genes were truly differentially expressed (shown with purple color), 7 were false genes (red color) and 34 genes were not available (grey color) as per databases search. For IVT, out of 62 significantly regulated genes, 18 were truly differentially expressed, 4 were false genes and 40 genes were not available as per databases. However, for SMART, out of 315 significantly regulated genes, 187 genes were truly differentially regulated which was 3X to the reference and 9X to the T7-IVT samples, with a least number of false genes (5 %) and 112 genes

were not available as per databases search. In conclusion, expression profiling after SMART™ based preamplification turned out to be more efficient, reliable and reproducible than T7-IVT.

5.2 Microarray Application in Animal Models

5.2.1 Monocrotaline Induced Pulmonary Hypertension

Monocrotaline (MCT) induced pulmonary hypertension (PH) is characterized by lumen-obliterating endothelial cell proliferation and vascular smooth muscle hypertrophy of the small precapillary pulmonary arteries.

In a rat model, subcutaneously injected MCT induces endothelial inflammation and structural remodelling of the lung arteries leading to PH with similar histological properties as seen in human PAH. Tolafentrine is known to attenuate the abnormalities in hemodynamics and gas exchange and the right-heart hypertrophy. Tolafentine is a phosphodiesterase inhibitor and possesses a strong antiproliferative effects in the pulmonary circulation.[47]

Following conditions were investigated compared to a control group without any treatment:

i) MCT_{28} (MCT): After systemic application of MCT animals are sacrificed at day 28: MCT application induces an endothelial inflammation with a structural remodelling of the lung arteries leading to pulmonary hypertension within 28 days.

ii) $MCT_{28}+Tola_{14}$ (MT): 28 days systemically applied MCT: 14 days after systemic application of MCT tola is continuously infused for further 14 days. The animals are sacrificed at day 28.

iii) Tola14 (tola): Control group with tola infused from day 14 to day 28 (without MCT application).

The expression profile of MCT-induced and tolafentrine-attenuated PH in the rat lung tissue was analysed using nylon filter arrays with 1176 cDNA probes (Atlas) as well as glass microarrays with 10K oligonucleotide probes (MWG).

5.2.1.1 Expression Profiles on Nylon Filter Arrays

Hybridization was performed on Atlas Rat 1.2 Array (1,176 spotted cDNAs). Two groups i.e. MCT (n=3) and MT (n=2) respectively were hybridized using control group as a reference. Figure 30 shows a representative scanned image of nylon filters.

A   **B**
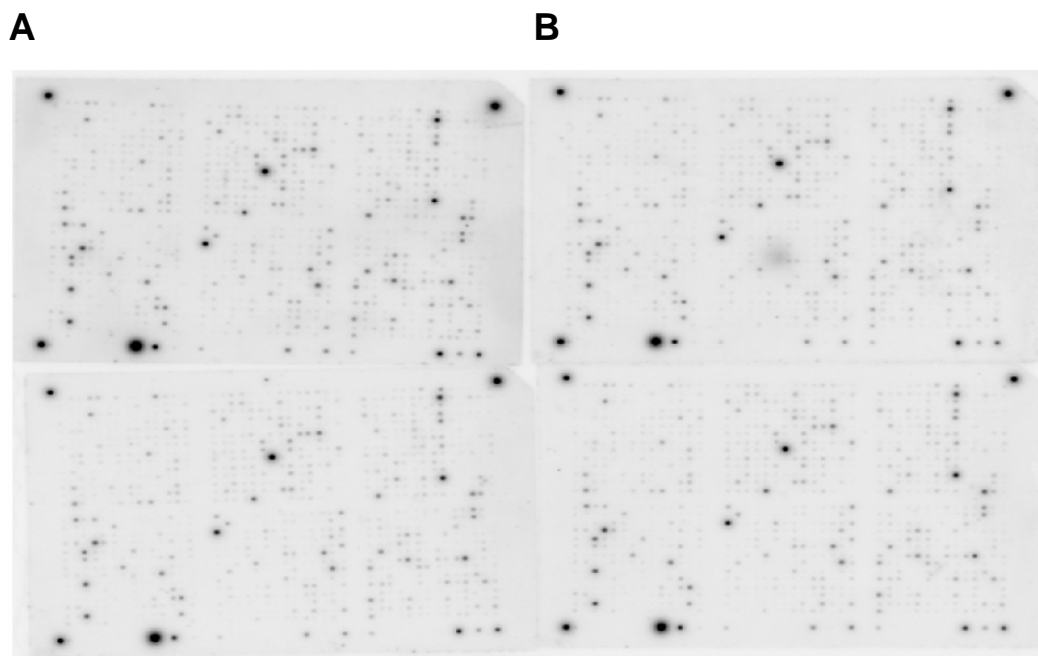
Figure 30. *cDNA macroarray nylon filter.* **Left side:** *duplicate control,* **Right side:** *duplicate MCT treated sample.*

The intensity dependent data distribution is shown in figure 31.
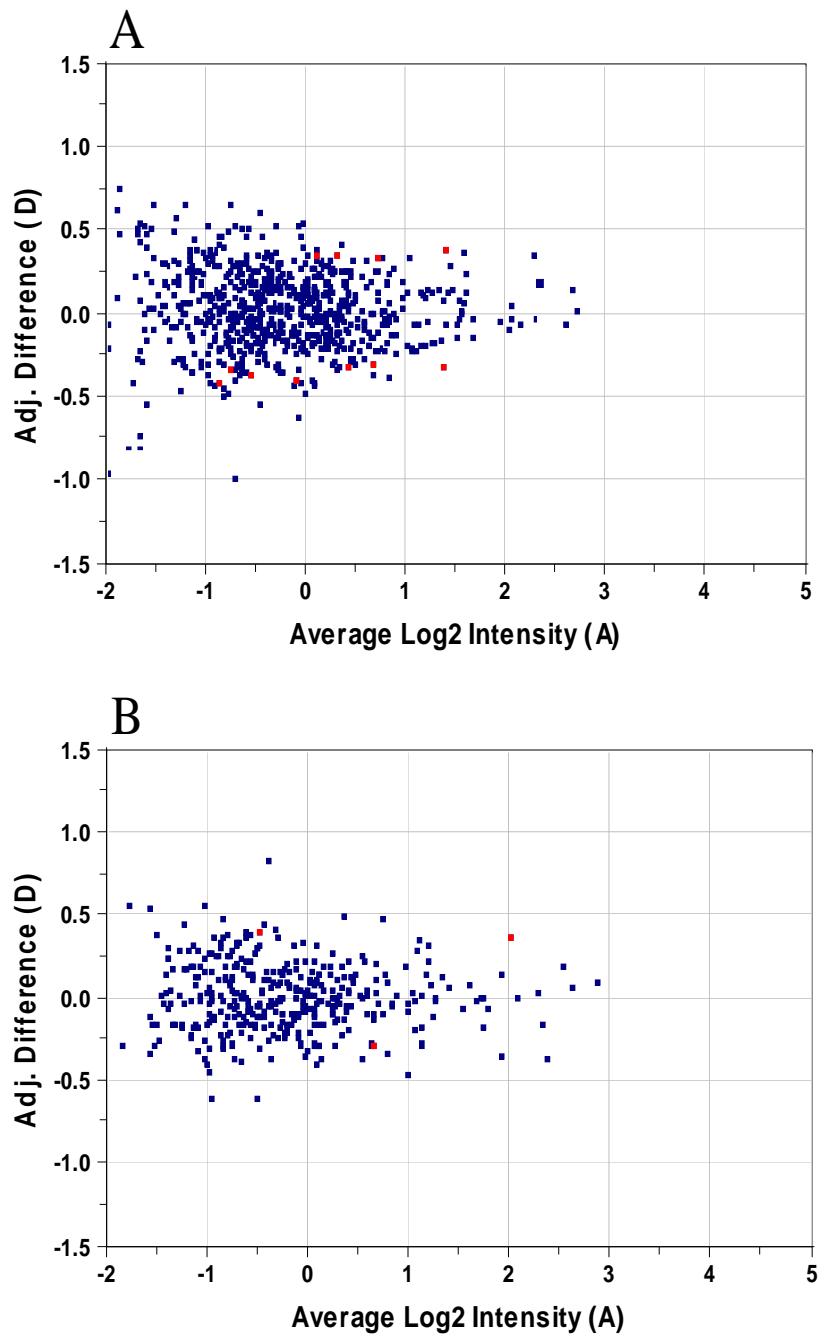
Figure 31. *D/A-Scatterplots for the averages. Control used as a reference for* **(A)** *MCT and* **(B)** *MT. Red dots: selected genes.*

From 703 evaluated genes (where at least one spot was above background), 11 genes were considered to be differentially expressed according to the selection criteria applied (4.6.1.4) after MCT treatment. Similarly, 3 genes from 379 genes were selected in the MT group (see table 12).

Table 12: *Selected Genes from the Nylon Macroarray Experiments. N: number of experiments, A: adjusted differences, M: average log2 intensity, P: p-values, SD: standard deviation of D*

Gene	GenBank Accession	N	A	M	D	P	SD
MCT versus Control							
MXI1	AF003008	2	-0.08	-0.79	-0.41	0.0361	0.033
PKB; AKT1	D30040	3	0.43	-0.57	-0.32	0.003	0.031
FABP4; ALBP	U75581	3	0.69	-0.54	-0.31	0.0303	0.095
GLCLC; g-ECS	J05181	2	-0.53	-0.69	-0.38	0.0001	<0.001
alkaline phosphatase	J03572	2	1.41	0.70	0.38	0.0181	0.015
neurotensin receptor 2	U51908	2	0.12	0.60	0.34	0.0217	0.016
GABRA1	L08490	3	0.33	0.60	0.34	0.0094	0.057
Ggamma8	L35921	2	0.74	0.58	0.33	0.0151	0.011
Rab-3b	Y14019	3	1.39	-0.57	-0.32	0.0313	0.100
PDGF-associated protein	U41744	2	-0.75	-0.61	-0.35	0.0046	0.004
proteasome component C3	J02897	2	-0.85	-0.81	-0.43	0.0025	0.002
MT versus Control							
CD68 antigen	D64050	2	0.66	-0.52	-0.3	0.04	0.027
CBPTP	M94043	2	1.92	-0.66	-0.36	0.0542	0.044
Rab-related GTP-binding	M12481	2	2.03	0.63	0.35	0.0274	0.021

A more detailed analysis of the intra-assay correlation revealed remarkable differences between the individual experiments (figure 32)
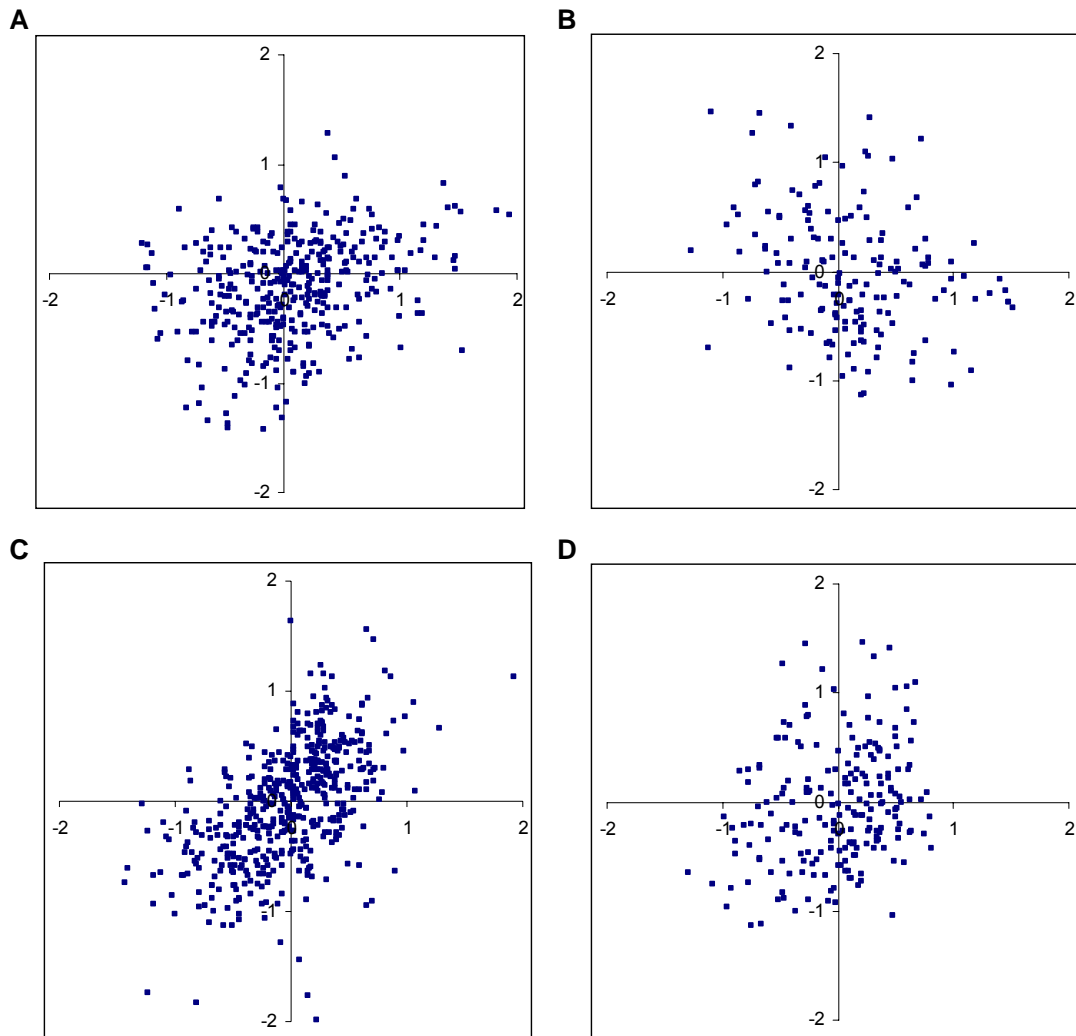
Figure 32. *Correlation of the expression profiles of individual MCT-treated samples. The diagrams show the adjusted differences (D values) of the experiments compared. **(A)** #1 versus #2, **(B)** #1 versus #4, **(C)** #2 versus #3, and **(D)** #3 versus #4.*

This inferior correlation can be due to biological and experimental variation. Interestingly, only the expression profiles from the experiments #2 and #3 exhibits a weak correlation (figure 32 C). Exactly these two experiments have been conducted in parallel by the same experimenter (the animals were prepared at the same day from the same person), whereas all other animals were prepared at different days from different experimenters. This demonstrates a major contribution of experimental variation to the overall variation and, hence, the necessity of a parallel sample

preparation. But even the expression profiles of samples prepared in parallel only correlate weakly ($R^2 \cong 0.3$), indicating considerable individual variations and limiting the power of a statistical analysis to identify differentially expressed genes. The power of a two-sided t-test to find a strong effect (observed value divided by the standard error > 1) is estimated in the experiment in question to be smaller than 10% (calculated with Gpower®).[86] The standard error can be reduced (and the power increased) by averaging more samples.

5.2.1.2 Expression Profiles on Glass Slides

The experiences from the nylon filter array experiments were considered for the experimental design using 10K oligonucleotide spotted glass arrays. All samples were prepared from the same person and whenever possible processed in parallel. Additionally, the number of individuals was considerably increased. For a power of 90% to identify genes that are regulated by more than 2-fold, the number of samples was calculated to be greater than 16 (Gpower®, the standard deviation of the M values was estimated to be ~ 0.5).

Three groups (i.e. MCT, MT, and Tola) with 6 individual per group were hybridized together with the control group (6 individuals) on rat 10K glass slides. A technical repetition of the hybridization was performed including a dye-swap to eliminate effects of any sequence-specific dye-bias. Figure 33 shows representative parts of the two scans of a dye-swap experiment.

(A) **(B)**
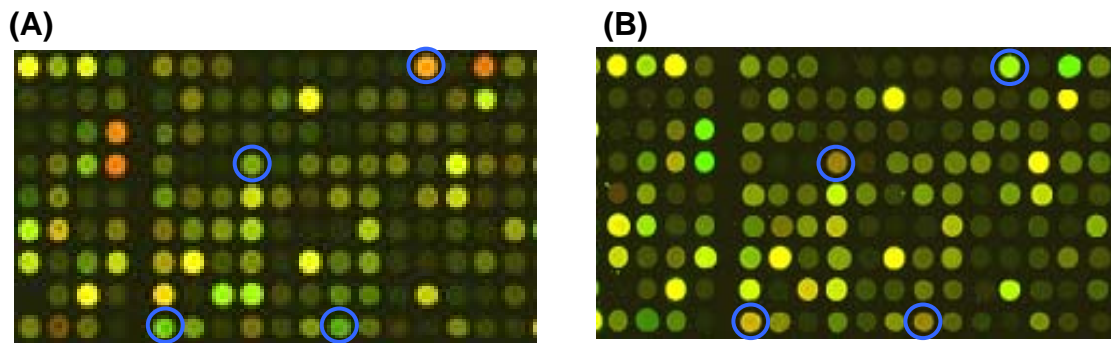
Figure 33. Dye swap on rat 10K oligonucleotide slides. (A) Slide where reference sample was labelled with Cy3 and treated sample with Cy5 while for dye swap approach (B) reference was

labelled with Cy5 and treated with Cy3. Blue rings are indicating how the color for spots in figure
(A) and (B) switched in dye swap appraoch.

The averaged results for each group are shown in figure 34. Clearly more genes were differentially regulated after treatment with MCT and MT than after Tolafentrine treatment. In all groups, more genes were found to be upregulated than genes to be downregulated.
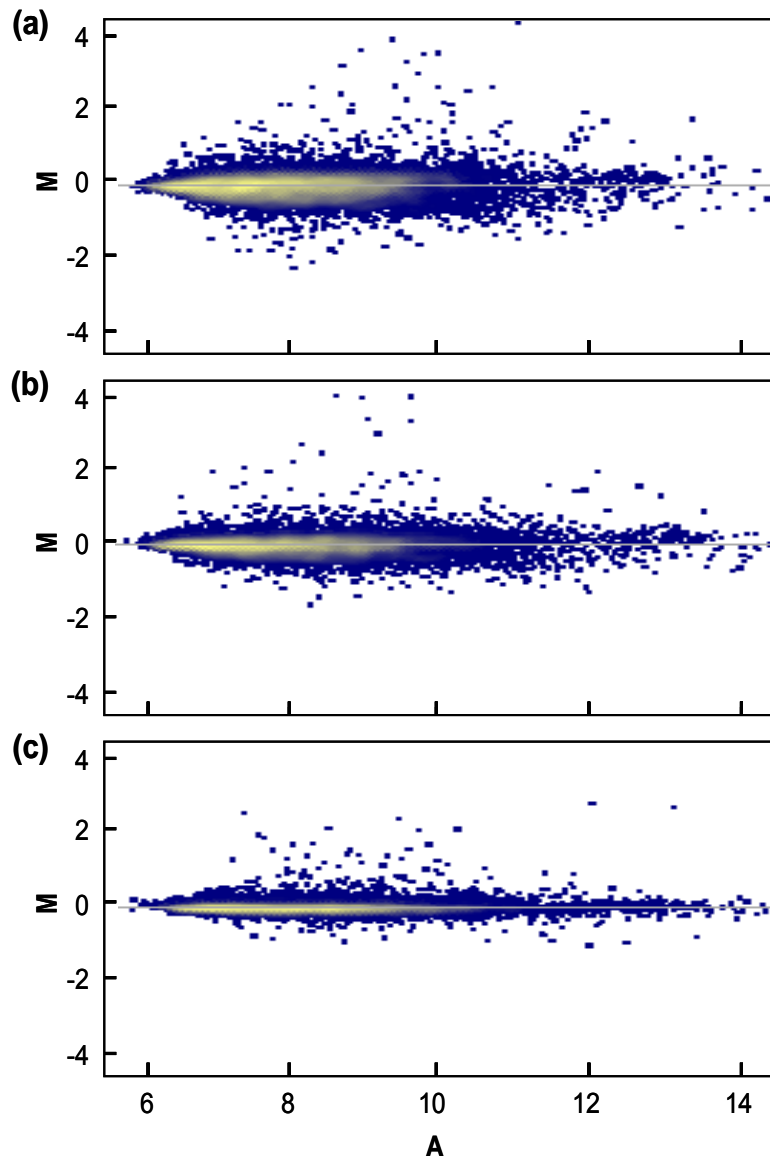
Figure 34. *A normalized MA-plot. Fits for the (A) MCT, (B) MT, and (C) Tola groups.*

The probability of differential expression was estimated using the Bayesian approach with a fraction of 0.1% of the genes being differentially expressed. Genes were considered to be differentially expressed (selected) when the odds-ratio was greater than 10 (log odds >1) and the absolute log fold-change was greater than 1 (|M|>1). The distribution of the log odds and M values is illustrated in figure 35.
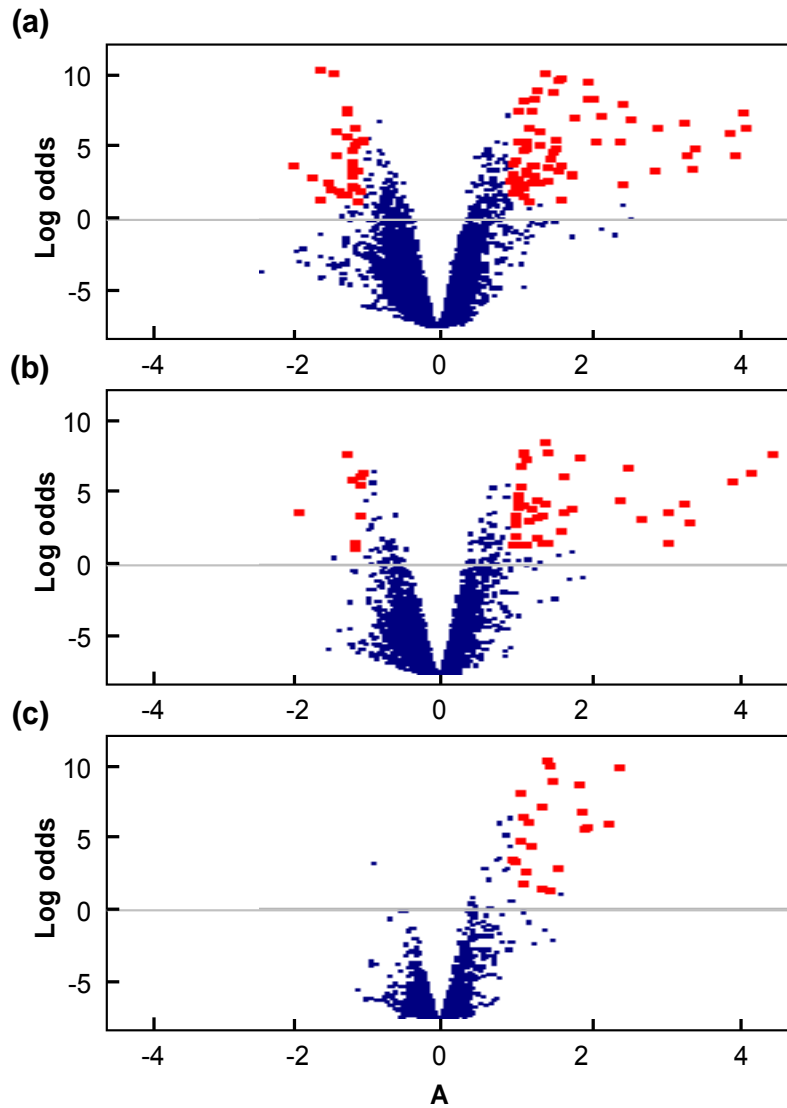
Figure 35. *Volcano plots.* ***(A)*** *MCT,* ***(B)*** *MT, and* ***(C)*** *Tola. Selected genes are indicated by grey dots.*

Figure 36 shows a comparison of the M values between the treatment groups to investigate the similarities and differences of gene regulation.
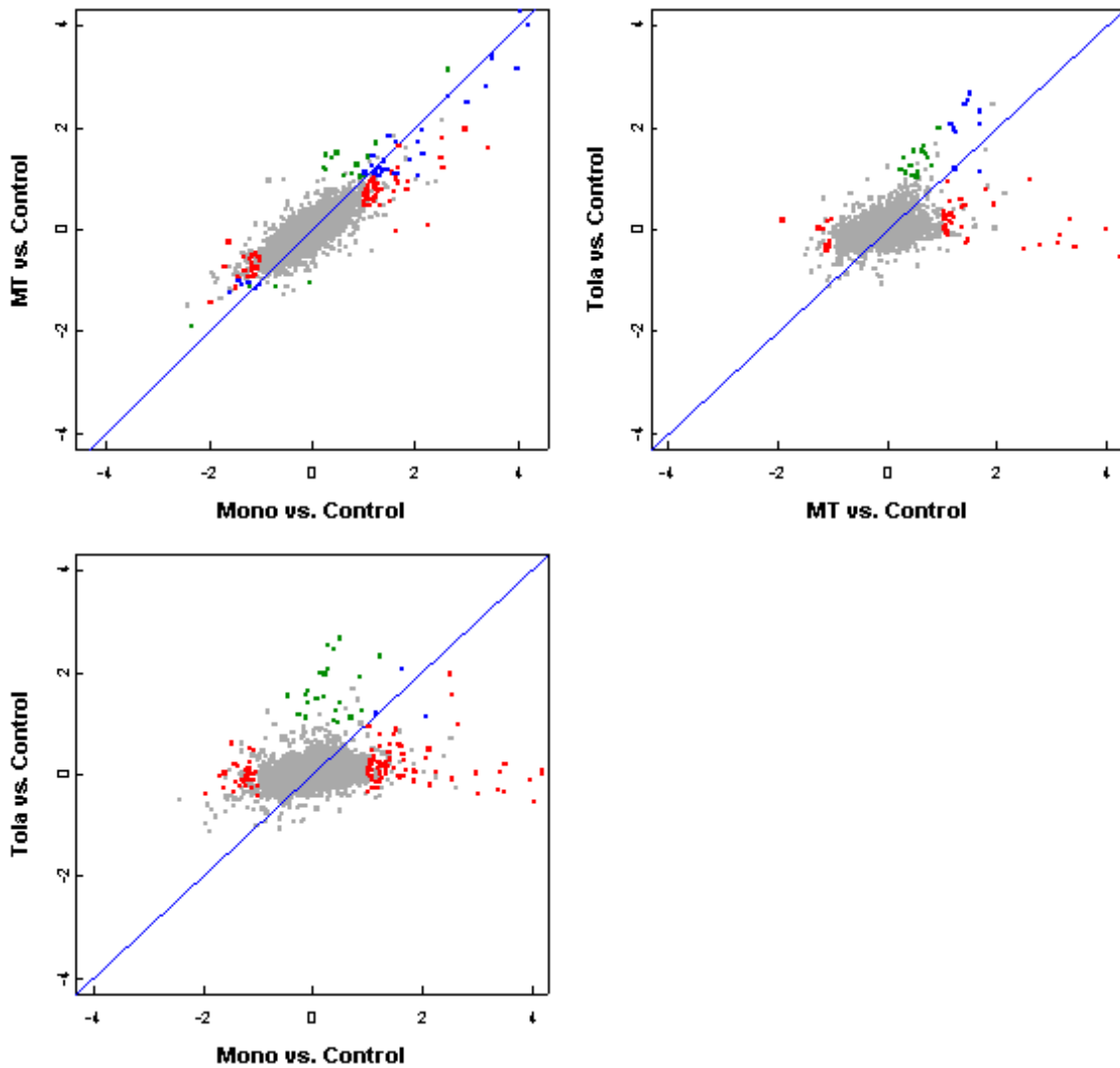
Figure 36. *Comparison of the M Values for Different Conditions. The compared conditions are given by the axis labels: Mono: MCT, Tola: tolafentrine, MT: MCT+Tola. Blue dots: similarly regulated in both conditions; red / green dots: regulated in one but not in the other condition.*

Genes that were found to be regulated in any of the three groups are listed in table 13. In total, 103, 54, and 25 genes were considered to be regulated, in the MCT, MT, and Tola groups, respectively.

Table 13. *Differentially expressed genes in MCT, MT, and Tola groups.*

Growth factor/Cytokines/Chemokines

Gene name	MCT	MT	Tola	GenBank accession
Chemoattractant protein-1	1.2	-	-	NM_031530
Bone morphogenetic protein type ii receptor	- 2.0	-	-	AB073714
Insulin-like growth factor binding protein 6	- 1.0	- 1.1	-	NM_013104
Chemoattractant protein-1	1.2	-	-	NM_031530
Chemokine c-x-c receptor 2 il8rb	-	-	2.0	NM_017183

Transcription and Replication factors

Gene name	MCT	MT	Tola	GenBank accession
Topoisomerase dna ii alpha top2a	1.2	1.1	-	NM_022183
Hypoxia inducible factor 2 alpha hif-2a	- 1.2	-	-	NM_023090
Transcription factor fkhr	- 1.1	-	-	AF247812

Immunoglobin proteins

Gene name	MCT	MT	Tola	GenBank accession
Immunoglobulin light chain	2.1	1.7	1.1	M87786
Immunoglobulin heavy chain variable region	1.6	-	-	AF217571
Immunoglobulin kappa-chain igkv	2.1	1.1	-	L07406
t-cell receptor	-	1.3	1.9	L20987
Immunoglobulin gamma-2a chain	1.6	-	-	L22654

Signalling/ Transporter/ Receptor

Gene name	MCT	MT	Tola	GenBank accession
Sodium/potassium-transporting gamma chain;	1.2	-	-	NM_017349
Serine-threonine kinase receptor type i	- 1.7	-	-	NM_022441
Protein kinase c epsilon subspecies	- 1.4	-	-	M18331
Interleukin 1 receptor-1 fos-responsive gene	1.3	-	-	NM_013037
Interleukin 1 receptor; type ii	-	1.7	2.3	NM_053953
Melanocortin 5 receptor	-	1.2	1.0	NM_013182
t-cell receptor	-	1.3	1.8	L20987
Interleukin-3 receptor beta-subunit	1.2	1.2	1.2	AJ000555
Calcitonin receptor-like receptor	- 1.1	-	-	NM_012717
Adenosine deaminase	1.2	1.2	-	AB059655
Fit-1m fit-1	1.6	1.1	-	U04317
Cell division cycle control protein 2 cdc2a	1.2	1.5	-	NM_019296
Inositol hexakisphosphate kinase	- 1.1	-	-	AB049151
Equilbrative nitrobenzylthioinosine-sensitive	- 1.2	- 1.1	-	NM_031684
Putative g protein coupled receptor g10d	-1.4	- 1.0	-	NM_053302
Ephrin b1 efnb1	- 1.3	-	-	NM_017089
3';5'-cyclic amp phosphodiesterase pde3	-	1.4	2.5	U01280

Serine / Aspartic proteases /Metalloproteinases/ Metabolic enzymes

Gene name	MCT	MT	Tola	GenBank accession
Serine protease	1.5	1.8	-	D88250
Secretory leukocyte protease inhibitor	1.5	1.7	2.1	NM_053372
Convertase pc5	-	1.2	1.2	L14933
Alcohol dehydrogenase 3 adh3	-	1.1	-	NM_019286
Protease ii prt	-	3.1	-	J02712
Mast-cell protease 5 precursor	4.2	-	-	NM_013092
Mast-cell carboxypeptidase a precursor r-cpa	4.1	4.3	-	U67914
Mast-cell protease 1 precursor rmcp-1	4.2	4.0	-	U67915
Mast-cell protease 7 rmcp-7	4.0	3.2	-	NM_019322
Mast-cell protease 8 precursor rmcp-8	3.5	3.4	-	NM_019323
Rat mast-cell tryptase precursor	3.4	1.9	-	NM_019180
Cathepsin K	1.9	-	-	NM_031560
Cathepsin y	1.2	-	-	AB023781

Gene name	MCT	MT	Tola	GenBank accession
Cathepsin s precursor	1.4	1.2	-	NM_017320
Cytochrom c oxidase subunit viii-h heart/muscle cox8h	- 1.6	-	-	NM_012786
Angiotensin i-converting enzyme dipeptidyl carboxypeptidase 1	- 1.2	-	-	NM_012544
Matrix metalloproteinase 9 gelatinase b	-	-	1.1	NM_031055
Tissue inhibitor of metalloproteinase 1 timp1	1.6	-	-	NM_053819
Metallothionein 2	2.5	-	-	M11794

Other proteins

Gene name	MCT	MT	Tola	GenBank accession
Apolipoprotein e rapoe	1.4	1.4	-	S76779
s100 calcium-binding protein a9	-	1.5	2.5	NM_053587
s100 calcium-binding protein a8	-	1.5	2.7	NM_053822
Arachidonate 5-lipoxygenase	1.0	-	-	NM_012822

Several proteases, transporters, signalling, and immunoglobin proteins were regulated after MCT treatment. The additional application of tolafentrine (MT group) resulted in a reduced number of regulated genes, mainly growth factors, chemokines, and transcription factors (e.g., bmp2r, fkhr, il8rb). The regulation of most of the genes involved in inflammatory processes was not influenced by tolafentrine, whereas several genes were upregulated after tolafentrine (Tola) treatment (e.g., Il1Rii, Melanocortin 5 receptor, t-cell receptor, pc5, adh3, prt ii, s100a9, and s100a8).

5.2.2   Pneumolysin Induced Pulmonary Hypertension

To differentiate the local effect of PLY to the lung epithelium that covers the airways and constitutes the first border of innate defense against respiratory pathogens from its systemic effects we applied either the PLY toxin intratracheally (IT) or via the systemic i.e. intravenously (IV). Interestingly, while systemic application resulted in healthy animals similar to the untreated control group, the intratracheal application led to sever illness, respiratory distress and death of the mice. The lungs showed a remarkable increase in weight by development of an edema. Additionally, in an *ex-vivo* model of a ventilated and perfused mouse lung (established in the group of PD Dr. N. Weissmann,

Internal Medicine-II) a significant increase in pulmonary artery pressure (PAP) could be measured (figure 37). Using this observation as a template we investigated the gene expression regulation in the organ model and animal model.
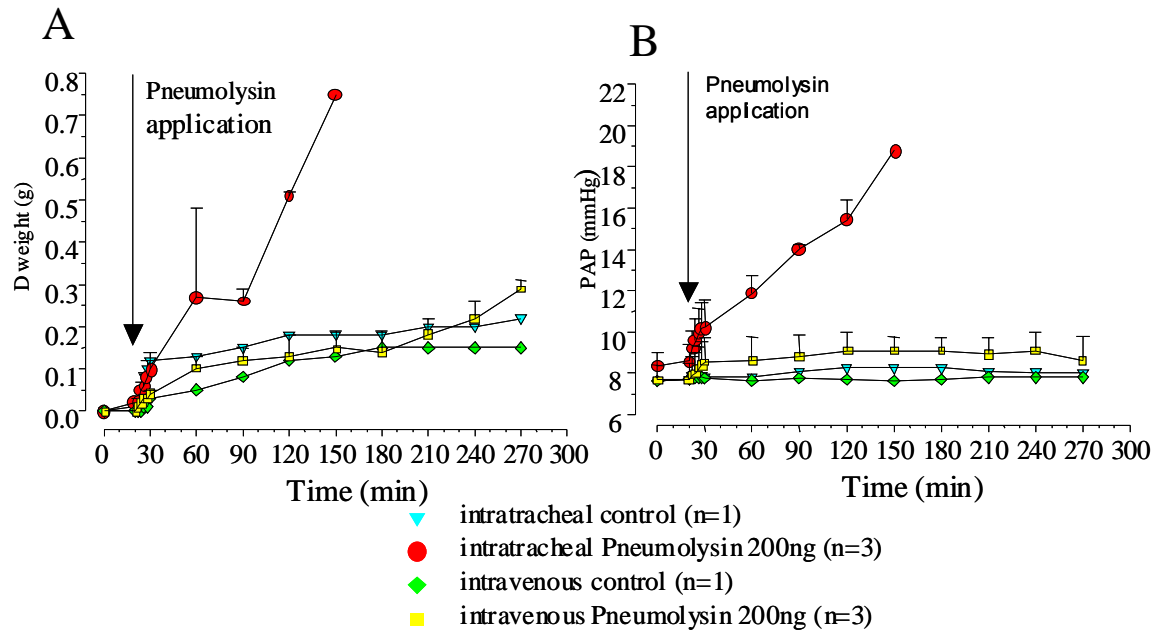
Figure 37. Effect of PLY in mouse lungs. PLY-toxin applied via IV and IT modes shows, increases in lungs weight (A) and PAP (B) via IT mode whereas, via IV mode there was no such changes. (Picture was adopted from N. Weissmann).

5.2.2.1 Expression Profiles on Affymetrix Arrays

Affymetrix arrays were applied to investigate the expression profiles in mouse lungs of mice treated with PLY via IT or via the IV. The lungs were obtained either from animal (*in-vivo*) or from organ (*ex-vivo*) ventilated and perfused lungs models. Total RNA was extracted from *in-vivo* and *ex-vivo* models as described in section 4.1.1. Applying 15 μg total RNA and one round of T7-linear preamplification, 40-50 μg labelled cRNA were generated. Figure 38 shows a representative electropherogram of the cRNA used for the hybridizations.
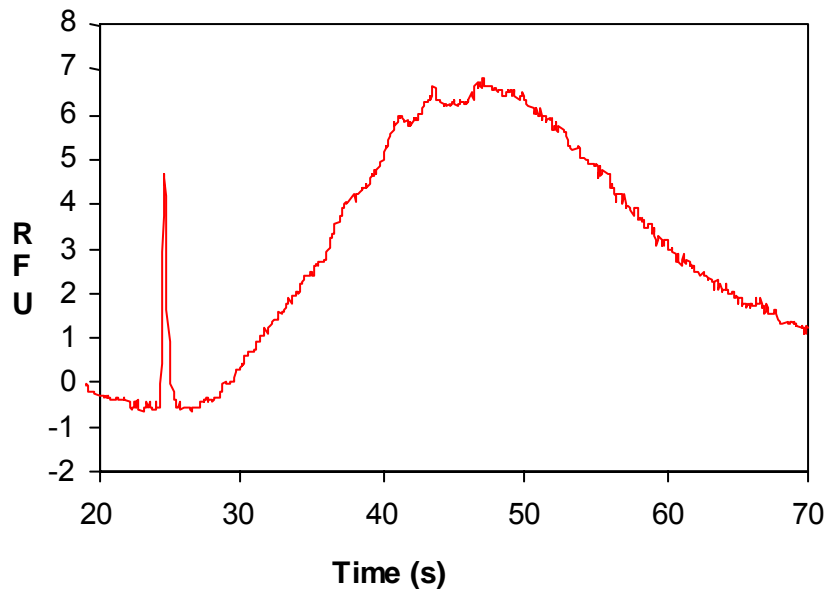
Figure 38. Electropherogram of cRNA. Electropherogram of cRNA obtained after one round of T7-IVT. RFU: relative fluorescence units.

5.2.2.2 PLY-Dependent Gene Expression in the Animal Model (*in-vivo*)

15 µg labelled and fragmented cRNA were hybridized to Affymetrix® GeneChip® U74Av2 arrays at the Max-von-Petemkofer Institute, Ludwig-Maximilian-University of Munich, Germany. Hierarchical cluster analyses were performed using dChip to examine the similarity of the expression patterns between the treatment groups and the controls. The results of the cluster analyses are show in figure 39.
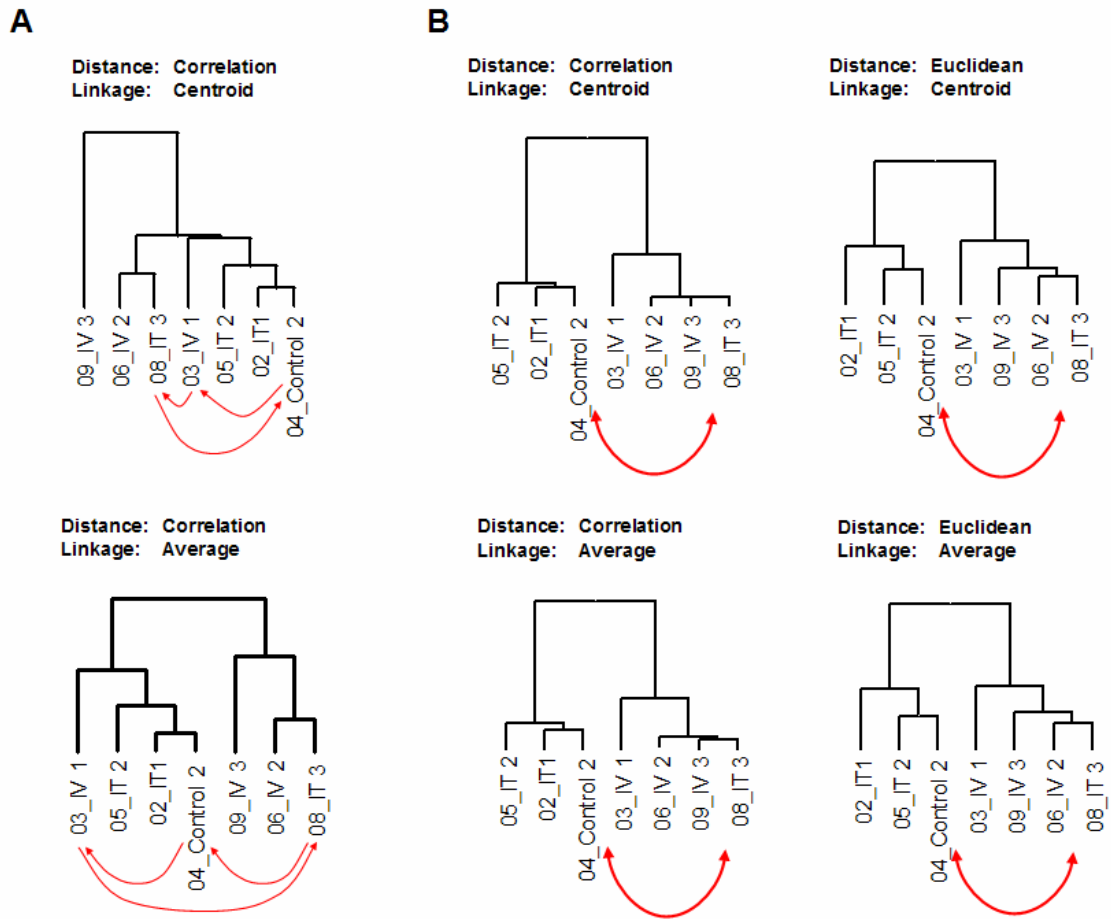
Figure 39. Hierarchical clustering. **(A)** With row and column standardization. **(B)** Without standardization. Distance measure and linkage type are given in the figure. The arrows indicate possible mixes of samples (see text).

The cluster analysis did not separate any of the treatment groups. A possible reason could be mixed-up samples. Using the standardized data, one has to assume the mix-up of at least three samples to get two major clusters clearly separating the IT treated samples (figure 39 a). Without standardization, the clusters seem to be more reasonable with a better separation of the IT group, and a perfect separation after exchanging only two of the samples (i.e., 04_Control 2 and 08_IT 3, fig 39 b). The connection of the clusters, including the propably interchanged samples, was robust with respect to the way the distance matrix and the linkage are calculated.

To confirm the interchange of the two samples, an additional control sample was measured and included in the cluster analysis (figure 40).
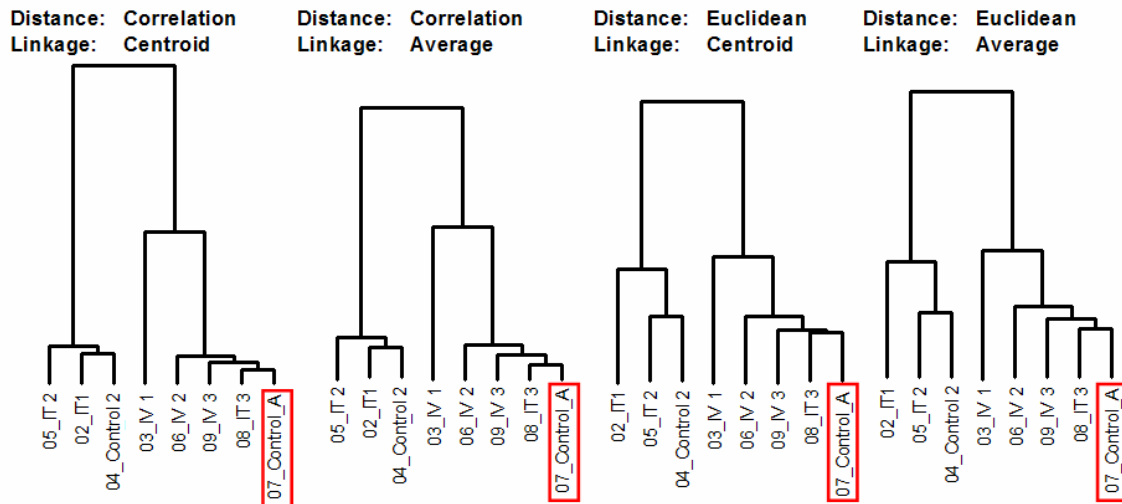
Figure 40. *Hierarchical clustering with an additional control sample. Distance measure and linkage type are given in the figure. A frame indicates the additional control sample.*

The additional control sample (07_Control_A) clusters next to 08_IT 3 which is suspected to be the other control sample, 04_Control 2. This result strongly supports the hypothesis that the samples 04_Control 2 and 08_IT 3 were mixed-up. Consequently, for the further analysis 04_Control 2 was assigned to be 08_IT 3 and *vice versa*. The corrected clusters show a perfect separation of the IT samples from the IV samples and from the controls, whereas there is only a very week separation between the IV's and the controls. Since there is no significant difference between the expression profiles of IV's and controls, the IV's were used as reference for calculating the differential expression of the IT samples.

The data obtained from PLY response via IT revealed 280 upregulated and 30 downregulated genes by more than a factor of 2. (see table I4).

Table 14. *Differentially expressed genes after PLY treatment in the animal model. The log fold changes between the conditions compared are shown.*

Probe ID	Gene Name	IT1/IV1	IT2/IV2	IT3/IV3
96192_at	Trans-acting transcription factor 3	3.48	2.45	5.17

Probe ID	Gene Name	IT1/IV1	IT2/IV2	IT3/IV3
104407_at	Activated leukocyte cell adhesion molecule	3.45	2.68	4.63
92579_at	Sjogren syndrome antigen B	3.42	2.58	4.93
98572_at	DnaJ (Hsp40) homolog, subfamily B, member 11	3.23	2,26	4.96
102906_at	T-cell specific GTPase	3.23	2.02	4.65
161184_f_at	Tyrosine kinase receptor 1	3.23	2.24	5.01
94939_at	CD53 antigen	3.04	2.39	4.14
98472_at	Histocompatibility 2, T region locus 23	3.04	2.19	4.68
161224_f_at	Angiotensin converting enzyme	3.04	2.31	4.29
161104_at	Expressed sequecnce AA408298	3.08	2.53	3.7
92647_at	Retinoblastoma binding protein 4	3.02	2.28	4.35
95120_at	RIKEN cDNA 1100001I23 gene	3.02	2.11	4.53
99643_f_at	Carboxypeptidase E	3.02	2.06	4.69
102904_at	Histocompatibility 2, class II antigen E alpha	3.02	2.15	4.8
92660_f_at	Ubiquitin-conjugating enzyme E2E 1,	2.96	2.15	4.97
96012_f_at	Matrin 3	2.95	2.16	4.46
99532_at	Transducer of ErbB-2.1	2.95	2.19	4.28
92291_f_at	Complement factor H-related protein	2.95	2.03	4.92
96852_at	cAMP dependent regulatory Protein kinase type I, alpha	2.91	2.07	4.59
93104_at	B-cell translocation gene 1, anti-proliferative	2.90	2.14	4.24
93351_at	Hydroxyprostaglandin dehydrogenase 15 (NAD)	2.89	2.00	4.93
160643_at	Histone deacetylase	2.88	2.22	3.91
100032_at	Trans-acting transcription factor 1	2.86	2.32	3.53
100344_at	CD2-associated protein	- 2.28	- 2.01	- 2.61
93908_f_at	Carbon catabolite repression 4 homolog (S. cerevisiae)	- 2.45	- 2.05	- 2.96
161341_f_at	GA repeat binding protein, beta 1	- 2.48	-.2.07	- 3.00
92306_at	Ovary testis transcribed	- 2.61	- 2.02	- 3.29
100914_at	CD84 antigen	- 2.63	- 2.19	- 3.12
100721_f_at	Recombinant antineuraminidase single chain Ig VH and VL domains	- 2.72	- 2.07	- 3.85
101732_at	Per-hexamer repeat gene 5	- 3.04	- 2.34	- 3.82
98772_at	Small inducible cytokine B subfamily, member 5	- 3.14	- 2.36	- 4.46
97127_f_at	Vomeronasal 2, receptor, 15	- 3.25	- 2.72	- 3.89
100687_f_at	Vomeronasal 2, receptor, 14	- 3.39	- 2.46	-4 .15
98524_f_at	RIKEN cDNA 2210039B01 gene	- 3.39	- 2.46	- 4.41
94028_f_at	CD84 antigen	- 3.94	- 2.74	- 5.53
103269_f_at	Zinc finger protein 125	- 4.07	- 3.00	- 5.43
98577_f_at	Endogenous retroviral sequence 4	- 4.28	- 2.94	- 7.50

Probe ID	Gene Name	IT1/IV1	IT2/IV2	IT3/IV3
103267_i_at	Zinc finger protein 125	- 4.60	- 3.56	-6.08
160934_s_at	Intracisternal A particles	- 5.30	- 4.52	- 6.22
160906_i_at	RIKEN cDNA 2210039B01 gene	- 7.72	- 4.52	- 11.4
100920_at	RIKEN cDNA 2210039B01 gene	- 8.12	- 5.34	-14.5
102818_at	Xlr-related, meiosis regulated	- 8.20	- 4.41	- 26.0

5.2.2.3 PLY-Dependent Gene Expression in the organ model (*ex-vivo*)

The genes found to be regulated by more than a factor of 2 in the *ex-vivo* PLY treated lungs are listed in table 15.

Table 15. *Differentially Expressed Genes after PLY Treatment in the ex-vivo Model. The log fold changes between the conditions compared are shown.*

Probe ID	Gene Name	log fold-change
	IT versus IT C	
100593_at	Troponin T2, cardiac	2.93
101071_at	Myosin heavy chain, cardiac muscle, adult	2.70
101028_i_at	Actin, alpha, cardiac	2.48
100921_at	Troponin I, cardiac	2.40
160487_at	Myosin light chain, alkali, cardiac atria	2.21
93534_at	Decorin	1.84
160242_at	Expressed sequence AU014660	1.76
98049_at	RIKEN cDNA 1300018I05 gene	1.70
103349_at	Yamaguchi sarcoma viral (v-yes-1) oncogene homolog	1.89
93617_at	Chemokine (C-C) receptor 1,-like 2	-1.98
97740_at	RIKEN cDNA 3830417M17 gene	-2.04
93869_s_at	B-cell leukemia/lymphoma 2 related protein A1d	-2.17
102658_at	Interleukin 1 receptor, type II	-2.54
161689_f_at	Interleukin 1 receptor, type II	-2.87
98423_at	Gap junction membrane channel protein beta 2	-3.17
93858_at	Small inducible cytokine B subfamily (Cys-X-Cys), member 10	-3.31
	IV versus IV C	
96875_r_at	RIKEN cDNA 1200003J11 gene	2.16
104046_at	Expressed sequence AU021774	2.10
92569_f_at	Nucleolar protein 5	2.01
102197_at	Nucleobindin 2	1.97

Probe ID	Gene Name	log fold-change
104340_at	Methyl-CpG binding domain protein 1	1.96
98465_f_at	Interferon activated gene 204	1.96
97205_at	Expressed sequence AA409117	1.91
99535_at	Carbon catabolite repression 4 homolog (S. cerevisiae)	1.91
93316_at	cDNA sequence AB017026	1.90
96041_at	RNA binding motif protein 3	1.86
161980_f_at	Bcl2-associated athanogene	1.84
95518_at	RIKEN cDNA 1810015C04 gene	1.82
92789_r_at	centrin 3	1.81
93430_at	chemokine orphan receptor 1	1.80
104419_at	DNA segment, Chr 14, ERATO Doi 453, expressed	1.79
103015_at	B-cell leukemia/lymphoma 6	1.71
99031_at	Expressed sequence AA407558	1.71
92660_f_at	ubiquitin-conjugating enzyme E2E 1, UBC4/5 homolog (yeast)	1.71
94939_at	CD53 antigen	1.69
96238_at	RAB11a, member RAS oncogene family	1.69
161104_at	Expressed sequence AA408298	1.68
95516_at	RAB9, member RAS oncogene family	1.67
99582_at	Tumor-associated calcium signal transducer	1.67
99462_at	Topoisomerase (DNA) II beta	1.65
103275_at	ATPase, H+ transporting, lysosomal (vacuolar proton pump) noncatalytic accessory protein 1A (110/160 kDa)	-1.80
102698_at	Endothelial PAS domain protein 1	-3.40

5.2.2.4 Intersection of the results found in the *in-vivo* and *ex-vivo* models

An intersection of the results between *in-vivo* (IT/IV) and *ex-vivo* (IT/IT-control) models was made to understand the similarities between them. Genes that were showing similar regulation pattern in *in-vivo* model (IT/IT-control) and *ex-vivo* model (IV/IV-control) are shown below:

Topoisomerase II beta

R- cDNA 18100115C04

R-cDNA C330007P06 gene

Sjogren syndrom antigenB

Bcl2-athanigene 3

CD53 antigen

R-cDNA 231000F16 gene

MAC kinase 1

Centrin 3

Phosphofructokinase, platelet

RA11a, member RAS oncogene family

Expressed sequence AA409117

Expressed sequence U13839

Syndecan binding protein

RAB9, member RAS oncogene family

Laminin B1 subunit 1

No genes were found to show similar regulation patterns in the *in-vivo* model (IT/IT-control) and in the *ex-vivo* model (IT/IT-control).

6 Discussion

6.1 Microarray technology

Microarray analysis is a very powerful technique that can provide important information. It is necessary to validate all data obtained through microarray analysis. Microarrays can provide information on global gene expression in an organism, tissue, or cell. Unfortunately, microarray technology is not a simple technique in practice. To establish the application of microarray technology in the laboratory, many technical parameters and methods need to be optimized to minimize technical errors associated with microarray studies. In particular, RNA extraction, preamplification, labelling, as well as the complete slide handling including pre-processing, hybridization, washing and drying have to be optimized carefully in order to obtain best possible results.

6.1.1 RNA Isolation and Labelling

The major factor that determines the quality of the microarray experiment is the quality of the sample RNA used. Since RNA quality and quantity is the most critical checkpoints to perform microarray experiments, three different known methods for RNA extraction were tested. The combination of RNA extraction by Trifast and the purification employing an RNeasy column including a DNase treatment was most productive (100 µg RNA / 60 mg tissue and yielded pure nucleic acids ($OD_{260}/OD_{280} \geq$ 1.8).

To investigate the expression profiles, the extracted and purified RNA sample has to be labelled, i.e., labelled cDNA or aRNA have to be made using the isolated RNA as template. The cDNA can either be labelled directly by introducing Cy-labelled deoxynucleotides during the reverse transcription or indirectly by introducing aminoallylated deoxynucleotides that are subsequently coupled to free reactive dye molecules. It is essential to generate sufficient amounts of labelled products to get

detectable signals for all present sequences. The presently available laser powers and sensitivities of the detection systems yield optimal results when more than 20 pmol CyDyes are hybridized. The dye molecules attached to the cDNA should be separated by an average of 100-200 nucleotides, what corresponds to a frequency of incorporation (FOI) of 5-10 CyDyes / kb. Lower FOIs make more cDNA necessary to get sufficient fluorescence signals. It can be problematic to get enough cDNA for low FOIs. Additionally, the absolute amount of cDNA required for sufficient signals might then be so high that the spotted probes get saturated. It is not yet solved if and how the fluorescence signals can be normalized, i.e., corrected for intensity-dependent artefacts, when a considerable fraction of the spots is saturated. In this case, some of the ratios would be the result of the total abundance of labelled target sequences, whereas others would be the result of an actually competitive hybridization and directly reflect the relative amounts of two samples. On the other hand, higher FOIs result in a steric hindrance during hybridization and to a loss of signal due to intermolecular energy transfer between the fluorophors.

The results presented in 5.1.3 suggest that it is much more likely to get relatively low FOIs. The FOI for indirectly labelled cDNA is expected to be the highest among the tested methods, because the amino-modified deoxynucleotides are much smaller than the comparably bulky CyDye-conjugates and thus are incorporated with a higher fidelity by the enzyme. Additionally, the aminoallylation is performed for three PCR cycles, enhancing the yield. However, the comparison of the amounts of generated cDNA reveals that the repetitive aminoallylation is the major factor for increased amounts of labelled products: whereas the FOI of the indirectly labelled products was only slightly higher than that of the directly labelled products (11 vs. 7.5), the total amount of incorporated dyes was more than eight times higher. Corrected for the FOI follows a total yield of about 8 nmol (2.5 nmol) cDNA for the indirectly (directly) labelled product. This demonstrates that the efficiency of the aminoallylation-PCR was considerably lower than 2 (~1.5), indicating some disturbing influence of the allylated deoxynucleotides. For oligonucleotide-spotted arrays, the effective difference between the two methods is less pronounced as indicated by the presented values, because only half of the indirectly labelled double-stranded cDNA can actually hybridize to the spotted sequences.

Furthermore, the results in 5.1.2 demonstrate that there are differences in the fidelities of different reverse transcriptases to incorporate Cy-labelled nucleotides, too. SuperScript II was more efficient and more productive (30 pmol) than OminiScript, followed by FluoroScript and CyScribe.

6.1.2 Hybridization and Washing

The quality of the scanned images has a major impact on the value of the results. A predominant problem during this work concerning the image quality was extraordinary high background fluorescence on the slides. This background was observed mainly as a "green" smear more or less equally distributed over the slides, but also as "red" rings around the spots (figure 18).

First, the red rings are likely to be a property of the slides itself. This is supported by the fact that they were observed exclusively on the cDNA-spotted slides obtained from the DKFZ. It is possible that these fluorescing structures are caused by a suboptimal composition of the spotting buffer and/or by suboptimal spotting conditions, e.g., by an inadequate humidity in the spotting chamber. It was not possible to remove these artefacts with extensive washing of the slides. A proper evaluation of such slides is not well possible, because the spot-finding algorithms are unable to identify spots surrounded by excessive fluorescence. Additionally, a local background correction would result in negative values when the intensity of the ring structures is higher than those of the spots.

Secondly, the green smear can have many different sources, so that the identification of the actual origin may be quite difficult. The most prominent sources for background fluorescence are dyes or labelled non-hybridized products remaining on the slide after insufficient washing. Alternatively, SDS as part of many washing buffers may remain on the slides and thus add to the background fluorescence.

Remaining dyes would give measurable background signals in both channels. This was not observed during the works. It is thus unlikely that insufficient washing was the reason for the observed high background. SDS was also implausible since the whole

amount of SDS in the wash buffers is not able to cause such high fluorescence as observed (figure 18 a).

To select a reliable set of series of wash buffers (i.e. initially with low-stringency wash buffer, then with high-stringency wash buffer, and finally with post-wash buffer), we have tested three different series of set of wash buffers on cDNA spotted slides from DKFZ and oligospotted slides from MWG. Our buffer tests show that test 3 (as described in 5.1.4.1) on DKFZ and MWG slides did not show green fluorescency while the other two tests i.e. test 1 and test 2 (as described in 5.1.4.1) showed fluorescency. This tests suggests us to use only a third set of buffers i.e. initially with low-stringency wash buffer 2XSSC; 0.2%SDS, then with high-stringency wash buffer (1X SSC), and finally with post-wash buffer (0.5% SSC).

Ethanol has also been discussed as a source of unspecific fluorescence.[81] This finding can be supported by the results of this work (see figure 19). It is a source of direct contamination of the slides that need to be preprocessed with ethanol, but additionally indirectly by the manifold and the slide covers of the hybridization station that are intensively washed with ethanol.

Unfortunately, the background fluorescence could not be eliminated by changing the ethanol brand, indicating a further source of the contaminations. Following the hints of personal communications with the members of the DKFZ, also the canned air used to dry the slides was tested. It turned out that the canned air itself does not seem to contain any fluorescent particles. Not any fluorescence was measured on dry slides that have been intensively sprayed with canned air. However, using wet slides, significant background signal was detected (figure 20). Again, it took another round of investigation until it became clear that the manifold – also dried with canned air– accumulates fluorescing particles that are flushed over the slides during the machine washing (figure 21).

Finally, oligonucleotide arrays appear to have some important advantages over cDNA arrays. In particular, specific, highly unique sequences can be selected for each gene and thus cross-hybridization can be minimized. Furthermore, most of the cDNAs in the cDNA libraries are insufficiently annotated. Apart from these advantages,

oligonucleotide-spotted arrays exhibit superior spot morphologies. This is demonstrated in 5.1.5. All key parameters of the slide quality, i.e signal-to-noise ratio foreground-to-background ratio, and spot morphology were clearly better for the oligonucleotide spotted arrays than for the cDNA spotted arrays.

6.1.3 RNA Preamplification

Amplification strategies represent the most promising approach currently being pursued to reduce the microgram quantities of RNA required to perform single microarray hybridization. At present, the most commonly used amplification methods are (i) linear amplification by *In-vitro* transcription (IVT) and (ii) PCR based exponential amplification with a switching mechanism at the 5' end of the RNA transcript (SMART). Here, the performances of both methods were compared. Although both methods have been tested for reliability and suitability,[87] a fair and direct comparison of both methods has not yet been published. Recently, a comprehensive comparison study for the expression profiling using one microgram of total RNA for IVT (one round) and SMART have been reported by M. Saghizadeh *et al*. They showed that the relative abundance of RNA species in the amplified probes (IVT and SMART) is highly maintained during the amplification process, independent of the method.[87] However, 1 µg total RNA is still hard to obtain from small biopsies of laser microdissected cells. Thus 50 ng total RNA were used in this work, which is 20 times less then used by M. Saghizadeh *et al*. Since one round of IVT does not yield enough product for a satisfactory hybridization from this little amount of starting material, two subsequent rounds IVT were performed.

The process of IVT preferably amplifies sequences close to the poly-A tail of the mRNAs.[88] This effect is responsible for the lower average length of aRNA compared to that of the mRNA. Although this fact has no significant influence on the outcome of microarray experiments when only one round is performed, it is likely that this may result in an accumulation of drastically shortened products after two subsequent rounds of IVT. These short products may lack the parts of the sequence complementary to the spotted probes. In contrast to the IVT, SMART is said to amplify full-length products avoiding the problems arising from poly-A biased products.[89] On

the other hand the exponential amplification possess the potential to amplify small initial errors and hence to alter the underlying transcription profile.

The results presented in 5.1.6.1 demonstrate that two rounds of IVT do in deed result in a strongly biased amplification of sequences close to the poly-A tail, whereas SMART amplifies all sequences equally well. After 2 rounds of IVT, the highest ΔCt values observed were about 10, that corresponds to a $2^{10} \approx$ 1000-fold overall amplification (GAPDH-3'UTR). The tested sequence of PBGD with a distance of 1400 bp to the poly-A tail revealed an amplification factor of just 5. The observed reduction of the amplification factors corresponds well with the ratios of 3'-to-5'-signals reported for affymetrix arrays.[90] These results demonstrate the ability of SMART to amplify longer products than T7-IVT.

It is reported that one round of IVT yields up to ~2 µg aRNA from 100 ng total RNA.[91] Under the assumption that about 1- 5% of total RNA are polyA RNAs, this corresponds to a 400 - 1000-fold amplification. After two rounds of IVT starting with 50 ng total RNA about 50 µg aRNA were obtained, corresponding to a $2 \cdot 10^4 - 10^5$-fold amplification of the polyA RNAs. This yield is marginally less than theoretically expected (~10^6), that could be explained by the fact that Cy-labeled ribonucleotides had to be incorporated in the second round of IVT likely reducing the efficiency of the RNA polymerase. Additionally, a loss-prone purification step had to be performed. Interestingly, the amplification factors of specific target sequences as determined by real-time PCR were considerably lower. The reason for this discrepancy remains unclear, but the amplification of non-polyA RNA may serve as a possible hypothesis.

The amplification factors obtained by 12 cycles SMART are already higher than those obtained by 2 rounds of IVT, and they still can be further increased by performing more PCR cycles. After 24 cycles of SMART, the ideal efficiency of amplification is not reached. Instead of a shift of the Ct values by 24, the shift observed was only 18. This can be attributed to the fact that the reaction ran into to plateau phase. Because the amplification processes become unpredictable when the accumulation of products starts to plateau, it must be taken care that PCR cycles have to be stopped in time. When the amount of starting material is not known, the optimum number of cycles yielding as much product as possible without running into the plateau phase should be

empirically determined. This can be done according to the procedure described in SMART Fluorescent Probe Amplification kit manual: after each (two) cycle(s), an aliquot of the SMART reaction can be introduced to a real-time PCR. Plotting the Ct values versus the numbers of SMART cycles will reveal a negative linear trend until the point where the SMART reaction started to plateau.

How accurately the transcription profiles were maintained by the amplification methods was analysed in microarray experiments. Here, aliquots of RNA from mouse liver and kidney were subjected to a direct labelling as well as to preamplification and labelling by 2 rounds IVT and by 15 cycles SMART. The direct comparisons of the M values from two independent replicates demonstrate a very bad correlation of profiles after IVT (figure 26). This extreme result is unexpected since the linear amplification should yield more constant or reliable results than the exponential amplification. To elucidate whether this low correlation was due to experimental errors, more repetitions would have to be performed. Anyway, these results show that two rounds of IVT hold a high risk of low reproducibility.

As already expected from the inferior correlation of technical repeats, the averaged profiles of the IVT amplified samples correlated only weakly with those of the unamplified reference (figure 27). In contrast, the SMART amplified samples correlated noticeably better with the reference (figure 27). Both comparisons show that the M values of the preamplified samples are compressed relative to the reference. This phenomenon is also reported by others.[90-91]

Another important property to address is the accuracy of the results. This point is difficult to assess and frequently not even touched in the respective publications. Ideally, samples with known expression profiles would be required to estimate the accuracy of microarray experiments, but such information is not (yet) available. At least parts of this information are increasingly more collected in expression databases. The comparison of the lists of differentially expressed genes between liver and kidney with the results presented in the databases showed that the number of false positives is low for all samples (figure 29, right one). The false-positive rate was low even for the IVT amplified samples, although the two individual experiments had a bad correlation / high variance. This high degree of correctly selected genes may be attributed to the robust Bayesian algorithm of candidate selection. Notably, the list obtained from the SMART

amplified samples was not only larger, but also contained more correct genes than the list of the unamplified reference sample (figure 29, right one). That fact that more genes were selected can be explained by the lower inter-assay variance of the SMART samples. Again, this might be a general effect of the SMART reaction itself or just the result of lucky circumstances. To comprehensively evaluate this aspect, considerably more repetitions have to be done.

In conclusion, SMART turned out to be the preferred technique to amplify very small amounts of RNA. It was more reliable, precise, and accurate and considerably less time-consuming than two rounds IVT. Moreover, in contrast to IVT that produces relatively unstable aRNA, SMART yields labelled cDNA that is less prone to degradation by prolonged storage and repeated freezing/thawing cycles.

6.2 MCT-Dependent Gene Expression

6.2.1 Differences between Nylon- and Glass-Arrays

Microarray technology permits the analysis of the gene expression profile of rats lung tissue obtained from MCT-induced and Tola-attenuated PH to compare to that found in normal lung tissue. In this rat model, the subcutaneouslly applied monocrotaline (an alkaloid toxin) induces on the basis of inflammation changes in the structure and function of endothelial cells, smooth muscle cells, and fibroblasts contributing to the vascular remodelling, altered tone, and vasoreactivity that are characteristics of chronic pulmonary hypertension.[92-93].

For the expression profiling study we used small pieces of lung tissue samples keeping in consideration that these samples are representative for the entire lung. Starting with nylon filters and 1,176 spotted cDNAs, we investigated the expression profile of MCT-induced and Tola-attenuated PH in rats.

In MCT group, out of 703 evaluated genes, 11 genes were selected. Among the selected genes, one of the most upregulated genes was Gamma-aminobutyric acid (GABA) receptor alpha 1. GABA is an important inhibitory neurotransmitter in the

mammalian CNS and also found in peripheral tissues, including the lung. It has recently been shown to modulate the contraction of airway smooth muscle.[94] Thus, it has to be evaluated now which compartment has caused the regulation of this receptor.

Alkaline phosphatase (ALP) was also found to be upregulated. In lung lavage fluids, an increased level of ALP is a marker for tissue damage and type II cell proliferation. Type II pneumocytes are extensively involved in the inflammatory process within the alveolar septum that may explain the upregulation. Moreover, an increase of the ALP: albumin ratio in bronchoalveolar lavage fluids from patients with chronic interstitial disorders may reflect a fibrosing progression.[95]

Alterations in the levels of the growth factor transcripts such as Platelet-derived growth factor (PDGF)-associated protein may have a significant role in the development of pulmonary hypertensive disease. PDGF-associated protein has been implicated in myointimal proliferative arteriopathy, a lesion seen in monocrotaline-induced pulmonary hypertension. Arcot SS *et al.* showed that transcripts of PDGF were increased in the early stages but declined in the later stages of MCT-induced hypertension.[96] Well in line with this finding we found the PDGF associated protein downregulated after 4 weeks as well.

Additionally, rac-alpha serine/ threonine kinase and Rab-3b ras-related protein, two members of the group of oncogenes and tumour suppressor proteins, were found to be downregulated indicating changes in the proliferation rate and induction of apoptosis.

However, the most important result of the approach with nylon filters is the weak or even absent correlation of the single experiments. Obviously, preparation of animals by different experimenters at different time points contributed in a way to the overall variation that it may almost completely prevent a reasonable statistical analysis. Only the expression profiles from the experiments #2 and #3 exhibit a weak correlation (figure 32 C). Exactly these two experiments have been conducted in parallel by the same experimenter (the animals were prepared at the same day from the same person), whereas all other animals were prepared at different days from different experimenters. This demonstrates the necessity of strategical planning of the process of sample collection and the importance of a parallel sample preparation.

6.2.2 Effects of MCT Treatment

Using oligonucleotides spotted glass chips, we characterized the expression pattern in the lung tissue obtained from the three different groups i.e. MCT, MCT+Tola (MT) and Tola alone to compare with that found in normal lung tissue. So far, less work has been performed in context to identified candidate genes that are involving in PH disease. Recently, Norbert F. Voelkel *et al.* investigated differentially regulated genes in PPH human samples.[97] Here, for selecting differentially regulated genes in each groups, we applied a regulation criterion that is a twofold change in expression [log2 ratio of 1.0 (upregulation) or -1.0 (downregulation)].

As the inflammatory mechanisms appear to play a significant role in MCT-PH model,[36] we hypothesized that factors such as inflammatory mediators, proteases and elastase, matrix metalloproteinase, ion channels, or vascular endothelial growth factors may have role in progression of the disease. We obtained 103 genes, which were regulating with a 2-foldchange. Few of them are discussed here.

A link between MCT-induced inflammation and smooth muscle cell (SMC) proliferation was first suggested by certain findings in pulmonary hypertension. SMC proliferation has also been demonstrated in the pulmonary vasculature in chronic PH of animal models.[98] Proinflammatory interleukins are intriguing candidates for a MCT-induced SMC-derived autocrine growth factor. As expected, pro-inflammatory genes like IL-3 receptor beta and IL-1 receptor 1, excessively produced in the lungs of rats treated with monocrotaline,[99] were upregulated here. Overexpressions of these cytokines stimulate proliferation of SMC. Such proliferation may contribute to the pathophysiological effects of chronic MCT induced PH and thus may play a role in the development of pulmonary hypertension.

Overexpression of arachidonate 5-lipoxygenase and chemoattractant protein-1 (MCP-1) was shown in endothelial cells of plexiform lesions and inflammatory cells in patients with PPH.[100] Interestingly, these genes were upregulated with more than a factor of 2.0, suggesting that upregulation of these enzymes involved in generation of inflammatory mediators and may play a role in the pathogenesis of PH.

Mast cells are specialized immune effector cells that synthesize and store in their granules large amounts of serine proteases, marked, statistically significant increases in proteases (particularly derived from mast cells) of vascular obliteration and pulmonary hypertension. Mast-cell-derived proteases may play a role in regulating the development of neointimal pulmonary vascular occlusion and pulmonary hypertension in response to injury. Indicating involvement in the remodelling process, our array data show that several mast-cell-derived proteases like mast-cell protease 1, 5, 7 and 8 precursors were highly upregulated by more than a factor of 5.0. Similar regulation pattern for mast cell proteases in MCT rat model was reported by Laszlo T *et al.*[101] In addition to this, other proteases like serine protease was found to be upregulated. Increased activity of serine proteases in pulmonary arteries has been observed during early remodelling in MCT-induced pulmonary hypertension.[102]

Besides mast cell proteases and serine proteases, some other proteases expression was found to be significantly elevated during the development of disease, for example, cathepsin K (3.0-fold) and cathepsin Y (approx. 2.0-fold) which has an influence on developing PH. Cathepsin K is a protease with potent fibrinolytic activity that may play an important role in extracellular matrix degradation. Again Laszlo T *et al.* showed upregulation of cathepsin K in MCT rat model.

Important changes occur in PH in the vascular adventitia, with increased production of the extracellular matrix. Cowan *et al.* recently showed that direct inhibition of serine elastases led to complete regression of pathological changes in experimental PH caused by monocrotaline.[103] Because metalloproteinases are potentially destructive agents, their production is tightly controlled at several levels. A way in which the activity of MMPs is regulated is based on the presence and activity of specific inhibitors such as TIMP-1,[104-105] which was upregulated, such overexpression is due to the interaction of MMPs with their specific inhibitors that determines the net activity of secreted enzymes during pulmonary artery remodelling. Because our results showing that mast cell proteases, cathepsins, and TIMP are increased during progression of pulmonary hypertension that extends the observations that experimental pulmonary hypertension involves extensive remodelling of extracellular matrix. [103]

Upregulation of Insulin-like growth factor-1 IGF has been recognized as likely having a role in stimulating smooth muscle hyperplasia.[106] IGF-I directly stimulate fibroblast

proliferation and perhaps collagen synthesis.[107] We found upregulation of IGF, such overexpression of IGF-1 can leads to increased cell proliferation decreased apoptosis and increased smooth muscle elastin synthesis that may play an important role in vascular remodelling in chronic pulmonary hypertension.

A member of the metal binding protein family is metallothionein 2 (MT-2), a low–molecular weight, cysteine-rich, heavy metal-binding protein can be easily induced by heavy metals, hormones, acute stress, and various chemicals.[108] In our approach, MT-2 was upregulated. This enzyme might play a role in the pulmonary defense against zinc toxicity and free radicals. As MCT rat model is a chronic PH model it influences upregulation of MT-2 against toxicity and free radicals. Interestingly, upregulation of metallothionein 1 and 2 in pulmonary arteries were found in parallel during hypoxia induced pulmonary hypertension (unpublished data communicated by L. Fink). Furthermore, MT-2 previously has been shown to increase after an ischemic insult.[109] Flavin-containing monooxygenase 1 (FMO) is a member of xenobiotic-metabolizing enzymes family. In normal condition, FMO oxidatively metabolizes a wide variety of nitrogen-, sulfur-, and phosphorous-containing xenobiotics compounds. In our setting, downregulation of FMO indicates the increased deposition of toxic reactive intermediates that might involve in a vascular injury.

On the other hand several genes were differentially downregulated in response to MCT. Among downregulated genes most of them are belongs to kinases family, for example; fms-related tyrosine kinase 1, protein kinase c, serine-threonine kinase receptor type I activin, and Inositol hexakisphosphate kinase (IP$_6$) enzymes were found to be downreguled. Kinases have been shown in vascular smooth muscle cells to regulate the expression of p27KIP1 leading to an enhanced G1/S transition of vascular smooth muscle cells.[110] A member of apoptosis regulation family i.e. IP$_6$ in response to MCT was downregulated. Members of this family involved in apoptosis regulation.[111] Furthermore, IP$_6$ is a naturally occurring polyphosphorylated carbohydrate that is present in substantial amounts in almost all mammalian cells, which are important for regulating vital cellular functions. It was recently recognized to possess multiple biological functions. A striking anticancer effect of IP$_6$ was demonstrated in different experimental models IP$_6$ is involved in apoptosis and vessel maintenance.[112]

Some receptors play a key role in angiogenesis. Ephrin b1 was downregulated and is known to be involved in vascular development and angiogenesis.[113] Downregulation of ephrin b1 results in reduced vessels sprouting and development.

Interestingly, the most downregulated gene in our approach is BMPR-II that is known to have an important role in PPH. Diverse mutations in BMPR-II receptor followed by functional loss of BMPR II have been reported in patients with PPH.[114] BMPR2 encodes a type II receptor member of the transforming growth factor-ß (TGF-ß) superfamily. Type II receptors have serine/threonine kinase activity and act as cell-signallimg molecules. Following ligand binding, type II receptors form heterodimeric complexes with membrane-bound type I receptors. This initiates phosphorylation of the type I receptor and downstream signalling via intracellular Smads.[115] This pathway is diverse and the specificity in cell growth and differentiation is mediated through transcriptional control. Thus, for the first time downregulation of BMPR2 was found in an animal model of PH.

6.2.3   Effects of MCT attenuation with Tolafentrine

For the MT group we hypothesized that some functionally related genes would be consistently and statistically significantly coexpressed during the development of disease and downregulated in response to treatment. Our first hypothesis came out to be true and 33 genes found to be regulated in MCT group showed similar regulation pattern in the MT group as well. Among these genes, 28 (5) were up-(down-) regulated. Many of them belong to the mast cell proteases, proteases inhibitors (TIMP-1), and immunoglobulin molecules. This similar regulation pattern in MCT and MT groups (typically seen for mast cell proteases) might have the reason that tolafentrine (a synthetic PDE 3/4 inhibitor) does not effect the structural matrix remodelling process. In continuation, Kohyama T e*t al.* showed that out of three types of PDE4 inhibitors (cilomilast, amrinone, and zaprinast), only cilomilast significantly inhibited the MMP-1 release and activation while neither amrinone nor zaprinast had any effect on collagen degradation and MMP-1 activity.[116]

Adenosine has been implicated as a modulator of inflammatory processes central to asthma.[117] Adenosine is a signalling nucleoside that is generated in hypoxic

environments such as that found in the inflamed lung, suggesting that it might serve a regulatory role in chronic lung diseases. High expression of this gene is associated with persistent lung inflammation and damage. In our findings the gene encoding the adenosine deaminase was upregulated in both groups.

Among the 5 most down regulated genes, adrenomedullin was downregulated in both, MCT and MT group. Adrenomedullin is a potent vasodilator peptide that is secreted constitutively by vascular endothelial and smooth muscle cells[118] and is expressed at high levels in the lung.[119] The downregulation of adenosine could lead to the restriction of vasodilator molecules resulting in an imbalance between vasoconstrictors and vasodilators.

Bone morphogenic proteins (BMPs) play pivotal roles in the regulation of embryonic lung development and branching of airways and have recently been considered to influence inflammatory processes in adults due to their chemotactic activity on fibroblasts, myocytes, and inflammatory cells. BMP-6 or vgr, is a member of the TGF-beta superfamily appearing to modulate mesenchymal differentiation, including the processes of cartilage and bone formation. This factor may be considered as a prototype for the largest subgroup of related factors within the TGF-beta superfamily. Nothing is yet known about the function of the TGF-beta- related factor vgr, only limited studies have been conducted on the most closely related factors BMP-5, osteogenic protein-1 (OP-1) or BMP-7, and OP-2. Because vgr-1 mRNA has been localized in hypertrophic cartilage, this factor may play a vital role in endochondral bone formation. Downregulation of Vgr/BMP-6 suggests that this molecule is involved somewhere in TGF-beta signalling pathway to inhibit ongoing BMP signalling and downstream intracellular smads process.

According to our second hypothesis, we did not detect any single gene that was attenuated after Tola infusion. Nevertheless, we have detected several genes that are regulated in MT and not in MCT (18 genes), and similarly, in MCT and not in MT (67 genes; see MCT discussion section). Among the 18 genes some gene likes protease II, protease inhibitor, stromal cell-derived factor-1 (an angiogenic cytokine), and cell division cycle control protein 2 cdc2a may be involved in angiogenesis and vessel maintenance. Very interestingly, BMPR2 that was found to be downregulated in the MCT group was no longer regulated in the treated group.

In the Tola group, we detected (as expected) only a low number of differentially regulated genes (19 genes). We further did not detect genes that are involved in MCT induced PH, especially no mast cell proteases, tissue inhibitors of metalloproteinases, or BMPR-II. Furthermore, we have detected 10 genes that are upregulated in MT in similar fashion as well. Such similar behaviour suggests that these genes were regulated by Tola influence. Among 10 genes S100A8 and S100A9 were upregulated. Recently, pro-inflammatory activities had been described for S100A8 and S100A9, two proteins found at inflammatory sites and within the neutrophil cytoplasm. Elevated serum levels of S100A8 and S100A9 have been found in patients suffering from a number of inflammatory disorders including cystic fibrosis, rheumatoid arthritis and chronic bronchitis.[120] Upregulation with 3.0-fold of these proteins in MT group suggests that S100A8 and S100A9 play a role in the inflammatory response against inflammatory agent (MCT) by inducing the release of neutrophils from the bone marrow and directing their migration to the inflammatory site. In the Tola group an upregulation by a factor of 5.0 suggests that Tola has a very strong influence on recruiting these pro-inflammatory proteins while in MT group the increase dropped to the factor of 2.0.

Another molecule that was regulated in MT and Tola group was Melanocortin 5-receptor (MC5-R). MC5-R belongs to a family of pro-opiomelanocortin-derived peptides that have the melanocyte-stimulating hormone (MSH) core sequence. Melanocortins have been described as having a variety of cardiovascular effects.[121] Moreover, very low expression levels have been detected in brain, while high levels are found in adrenals, stomach, lung and spleen.[122] This gene was upregulated in MT (Tola) with a foldchange of 2.0 (4.0).

6.3   Pneumolysin-Dependent Gene Expression

Among different toxins streptococcus pneumoniae is able to synthesize the pore-forming exotoxin pneumolysin. When investigating the effects of this exotoxin (kindly provided by Prof. Dr. T. Chakraborty, Department of Medical Microbiology) we found that IT application resulted in severe illness and respiratory distress and lung edma of the mice while IV applications of same dosage was tolerated well by the animals

(performed by PD Dr. U.A. Maus). Additionally, PLY was applied to the *ex-vivo* ventilated and perfused lung organ model (performed by PD Dr. N. Weissmann). Here, IT application showed a remarkable increase in weight by development of an edema and significant increase in pulmonary artery pressure (PAP; figure 37 b). Based on these observations we investigated the gene expression regulation in the *in-vivo* and *ex-vivo* model. Only few studies on streptococcus pneumoniae induced transcriptional regulation were published. Roger PD *et al*. differentiated the PLY dependent and PLY independent expression changes of streptococcus pneumonaie in mononuclear cells.[123]

6.3.1 Animal Model (*in-vivo*)

Expression profiling was performed on Affymetrix MG U74 Chips. Analyzing the data, the hierarchical clustering resulted in a conclusion that there was a high degree of similarity between IV group and control group for both the models suggesting that PLY application via IV mode does not alter gene expression pattern considerably. The reason for this finding might be that PLY in the given dosage is completely bound by serum proteins and therefore does not develop effects. Consequently, we put IV and control in one group. Afterwards, differential expression of IT group versus control+IV group was calculated. As expected, we found several genes that are regulating in PLY dependent manner. Lysyl oxidase (LOX), an enzyme secreted by activated vascular smooth muscle cells and fibroblasts, was upregulated with a more than a factor of 4.0. LOX catalyzes a key step in the cross-linking and stabilization of collagen and elastin in the vascular wall and involved in extracellular matrix maturation. Upregulation of LOX could be a sign for instability between collagen and elastin in vascular wall and impairs the endothelial barrier function and could be involved in homocysteine (HC)-induced endothelial dysfunction and leakage.[124]

An imbalance between vasoactive and vasocontrictor factors contributes to the vascular remodelling and increases pulmonary artery pressure. Among vasoconstriction factor, here, angiotensin converting enzyme (ACE) was upregulated. ACE is an ectoenzyme that catalyzes the conversion of angiotensin I to the vasoconstrictor angiotensin II as well as the degradation of the potent vasodilator

bradykinin.[125] ACE is thought to play a crucial role in blood pressure regulation and in processes involved in vascular remodelling.

CD53 is also an integral membrane protein. It is expressed on a broad range of different hematopoietic cell types, including monocytes and macrophages and is involved in association with integrins and protein kinase C to facilitate their interaction and thus their engagement in growth regulation of these cells.[126-127] Although, its biological role remains unknown. Here, the expression of CD53 was upregulated with more than a factor of 3.0, suggesting a defence mechanism of lung cells against pneumococcus.

A number of factors involved in cell cycle control were found to be upregulated in a PLY-dependent fashion, for example, ubiquitin-conjugating enzyme E2 was upregulated. Upregulation of ubiquitin-conjugating enzyme E2 mediating degradation of the cyclin-dependent kinase inhibitor p27Kip1 thereby triggering the onset of DNA replication and cell cycle progression. Moreover, ubiquitinylation induced proteolysis may disrupt cell regulation itself by degradation of regulatory proteins.[128]

On the other hand several genes were differentially downregulated in response to PLY. Among them, CD84, a newly described cell surface molecule is a member of the CD2 subset of the immunoglobulin superfamily of cell surface receptors.[129] Recently, it had been described that CD84 may play a significant role in leukocyte activation.[130] Its structural similarity with other members of the Ig superfamily as well as the presence of four potential SH2 domain binding motifs found in the cytoplasmic domain suggest that it may be involved in cellular interactions, activating lymphocytes and natural killer cells, and signal transduction.[130] Downregulation of CD84 would lead to severe curtailment of above processes.

In conclusion, the found differential expression indicates changes that lead to acute disruption of the endothelium barrier and dysregulation of the vascular tone.

6.3.2 Organ Model (*ex-vivo*)

Several genes were regulated after applying PLY via IT mode to the ex-vivo model. The first five upregulated genes are troponin T2, myosin heavy chain, cardiac actin,

troponin I and myosin light chain. These muscle cell filaments necessary for contraction point to an increased pressure that is answered by increased muscle filament synthesis. Myosin light chain (MLC) additionally playes a role in maintaining endothelium cell (EC) barrier integrity between the vascular spaces and underlying tissues. Any compromise of endothelial cell (EC) barrier integrity leads to an increase in vascular permeability, a cardinal feature of inflammation resulting in tissue edema and hypoxemia. Edemagenic agents such as the serine protease thrombin induce EC barrier dysfunction, primarily via actomyosin-driven contraction initiated by myosin light chain (MLC) phosphorylation and tightly linked to microfilament reorganization.[131]

On the other hand chemokine c-c receptor 1, which may play an important role in lung inflammatory cell recruitment because of having a leukocyte chemotactic and activating properties, was downregulated in response to PLY via IT. Less is known about the relationship of complement activation products to chemokine generation and attendant effects on lung injury. Here, downregulation of chemokine c-c gene as well as interleukin I receptor suggest an involvement in lung inflammatory cell recruitment process and edema induction.[132]

In the *ex-vivo* model and PLY application via IV mode, the toxin via IV mode has obviously no strong effects. Few genes were found to be regulated which are independent to PLY toxin effect; for example, Bcl-2-associated athanogen was upregulated. Bcl-2-associated athanogen consists of a homologous network of genes that regulate apoptosis or programmed cell death. Overexpression of Bcl-2 might be implicated in genome degradation during apoptosis.

Next we asked how many genes are regulated commonly in *in-vivo* and an *ex-vivo* model? Interestingly, no single gene was detected after comparing *in-vivo* (IT/IV) model to an *ex-vivo* (IV/IVC) group while several genes were detected in *in-vivo* (IT/IV) and an *ex-vivo* (IT/ITC) group. This suggests that the expression profiling for IT application of PLY results in severe changes *in-vivo* and in an *ex-vivo* organ model that differ remarkably from the IV treatment. PLY toxin via IV mode does not have strong influences on these genes.

7   Conclusions

The presented thesis work provides a broad overview of different gene array technology platforms. The optimization of glass array technology is shown in a stepwise manner. Pitfalls that appeared are shown from the sample preparation of different experimenters leading to completely different expression profiles to the cluster analysis of affymetrix arrays pointing to a sample mix-up. Moreover, two different RNA preamplification techniques were extensively compared due to the generated product length, reproducibility, and validity of the correspinding unamplified samples. This technical part gives other investigators suggestions how to plan and perform array experiments and what details have to be noticed.

This kind of screening technique was applied to the analysis of two animal models of pulmonary hypertension. At first sight, we could not detect new key player genes that have not been described yet in the setting of vascular remodelling. On closer inspection, a set of genes was found that confirm published knowledge of signalling mechanisms during the remodeling process indicating reliable performance of the experiments. Furthermore, some genes were found that fit well into the expectations of signalling. Especially the downregulation of BMPR2 in the monocrotaline model is an interesting finding showing for the first time disease involvement of this receptor in an animal model. Nevertheless, an independent confirmation of the RNA regulation should be performed before further investigations on protein level (western blot, immunohistochemistry) and functional experiments follow.

8 Summary

Differential gene expression can be investigated effectively by microarrays. Therefore, the respective technical steps and parameters, in particular RNA extraction, cDNA labelling, hybridization and washing for low-fluorescence background on slides have to be optimized. Comparing different RNA extraction techniques, we found that Trifast™ method followed by column purification combined with DNase digestion resulted in highest RNA quality of the samples. Ten to 20 µg RNA, direct labelling of the RNA with Cy-dNTPs and SuperScript II reverse transcriptase generated an efficient incorporation rate and sufficient amounts of labelled samples for microarray analysis. Furthermore, technical parameters of the hybridization process were adapted to optimize the signal to noise ratio. Particular importance was addressed to the comparison of RNA preamplification methods that allow the use of trace amounts of sample material for array analyses. Starting from as few as 50 ng initial total RNA, the performance of two preamplification techniques, two rounds of T7 based *In-vitro* transcription and PCR based SMART™ amplification were compared due to 1) the length of the generated products, 2) the inter-assay reproducibility using two independently performed repetition of the hybridization experiments, and 3) the validity of the expression profile when compared to the identical unamplified samples. We could show that the sequences close to the polyA-tail (<1kb distance) were amplified in two rounds IVT by a factor of 300-1000, comparable to the factor obtained by 12 cycles SMART™. In contrast, sequences with a distance of >1kb from the polyA-tail were only <100-fold amplified by IVT but again about 1000-fold with 12 cycles SMART™. The reproducibility of SMART™ was higher (R^2=0.91) than of IVT (R^2=0.68). Finally, higher correlation was seen for the comparison of SMART™ amplified samples to unamplified material versus IVT samples. Thus, SMART™ turned out to be superiour for minute amounts of total RNA (~ 50 ng) when introducing to microarray experiments.

Applying our established cDNA-macroarrays and oligonucleotide-microarrays to investigate pulmonary hypertension we expected to expand our knowledge about the disease signalling pathways. Differential gene expression was studied using a rat model of monocrotaline-induced pulmonary hypertension and attenuation of the

disease by application of the phosphodiesterase inhibitor tolafentrine. In cDNA macroarrays with 1,176 genes, we detected 11 regulated genes after monocrotaline treatment and 3 after treatment with monocrotaline together with tolafentrine. Using microarrays with 10,000 spotted sequences, we detected 103 and 54 regulated genes, respectively. Interestingly, tolafentrine given alone had only little influence on the expression profile.

In the second model of pulmonary hypertension pneumolysin, a pore-forming exotoxin of *Streptococcus pneumoniae* was instillated intratreacheally (IT) or intravenously (IV) to mice. While IT application resulted in severe illness and respiratory distress, IV application was tolerated well. Differential gene expression of lung homogenates was analysed by Affymetrix GeneChips™. Afterwards, IT and IV instillation was applied to an *ex-vivo* ventilated and perfused lung organ model. Here, IT application resulted in significant increase of pulmonary artery pressure and lung oedema. Comparing expression profiles after *in-vivo* application to that of the *ex-vivo* treated lungs showed more than 100 genes regulated in the IT groups of both models. In contrast, the profiles differed remarkably to those of IV treatment, where only minor changes in the expression profiles were observed in comparison to the controls.

9   Zusammenfassung

Mikroarrays erlauben eine effektive Untersuchung differenzieller Genexpression. Zunächst müssen hierzu jedoch die entsprechenden technischen Schritte und Parameter, insbesondere die RNA Extraktion, die Markierung der cDNA, die Hybridisierung sowie Waschschritte zur Minimierung des Hintergrunds auf den Objektträgern optimiert werden. Beim Vergleich verschiedener RNA Extraktionsprotokolle fanden wir, dass die Trifast™ Methode mit anschließender Silicasäulenaufreinigung und kombiniertem DNase Verdau die höchste RNA Qualität ergab. Einsatz von 10 bis 20 µg RNA, die Verwendung Cy-gekoppelter dNTPs sowie die SuperScript II reverse Transkriptase resultierten in einer effizienten Einbaurate und ausreichenden Mengen an markierter cDNA für die anschließende Mikroarray Hybridisierung. Zudem mussten aber auch die technischen Parameter dieses Hybridisierungsprozesses ausgetestet werden, um den Quotienten von Signal/Hintergrund zu optimieren.

Ein besonderes Augenmerk wurde auf den Vergleich von RNA Präamplifikationstechniken gelegt, die das Einsetzen auch geringer RNA Mengen in Array Experimente erlauben. Ausgehend von nur 50 ng Gesamt-RNA wurden als Präamplifikationstechniken zwei Runden der T7 basierten In-vitro Transkription (IVT) mit der PCR basierten SMART™ PCR verglichen bezüglich 1) der Länge der generierten Produkte, 2) ihrer (inter-assay) Reproduzierbarkeit bei jeweils zwei unabhängig voneinander durchgeführten Hybridisierungsexperimenten sowie 3) der Validität der Expressionprofile im Vergleich zu Profilen von identischen unamplifizierten Proben. Wir konnten dabei zeigen, dass Sequenzen nahe des poly-A-Schwanzes (<1kb Abstand) mit zwei Runden IVT um einen Faktor von 300-1000 amplifiziert wurden, vergleichbar zu dem mit 12 Zyklen SMART™ erzielten Ergebnis. Dagegen wurden Sequenzen mit einem Abstand von >1kb vom poly-A-Schwanz durch die IVT weniger als 100-fach amplifiziert, während 12 Zyklen SMART™ wiederum eine Vervielfältigung um Faktor 1000 zeigten. Zudem erwies sich die Reproduzierbarkeit von SMART™ (R^2=0.91) höher als die der IVT (R^2=0.68). Schließlich erwies sich auch die Korrelation beim Vergleich von SMART™ amplifizierten Proben zu ihren unamplifizierten Pendants als höher als der entsprechende Ansatz mit IVT Proben. Insofern bleibt festzuhalten, dass

die SMART™ Amplifikation bei sehr geringen initialen RNA Mengen (~ 50 ng) der IVT über zwei Runden für Hybridisierungsexperimente deutlich überlegen ist.

Anschließend wurden die in der Arbeitsgruppe bereits etablierten Nylon-Membran basierten Makroarrays sowie die neu optimierten Oligonukleotid-Mikroarrays eingesetzt, um pulmonalarterielle Hypertonie in zwei Tiermodellen zu untersuchen und mögliche Signalkaskaden aufzufinden. Zum einen kam das Rattenmodell der Monokrotalin-induzierten pulmonalen Hypertonie zur Verwendung sowie deren Abschwächung durch Gabe des Phosphodiesterase Inhibitors Tolafentrine. Mittels cDNA Makroarrays mit 1,176 gespotteten Genen detektierten wir 11 regulierte Gene in Lungen von Monokrotalin-behandelten Ratten sowie 3 Gene in Lungen von Ratten, denen Monokrotalin und Tolafentrine appliziert wurde. Bei Einsatz der Mikroarrays mit 10,000 gespotteten Sequenzen fanden wir 103 regulierte Gene in erstbeschriebener und 54 in zweitbeschriebener Gruppe. Interessanterweise hatte die alleinige Gabe von Tolafentrine nur einen geringen Effekt auf die Expressionsprofile.

Im zweiten Modell der pulmonalarteriellen Hypertonie wurde Pneumolysin, ein porenbildendes Exotoxin von *Streptococcus pneumoniae,* Mäusen entweder intratracheal (IT) oder intravenös (IV) instilliert. Während die IT Gabe zu schwerer Erkrankung und Luftnot führte, verhielten sich die Tiere nach IV Gabe unauffällig. Die differenzielle Genexpression der Lungenhomogenate wurde mittels Affymetrix GeneChips™ untersucht. Zudem erfolgte auch die IT und IV Instillation am Organmodell der ex-vivo ventilierten und perfundierten Lunge. Dabei resultiere die IT Applikation in einem signifikanten Anstieg des pulmonalarteriellen Druckes und Ausbildung eines Lungenödems. Der Vergleich der Expressionsprofile nach *in-vivo* Applikation zu denen von *ex-vivo* behandelten Lungen zeigte mehr als 100 Gene reguliert in den IT Gruppen beider Modelle. Im Gegensatz hierzu unterschieden sich die Profile beträchtlich zu denen nach IV Behandlung, wobei insgesamt nur geringe Veränderungen letztgenannter Expression gegenüber den Kontrollen zu beobachten waren.

10 References

1. Schena, M., Shalon, D., Davis, R.W., Brown, P.O. Quantitative monitoring of gene expression patterns with a complementary DNA microarray. *Science 1995,* **270**:467-470

2. Shioda, T. Application of DNA microarray to toxicological research. *J Environ Pathol Toxicol Oncol 2004*, **23**:13-31

3. Carella, M., Volinia, S., Gasparini, P. Nanotechnologies and microchips in genetic diseases. *J Nephrol 2003*, **16**:597-602

4. Chin, KV., Kong, AN. Application of DNA microarrays in pharmaco genomics and toxicogenomics. *Pharm Res 2002*, **19**:1773-1778

5. Butte, A. The use and analysis of microarray data. *Nat Rev Drug Discov 2002* **1**:951-960

6. Pollock, JD. Gene expression profiling: methodological challenges, results, and prospects for addiction research. *Chem Phys Lipids 2002*, **121**:241-256

7. Jenkins, ES., Broadhead, C., Combes, RD. The implications of microarray technology for animal use in scientific research. *Altern Lab Anim 2002*, **30**:459-465

8. Xiang, Z., Yang Y., Ma, X., Ding, W. Microarray expression profiling: Analysis and applications. *Curr Opin Drug Discov Devel 2003*, **6**:384-395

9. http://www.ncbi.nlm.nih.gov/entrez/

10. Southern, EM. Detection of Specific Sequences among DNA Fragments Separated by Gel Electrophoresis. *Journal of Molecular Biology 1975*, **98**:503-517

11. Dubitsky, A., Defiglia, J. Stripping of Digoxigenin-Labelled Probes from Nylon Membranes. *BioTechniques 1995*, **19**:210-212

12. Noppinger, K., Duncan, G., Ferraro, D. Evaluation of DNA Probe Removal from Nylon Membrane. *BioTechniques 1992*, **13**:572-575

13. Fodor, S., Read, JL., Pirrung, MC., Stryer, L.., Tsai, Lu A., Solas, D. Light-directed, spatially addressable parallel chemical synthesis. *Science 1991*, **251**: 767-773

14. Pease, AC., Solas, D., Sullivan, EJ., Cronin, MT., Holmes, CP., Fodor, SPA. Light-generated oligonucleotide arrays for rapid DNA sequence analysis. *Proc Natl Acad Sci USA 1994*, **91**:5022-5026

15. Barone, AD. Photolithographic synthesis of high-density oligonucleotide probe arrays. *Nucleosides Nucleotides Nucleic Acids 2001*, **20**:525-531

16. Wong, KK., Tsang, YT., Shen, J., Cheng, RS., Chang, YM., Man, TK., Lau CC. Allelic imbalance analysis by high-density single-nucleotide polymorphic allele

(SNP) array with whole genome amplified DNA. *Nucleic Acids Res 2004*, **32**:e69

17. Rubin, L. ACCP consensus statement; primary pulmonary hypertension. *Chest 1987*, **104**:236-250

18. Edwards, WD., Edwards, JE. Clinical primary pulmonary hypertension: three pathologic types. *Circulation 1977*, **56**:884-888

19. Romberg, E. Ueber sklerose der lungen arterie. *Dtsch Archiv Klin Med 1891*, **48**:197-206

20. Dresdale, DT., Schultz, M., Michtom, RJ. Primary pulmonary hypertension: Clinical and haemodynamic study. *Am J Med 1951*, **11**:686-705

21. Dresdale, DT., Michtom, RJ., Schultz, M. Recent studies In PPH, including pharmacodynamics observations on pulmonary vascular resistance. *Bull NY Acad Med 1954*, **30**:195-207

22. Rich, S., Dantzker, D., Aryers, SM. Primary Pulmonary Hypertension: a national prospective study. *Ann Intern med 1987*, **107**:216-223

23. Loyd, JE., Butler, MG., Foroud, TM., Conneally, PM., Phillips, JA., Newman, JH. Genetic anticipation and abnormal gender ratio at birth in familial primary pulmonary hypertension. *Am J Respir Crit Med 1995*, **152**:93-97

24. Wood, P. Pulmonary hypertension with special reference to the vasoconstrictive factor. *Br Heart J 1958*, **2**:557-570

25. Rubin, LJ. Diagnosis and Management of Pulmonary Arterial hypertension: ACCP Evidence-Based Practical Guidelines. *Chest 2004*, **126**:7S-10S

26. Romberg, E. Ueber slerose der lungenarterien. *Dtsch Arch Klin Med 1891*, **48**:197-199

27. Chazova, I., Loyd, JE., Zhdanov, VS., Newman, JH., Belenkov, Y., Meyrick, B. Pulmonary artery adventitial changes and venous involvement in PPH. *Am J Pathol 1995*, **146**:389–397

28. Cool, CD., Stewart, JC., Werahera, P., Miller, GJ., Williams, RL., Voelkel NF., Tuder, RM. Three-dimensional reconstruction of pulmonary arteries in plexiform pulmonary hypertension using cell-specific markers. *Am J Pathol 1999*, **155**:411-419

29. Voelkel, NF., Cool, C., Lee, SD., Wright, L., Geraci, MW., Tuder, RM. Primary pulmonary hypertension between inflammation and cancer. *Chest 1998*, **114**:225S-230S

30. Deng, Z., Morse, JH., Slager, SL., Cuervo, N., Moore, KJ., Venetos, G., Kalachikov, S., Cayanis, E., Fischer, SG., Barst, RJ., Hodge, SE., Knowles, JA. Familial primary pulmonary hypertension (gene PPH1) is caused by mutations in the bone morphogenetic protein receptor-II gene. *Am J Hum Genet 2000*, **67**:737-744

31. Strange, JW., Wharton, J., Philips, PG., Wilkins, MR. Recent insights into the pathogenesis and therapeutics of pulmonary hypertension. *Clinical Science 2002*, **102**:253-268

32. Will, DH., Alexander, AF., Reeves, JT., Grover, RF. High altitude-induced pulmonary hypertension in normal cattle. *Circ. Res 1962*, **10**:172-177

33. Huxtable, RJ. Activation and pulmonary toxicity of pyrrolizidine alkaloids. *Pharmacol Ther 1990*, **47**:371-389

34. Roth, RA., Reindel, JF. Lung vascular injury from monocrotaline pyrrole, a putative hepatic metabolite. *Adv Exp Med Biol 1991*, **283**:477-487

35. Schermuly, RT., Kreisselmeier, KP., Ghofrani, HA., Yilmaz, H., Butrous, G., Ermert, L., Ermert, M., Weissmann, N., Rose, F., Guenther, A., Walmrath, D., Seeger, W., Grimminger, F. Chronic sildenafil treatment inhibits MCT-induced pulmonary hypertension in rats. *Am J Respir Crit Care Med 2004*, **169**:39-45

36. Wilson, DW., Segah, HJ., Pan, LCW. Progressive inflammatory and skeletal changes in the pulmonary vasculature of monocrotaline-treated rats. *Microvasc Res 1989*, **80**:1207-1221

37. Romberg, E. Ueber slerose der lungenarterien. *Dtsch Arch Klin Med 1891*, **48**:197-199

38. Chazova, I., Loyd, JE., Zhdanov, VS., Newman, JH., Belenkov, Y., Meyrick, B. Pulmonary artery adventitial changes and venous involvement in PPH. *Am J Pathol 1995*, **146**:389-397

39. Rosenberg, HC., Rabinovitch, M. Endothelial injury and vascular reactivity in monocrotaline pulmonary hypertension. *Am J Physiol 1988*, **255**:1484-1491

40. Reindel, JF., Ganey, PE., Wagner, JG., Slocombe, RF., Roth, RA. Development of morphologic, hemodynamic, and biochemical changes in lungs of rats given monocrotaline pyrrole. *Toxicol Appl Pharmacol 1990*, **106**:179-200

41. Dorfmüller, P., Perros, F., Balabanian, K., and Humbert, M. Inflammation in pulmonary arterial hypertension. *Eur Respir J 2003*, **22**:358-363

42. Christman, BW., McPherson, CD., Newman, JH., King, GA., Bernard, GR., Groves, BM., Loyd, JE. An imbalance between the excretion of thromboxane and prostacyclin metabolites in pulmonary hypertension. *N Engl J Med 1992*, **327**:70-75

43. Wagner, RS., Smith, CJ., Taylor, AM., Rhoades, RA. Phosphodiesterase inhibition improves agonist-induced relaxation of hypertensive pulmonary arteries. *J Pharmacol Exp Ther 1997*, **282**:1650-1657

44. Uder, M., Heinrich, M., Jansen, A., Humke, U., Utz, J., Trautwein, W., Kramann, B. cAMP and cGMP do not mediate the vasorelaxation induced by iodinated radiographic contrast media in isolated swine renal arteries. *Acta Radiol 2002*, **43**:104-110

45. De Boer, J., Philpott, KJ, Van Amsterdam, RGM., Shahid, M., Zaagsma, J., Nicholson, CD. Human bronchial cyclic nucleotide phosphodiesterase

isoenzymes: Biochemical and pharmacological analysis using selective inhibitors. *Br J Pharmacol 1992*, **106**:1028-1034

46.   Torphy, TJ. Phosphodiesterase isoenzymes. *Am J Respir Crit Care Med 1998*, **157**:351-370

47.   Schermuly, RT., Roehl, A., Weissmann, N., Ghofrani, HA., Schudt, C., Tenor. H., Grimminger, F., Seeger, W., Walmrath, D. Subthreshold doses of specific phosphodiesterase type 3 and 4 inhibitor enhance the pulmonary vasodilatory response to nebulized prostacyclin with improvement in gas exchange. *JPET 2000*, **292**:512-520

48.   Hoeper, MM., Galie, N., Simonneau, G., Rubin, LJ. New treatment for pulmonary arterial hypertension. *Am J Respir Crit Care Med 2002*, **165**:1209-1216

49.   Johnston, RB. Pathogenesis of pneumococcal pneumonia. *Jr Rev Infect Dis 1991*, **13**:S509-S517

50.   Qadri, SM., Berotte, JM., Wende, RD. Incidence and etiology of septic meningitis in a metropolitan county hospital. *Am J Clin Pathol 1976*, **65**:550-556

51.   Klein, JO. The epidemiology of pneumococcal disease in infants and children. *Rev Infect Dis 1981*, **3**:246-253

52.   Yangco, BG., Deresinski, SC. Necrotizing or cavitating pneumonia due to *Streptococcus Pneumoniae*: report of four cases and review of the literature. *Medicine (Baltimore) 1980*, **59**:449-457

53.   Schwandner, R., Dziarski, R., Wesche, H., Rothe, M., Kirschning, CJ. Peptidoglycan- and lipoteichoic acid-induced cell activation is mediated by Toll-like receptor 2. *J Biol Chem 1999*, **274**:17406-17409

54.   Jedrezejas, MJ. Pneumococcal virulence factors: structure and function. *Microbiol Mol Biol Rev 2001*, **65**:187-207

55.   McDaniel, LS., Thornton, JA., McDaniel, DO. Use of cDNA microarrays to analyze responses to pneumococcal virulence factors. *Indian J Med Res 2004*, **119**:99-103

56.   Paton, JC. The contribution of pneumolysin to the pathogenicity of *Streptococcus pneumoniae. Trends Microbiol 1996*, **4**:103-106

57.   Rossjohn, J., Feil, SC., McKinstry, WJ., Tweten, RK., Parker, MW. Structure of a cholesterol-binding, thiol-activated cytolysin and a model of its membrane form. *Cell 1997*, **89**:685-692

58.   Bhakdi, S., Tranum-Jensen, J. Alpha-toxin of Staphylococcus aureus. *Microbiological Reviews 1991*, **55**:733-751

59.   Chomczynski, P., Sacchi, N. Single-step method of RNA isolation by acid guanidinium thiocyanate-phenol-chloroform extraction. *Anal. Biochem 1987*, **162**:156-159

60. Van Gelder, RN., Von Zastrow, ME., Yool, A., Dement, WC., Barchas, JD., Eberwine, JH. Amplified RNA synthesized from limited quantities of heterogeneous cDNA. *Proc Natl Acad Sci USA* 1990, **87**:1663-1667

61. Eberwine, J. Amplification of mRNA populations using aRNA generated from immobilized oligo-dT-T7 primed cDNA. *BioTechniques 1996*, **20**:584-591

62. Zhumabayeva, B., Chenchik, A., Siebert, PD., Herrler, M. Disease profiling arrays: reverse format cDNA arrays complimentary to microarrays. *Adv Biochem Eng BioTechnol 2004*, **86**:191-213

63. Seth, D., Gorrell, MD., McGuinness, PH., Leo, MA., Lieber, CS., McCaughan, GW., Haber, PS. SMART amplification maintains representationof relative gene expression: quantitative validation by real time PCR and application to studies of alcoholic liver disease in primates. *Biochem Biophys Methods 2003*, **55**:53-66

64. Eberwine, J., Yeh, H., Miyashiro, K., Cao, Y., Nair, S., Finnell, R., Zettel, M., Coleman, P. Analysis of gene expression in single live neurons. *Proc Natl Acad Sci USA 1992*, **89**:3010–3014.

65. Chenchik, A. *Clontechniques IX (1) 1998*, 9–12

66. Freeman, WM., Walker, SJ., Vrana Freeman, KE. Quantitative RT-PCR: pitfalls and potential. *BioTechnique 1999*, **26**:112-122

67. http://www.r-project.org/ and http://www.bioconductor.org/

68. Smyth, GK., Michaud, J., Scott, H. The use of within-array replicate spots for assessing differential expression in microarray experiments. *Bioinformatics 2005*, **21**:2067-2075

69. Smyth, GK., Speed, TP. Normalization of cDNA microarray data. *Methods 2003*, **31**:265-273

70. Smyth, GK. Limma: linear models for microarray data. In: Bioinformatics and Computational Biology Solutions using R and Bioconductor, R. Gentleman, V. Carey, S. Dudoit, R. Irizarry, W. Huber (eds.), Springer, New York, Chapter 23. (To be published in 2005)

71. Yang, YH., Dudoit, S., Luu, P., Lin, DM., Peng, V., Ngai, J., Speed, TP. Normalization for cDNA microarray data: a robust composite method addressing single and multiple slide systematic variation. *Nucleic Acids Research* 2002, **30**:e15

72. Cleveland, WS. Robust locally weighted regression and smoothing scatterplots. *Jour Amer Stat Assoc 1979*, **74**:829-836

73. Smyth, GK. Linear Models and Empirical Bayes Methods for Assessing Differential Expression in Microarray Experiments. *Statistical Applications in Genetics and Molecular Biology 2004*, **3**: Issue 1

74. http://www.dchip.org/

75. Bustin, SA. Absolute quantification of mRNA using reverse transcription polymerase chain reaction assays. *Jour Mol Endocrinol 2000*, **25**:169-193

76. Tavangar, K., Hoffman, AR., Kraemer, FB. A micromethod for the isolation of total RNA from adipose tissue. *Anal Biochem 1990*, **186**:60-63

77. Smale, G., Sasse, J. RNA isolation from cartilage using density gradient centrifugation in cesium trifluoroacetate: an RNA preparation technique effective in the presence of high proteoglycan content. *Anal Biochem 1992*, **203**:352-56

78. Briscoe, PR., Jorgensen, TJ. Improved RNA isolation from cells in tissue culture using a commercial nucleic acid extractor. *BioTechniques 1991*, **10**:594-96

79. http://homer.hsr.ornl.gov/CBPS/Arraytechnology/Hyb.html

80. http://www.bri.nrc.gc.ca/pdf/microarray_Direct_Incorporation_Labeling%20_Pro tocol_e.doc

81. Mateos, A. Effect of ethanol consumption on adult rat liver mitochondrial population analyzed by flow cytometry. *Alcohol Clin Exp Res 1995*, **19**:1327-1330

82. Velculescu, VE., Zhang, L., Vogelstein, B., Kinzler, KW. Serial analysis of gene expression. *Science 1995*, **270**:484-487

83. Watson, A., Mazumder, A., Stewart, M., Balasubramanian, S. Technology for microarray analysis of gene expression. *Curr Opin Biotechnol 1998*, **9**:609-614

84. Luo, L., Salunga, RC., Guo, H., Bittner, A., Joy, KC., Galindo, JE., Xiao, H., Rogers, KE., Wan, JS., Jackson, MR.,Erlander, MG. Gene expression profiles of laser-captured adjacent neuronal subtypes. *Nat Med 1999*, **5**:117-122

85. http://www.ncbi. nlm. nih.gov /Uni Gene /ddd.cgi AND http://genecards.weiz mann. ac.il/cgi-bin/ genenote

86. Morrison, DA., Ellis, JT. The Design and Analysis of Microarray Experiments: Applications in Parasitology. DNA and Cell Biology, 2003, **226**:357-394

87. Saghizadeh, M., Brown, DJ., Tajbakhsh, J., Chen, Z., Kenney, MC., Farber, DB., Nelson, SF. Evaluation of techniques using amplified nucleic acid probes for gene expression profiling. *Biomolecular Engineering 2003*, **20**:97-106

88. www.arctur.com

89. Wang E., Miller, LD., Ohnmacht, G.A., Liu, E.T., Arincola, FM. High-fidelity mRNA amplification for gene profiling. *Nat Biotechnol 2000,* **18**:457-459

90. Wilson, CL., Pepper, SD., Hey, Y., Miller, CJ. Amplification protocols introduce systematic but reproducible errors into gene expression studies. *BioTechniques 2004*, **36**:498-506

91. Schneider, J., Buness, A., Huber, W., Volz, J., Kioschis, P., Hafner, M., Poustka, A., Sultmann, H. Systematic analysis of T7 RNA polymerase based *in-vitro* linear RNA amplification for use in microarray experiments. *BMC Genomics 2004*, **5**:29-38

92. Stenmark, KR., Durmowicz, AG., Dempsey, EC. Modulation of vascular wall cell phenotype in pulmonary hypertension. *Portland Press Ltd, London 1995*, 171-212

93. Huxtable, RJ. Activation and pulmonary toxicity of pyrrolizidine alkaloids. *Pharmacol Ther 1990*, **47**:371–389

94. Tohda, Y. Role of GABA receptors in the bronchial response: studies in sensitized guinea-pigs. *Clin Exp Allergy 1998*, **28**:772-77

95. Capelli, A., Lusuardi, M., Cerutti, CG., and Donner, CF. Lung alkaline phosphatase as a marker of fibrosis in chronic interstitial disorders. *Am J Respir Crit Care Med 1997*, **155**:249-253

96. Arcot, SS. Alterations of growth factor transcripts in rat lungs during development of monocrotaline-induced pulmonary hypertension. *Biochem Pharmacol 1993*, **46**:1086-91

97. Geraci, MW., Moore, M., Gesell, T., Yeager, ME., Alger, L., Golpon, H., Gao, B., Loyd, JE., Tuder, RM., Voelkel, NF. Gene Expression Patterns in the Lungs of Patients with Primary Pulmonary Hypertension. *Circ Res 2001*, **88**:555-562

98. Meyrick, B., Reid, L. The effect of continued hypoxia on rat pulmonary arterial circulation: An ultrastructural study. *Lab Invest 1978*, **38**:188-199

99. Voelkel, NF., Tuder, RM., Bridges, J., Arend, WP. Interleukin-1 receptor antagonist treatment reduces pulmonary hypertension generated in rats by monocrotaline. *Am J Respir Cell Mol Biol 1994*, **11**:664-675

100. Wright, L., Tuder, RM., Wang, J., Cool, CD., Lepley, RA., Voelkel, NF. 5-Lipoxygenase and 5-lipoxygenase activating protein (FLAP) immunoreactivity in lungs from patients with primary pulmonary hypertension. *Am J Respir Crit Care Med 1998*, **157**:219-229

101. Vaszar, LT., Nishimura, T., Storey, JD., Zhao, G., Qiu, D., Faul, JL., Pearl, RG., Kao, PN. Longitudinal transcriptional analysis of developing neointimal vascular occlusion and pulmonary hypertension in rats. *Physiol Genomics 2004*, **17**:150-156

102. Ye,C., Rabinovitch, M. Inhibition of elastolysis by SC-37698 reduces development and progression of monocrotaline pulmonary hypertension. *Am J Physiol 1991*, **261**:12551267

103. Cowan, KN., Heilbut, A., Humpl, T., Lam, C., Ito, S., Rabinovitch, M. Complete reversal of fatal pulmonary hypertension in rats by a serine elastase inhibitor. *Nat Med 2000*, **6**:698-702

104. Kleiner, DE., Stetler-Stevenson, WG. Structural biochemistry and activation of matrix metalloproteases. *Curr Opin Cell Biol 1993*, **5**:891-897

105. Docherty, AJP., Lyons, A., Smith, BJ., Wright, EM., Stephens, PE., Harris, TJR. Sequence of human tissue inhibitor of metalloproteinases and its identity to erythroid-potentiating activity. *Nature 1985*, **318**:66-69

106. Dempsey, EC., Stenmark, KR., McMurtry, IF., O'Brien, RF., Voelkel, NF., Badesch, DB. Insulin-like growth factor-I and protein kinase C activation stimulate pulmonary artery smooth muscle cell proliferation through separate but synergistic pathways. *J Cell Physiol 1990*, **144**:159-165

107. Olbruck, H., Seemayer, NH., Voss, B., Wilhelm, M. Supernatants from quartz dust treated human macrophages stimulate cell proliferation of different human lung cells as well as collagen-synthesis of human diploid lung fibroblasts *in-vitro*. *Toxicol Lett 1998*, **96**-97:85-95

108. Kagi, JHR. Evolution, structure and chemical activity of class I metallothioneins: an Overview, In: Metallothionein, vol. III (K.T Suzuki, N. Imura and M. Kimura, eds.). Berlin: *Birkhausen Verlag 1993*, pp29-56

109. Ebadi, M., Iversen, PL., Hao, R., Cerutis, DR., Rojas, P., Happe, HK., Murrin, LC., Pfeiffer, RF. Expression and regulation of brain metallothionein. *Neurochem Int 1995*, **27**:1-22

110. Bacqueville, D., Casagrande, F., Perret, B., Chap, H., Darbon, JM., Breton-Douillon, M. Phosphatidylinositol 3-kinase inhibitors block aortic smooth muscle cell proliferation in mid-late G1 phase: effect on cyclin-dependent kinase 2 and the inhibitory protein p27KIP1. *Biochem Biophys Res Commun 1998*, **244**:630-636

111. Blackshaw, S., Sawa, A., Sharp, AH., Ross, CA., Snyder, SH., Khan, AA. Type 3 inositol 1,4,5-trisphosphate receptor modulates cell death. *FASEB J 2000*, **14**:1375-1379

112. Yamamoto-Hino, M., Sugiyama, T., Hikichi, K., Mattei, MG., Hasegawa, K., Sekine, S., Sakurada, K., Miyawaki, A., Furuichi, T., Hasegawa, M. Cloning and characterization of human type 2 and type 3 inositol 1,4,5-trisphosphate receptors. *Receptors Channels 1994*, **2**:9-22

113. Oike, Y., Ito, Y., Hamada, K., Zhang, XQ., Miyata, K., Arai, F., Inada, T., Araki, K., Nakagata, N., Takeya, M., Kisanuki, YY., Yanagisawa, M., Gale, NW., Suda, T. Regulation of vasculogenesis and angiogenesis by EphB/ephrin-B2 signalling between endothelial cells and surrounding mesenchymal cells. *Blood 2002*, **100**:1326-1333

114. Thomson, JR., Machado, RD., Pauciulo, MW., Morgan, NV., Humbert, M., Elliot, GC., Ward, K., Yacoub, M., Mikhail, G., Rogers, P., Newman, J., Wheeler, L., Higenbottam, T., Gibbs, JS., Egan, J., Crozier, A., Peacock, A., Allcock, R., Corris, P., Loyd, JE., Trembath, RC., Nichols, WC. Sporadic primary pulmonary hypertension is associated with germline mutations of the gene encoding BMPR-II, a receptor member of the TGF-beta family. *Jour Med Genet 2000*, **37**:741-745

115. Massague, J., Blain, SW., Lo, RS. TGF-beta. signalling in growth control, cancer, and heritable disorders. *Cell 2000*, **103**:295-309

116. Kohyama, T., Liu, X., Zhu, YK., Wen, FQ., Wang, HJ., Fang, Q., Kobayashi, T., Rennard, SI. Phosphodiesterase 4 Inhibitor Cilomilast Inhibits Fibroblast-Mediated Collagen Gel Degradation Induced by Tumor Necrosis Factor-and Neutrophil Elastase. *Am J Respir Cell Mol Biol 2002*, **27**:487-494

117. Cushley, MJ., Tattersfield, AE., Holgate, ST. Inhaled adenosine and guanosine on airway resistance in normal and asthmatic subjects. *Br J Clin Pharmacol 1983*, **15**:161-165

118. Sugo, S., Minamino, N., Shoji, H., Kangawa, K., Kitamura, K., Eto, T., Matsuo, H. Production and secretion of adrenomedullin from vascular smooth muscle cells: augmented production by tumor necrosis factor-alpha. *Biochem Biophys Res Commun 1994*, **203**:719-726

119. Kitamura, K., Sakata, J., Kangawa, K., Kojima, M., Matsuo, H., Eto, T. Cloning and characterization of cDNA encoding a precursor for human adrenomedullin. *Biochem Biophys Res 1993*, **194**:720-725

120. Sorg, C. The calcium binding proteins S100A8 and S100A9 in acute and chronic inflammation. *Behring Inst Mitt 1992*, **91**:126-137

121. Versteeg, DH., Van Bergen, P., Adan, RA., De Wildt, DJ. Melanocortins and cardiovascular regulation: The MC5-R mediates increase in cAMP accumulation with a characteristic pharmacology. *Eur J Pharmacol 1998*, **360**:1-14

122. Griffon, N., Mignon, V., Facchinetti, P., Diaz, J., Schwartz, JC., Sokoloff, P. Molecular cloning and characterization of the rat fifth melanocortin receptor. *Biochem Biophys Res Commun 1994*, **200**:1007-1014

123. Rogers, PD., Thornton, J., Barker, KS., McDaniel, DO., Sacks, GS., Swiatlo, E., McDaniel, LS. Pneumolysin-Dependent and -Independent Gene Expression Identified by cDNA Microarray Analysis of THP-1 Human Mononuclear Cells Stimulated by *Streptococcus pneumoniae. Infection and Immunity 2003*, **71**:2087-2094

124. Raposo, B., Rodriguez, C., Martinez-Gonzalez, J., Badimon, L. High levels of homocysteine inhibit lysyl oxidase (LOX) and downregulate LOX expression in vascular endothelial cells. *Atherosclerosis 2004*, **177**:1-8

125. Jaspard, E., Costerousse, O., Wei, L., Corvol, P., Alhenc-Gelas, F. The angiotensin I-converting enzyme (kininase II): molecular and regulatoryaspects. *Agents Actions Suppl 1992*, **38**:349-358

126. Olweus, J., Lund-Johansen, F., Horejs, V. CD53, a protein with four membrane-spanning domains, mediates signal transduction in human monocytes and B cells. *J Immunol 1993*, **151**:707-716

127. Zhang, XA., Bontrager, AL., Hemler, ME. Transmembrane-4 superfamily proteins associate with activated protein kinase C (PKC) and link PKC to specific beta (1) integrins. *J Biol Chem 2001*, **276**:25005-25013

128. Butz, N., Ruetz, S., Natt, F., Hall, J., Weiler, J., Mestan, J., Ducarre, M., Grossenbacher, R., Hauser, P., Kempf, D., Hofmann, F. The human ubiquitin-conjugating enzyme Cdc34 controls cellular proliferation through regulation of p27Kip1 protein levels. *Exp Cell Res 2005*, **303**:482-493

129. Davis, SJ., Vander Merwe, PA. The structure and ligand interactions of CD2: implications for T-cell function. *Immunol Today 1996*, **617**:177-187

130. de la Fuente, MA., Pizcueta, P., Nadal, M., Bosch, J., Engel, P. CD84 Leukocyte Antigen Is a New Member of the Ig Superfamily. *Blood 1997*, **90**:2398-2405

131. Verin, AD., Birukova, A., Wang, P., Liu, F., Becker, P., Birukov, K., Garcia, Joe G. N. Microtubule disassembly increases endothelial cell barrier dysfunction: role of MLC phosphorylation. *Am J Physiol Lung Cell Mol Physiol 2001*, **281**:565-574

132. Proost, P., Wuyts, A., Van Damme, J. The role of chemokines in inflammation. *Int J Clin Lab Res 1996*, **26**:211-223

Eidesstattliche Erklärung

Ich erkläre: Ich habe die vorgelegte Dissertation selbständig, ohne unerlaubte fremde Hilfe und nur mit den Hilfen angefertigt, die ich in der Dissertation angegeben habe. Alle Textstellen, die wörtlich oder sinngemäß aus veröffentlichten oder nicht veröffentlichten Schriften entnommen sind, und alle Angaben, die auf mündlichen Auskünften beruhen, sind als solche kenntlich gemacht. Bei den von mir durchgeführten und in der Dissertation erwähnten Untersuchungen habe ich die Grundsätze guter wissenschaftlicher Praxis, wie sie in der „Satzung der Justus-Liebig-Universität Gießen zur Sicherung guter wissenschaftlicher Praxis" niedergelegt sind, eingehalten.

Place: Giessen, 2005

Signature

Curriculum Vitae

Name:	Jai Prakash
Date of Birth:	04-09-1974
Address:	34/4, Block No.4, Teg Bahadur Road, Dalanwala, Dehradun, Uttaranchal, India
E-mail:	jai_muyal@yahoo.com
Telephone No:	+91-135 –2676904 (Home)

SCHOOL EDUCATION:

1981-90	From 1st standard to 9 th standard	Kendriya Vidyalaya, Jawahar Lal Nehru University, New Delhi, India.
1990–91	Class 10 th (High School)	Kendriya Vidyalaya, Jawahar Lal Nehru University, New Delhi, India.
1991– 93	Class 12 th (Intermediate)	Goverment Boys Senior Secondary School, RK Puram, Sector-II, New Delhi, India. Subject: Biology, Mathematics, Physics, Chemistry and English. Final marks: 57 % (PCB)

UNIVERSITY EDUCATION:

1993 – 1997	Bachelors in Science (B.Sc.), From Collage of Sri Venketeshwara, Delhi University. Final marks: 51%
1997 – 1999	Masters of Science in Biotechnology (M.Sc. in Biotechnology), from Banaras Hindu University, Varanasi,

Uttar Pardesh, India.

Final marks: 56 %

1998 – 1999	During Masters programmed, I had done one year's complete lab project work on "Hybrid Enzyme: A manipulating enzyme design" under the supervision of Dr. A.M. Kayastha, Department of Biotechnology, Banaras Hindu University, Varanasi, India.
Aug 2000 – Sept 2001	Worked as a Junior Research Fellow under Dr. U.K. Pati (Associate Professor), Centre for Biotechnology, Jawaharlal Nehru University, New Delhi, India under the project entitled "Correlation between Kringle IV and Pentanucleotide repeat (PNR) polymorphism in atherosclerosis "funded by Indian council of medical research (ICMR) New Delhi, India.

POSTGRADUATE EDUCATION:

Oct 2001 – Oct 2004	PhD program in the Graduiertenkolleg "Kardiopulmonales Gefäßsystem" of the University of Giessen.
	Done Ph.D. thesis work on "Optimization of Microarray Technology-Based Expression Profiling for Investigation of Different Animal Models of Pulmonary Hypertension" under the supervision of PD Dr. Ludger Fink, Institute for Pathologie, University Klinikum, Justus Liebig University, Giessen - 35392, Germany.

Place: Giessen, 2005

Signature